

N71-34985

VOLUME I  
NONAME SYSTEM DESCRIPTION

Contract No.: NAS 5-11736 MOD 92  
PCN 550-24217

Prepared By:

R.G. Williamson  
C.F. Martin  
M.L. Dutcher

Wolf Research and Development Corporation  
Riverdale, Maryland

For

Goddard Space Flight Center  
Greenbelt, Maryland

15 February 1971

REPRODUCED BY  
**NATIONAL TECHNICAL**  
**INFORMATION SERVICE**  
U.S. DEPARTMENT OF COMMERCE  
SPRINGFIELD, VA. 22161

28X

## TABLE OF CONTENTS

	<u>PAGE</u>
1.0 INTRODUCTION TO THE SYSTEM	1.0-1
	:
2.0 THE NONAME PROGRAM	2.0-1
2.1 INTRODUCTION TO THE NONAME PROGRAM	2.1-1
2.2 THE ORBIT AND GEODETIC PARAMETER ESTIMATION PROBLEM	2.2-1
2.2.1 The Orbit Prediction Problem	2.2-2
2.2.2 The Parameter Estimation Problem	2.2-5
2.3 THE MOTION OF THE EARTH AND RELATED COORDINATE SYSTEMS	2.3-1
2.3.1 The True of Date Coordinate System	2.3-2
2.3.2 The Inertial Coordinate System	2.3-2
2.3.3 The Earth-Fixed Coordinate System	2.3-3
2.3.4 Transformation Between Earth- Fixed and True of Date Co- ordinates	2.3-4
2.3.5 Computation of $\theta_g$	2.3-6
2.3.6 Precession and Nutation	2.3-9
2.3.6.1 Precession	2.3-12
2.3.6.2 Nutation	2.3-16
2.4 LUNI-SOLAR EPHEMERIDES	2.4-1

TABLE OF CONTENTS (CONTD.)

	<u>PAGE</u>
2.5 THE OBSERVER	2.5-1
2.5.1 Geodetic Coordinates	2.5-2
2.5.2 Topocentric Coordinate Systems	2.5-14
2.5.3 Time Reference Systems	2.5-15
2.5.3.1 Time System Transformations	2.5-16
2.5.4 Polar Motion	2.5-18
2.6 MEASUREMENT MODELING AND RELATED DERIVATIVES	2.6-1
2.6.1 The Geometric Relationship	2.6-7
2.6.2 The Geometric Partial Derivatives	2.6-15
2.6.3 The Time Derivatives	2.6-21
2.7 DATA PREPROCESSING	2.7-1
2.7.1 Time Preprocessing	2.7-2
2.7.2 Reference System Conversion To True of Date	2.7-4
2.7.3 Transponder Delay and Gating Effects	2.7-4
2.7.4 Diurnal Aberration	2.7-5
2.7.5 Refraction Corrections	2.7-6
2.7.6 Tranet Doppler Observations	2.7-10

TABLE OF CONTENTS (CONT.)

	<u>PAGE</u>
2.8 FORCE MODEL AND VARIATIONAL EQUATIONS	2.8-1
2.8.1 Equations of Motion	2.8-1
2.8.2 The Variational Equations	2.8-3
2.8.3 The Earth's Potential	2.8-11
2.8.4 Solar and Lunar Gravitational Perturbations	2.8-26
2.8.5 Solar Radiation Pressure	2.8-27
2.8.6 Atmospheric Drag	2.8-30
2.8.7 Atmospheric Density	2.8-34
2.8.7.1 The Assumptions of the Model	2.8-39
2.8.7.2 The Exospheric Temperature Computations	2.8-42
2.8.7.3 The Density Computation	2.8-52
2.8.7.4 Density Partial Derivatives	2.8-56
2.9 INTEGRATION AND INTERPOLATION	2.9-1
2.9.1 Integration	2.9-1
2.9.2 The Integrator Starting Scheme	2.9-7
2.9.3 Interpolation	2.9-10

TABLE OF CONTENTS (CONT.)

	<u>PAGE</u>
2.10 THE STATISTICAL ESTIMATION PROCEDURE	2.10-1
2.10.1 Bayesian Least Squares Estimation	2.10-2
2.10.2 The Partitioned Solution	2.10-8
2.10.3 Data Editing	2.10-25
2.11 GENERAL INPUT/OUTPUT DISCUSSION	2.11-1
2.11.1 Input	2.11-1
2.11.2 Output	2.11-5
2.11.3 Computations for Residual Summary	2.11-12
2.11.4 Kepler Elements	2.11-16
2.11.4.1 Node Rate and Perigee Rate	2.11-24
2.11.4.2 Period Decrement and Drag Rate	2.11-26
3.0 NONAME ANALYSES AND GRAPHICS SUPPORT PROGRAMS	3.0-1
3.1 DELTA	3.1-1
3.2 GEORGE	3.2-1
3.3 GROUNDTRACK	3.3-1
3.4 WOLF SC4020 PLOT PACKAGE	3.4-1

TABLE OF CONTENTS (CONT.)

	<u>PAGE</u>
4.0 NONAME DATA HANDLING SUPPORT PROGRAMS	4.0-1
4.1 DODS SORT-MERGE	4.1-1
4.2 GEOS SORT-MERGE	4.2-1
4.3 ORB1 CONVERSION (9-7 TRACK)	4.3-1
5.0 REFERENCES	5.0-1
APPENDIX A INDEX OF SUBROUTINE REFERENCES FOR NONAME PROGRAM	A-1

## GLOSSARY OF SYMBOLS

<u>Symbol</u>	<u>Description</u>	<u>Page First Used</u>
A	Matrix partition of $U_{2C} + D_r$ associated with position partials.	2.9-4
A	Matrix partition of $(B^T WB + V_A^{-1})$ associated with <u>a</u>	2.10-11
$\bar{A}_D$	Acceleration of satellite due to drag	2.8-2
$A_k$	Matrix partition of $(B^T WB + V_A^{-1})$ accounting for effects between <u>a</u> and <u>k</u>	2.10-11
$A_p$	Daily planetary geomagnetic index	2.8-51
$\bar{A}_R$	Acceleration of satellite due to solar radiation pressure	2.8-2
$A_r$	Matrix partition of A associated with the $r^{\text{th}}$ arc	2.10-13
$A_{rk}$	Matrix partition of $A_k$ associated with the $r^{\text{th}}$ arc	2.10-14
$A_s$	Cross sectional area of satellite	2.8-51
$A_z$	Azimuth of satellite (measurement type)	2.6-15
a	Semi-major axis of reference ellipsoid	2.5-3

## GLOSSARY OF SYMBOLS (Cont.)

<u>Symbol</u>	<u>Description</u>	<u>Page</u> <u>First Usd</u>
a	Semi-major axis of orbit	2.11-16
<u>a</u>	Vector of parameters associated with individual arcs, partition of <u>x</u>	2.10-9
<u><math>\bar{a}_d</math></u>	Acceleration of satellite due to a third body potential	2.8-27
$a_e$	Earth's mean equatorial radius	2.6-10
$a_p$	Three-hourly planetary geomagnetic index	2.8-44
<u><math>\bar{a}_r</math></u>	Partition of <u>a</u> associated with the $r^{\text{th}}$ arc	2.10-13
B	Matrix partition of $U_{2C} + D_r$ associated with velocity partials	2.9-4
B	Matrix of partial derivatives of computed measurements with respect to the parameters being determined	2.10-5
b	A constant measurement bias	2.6-2
$C_D$	Satellite drag factor	2.8-4
$C_R$	Satellite emissivity factor	2.8-4

## GLOSSARY OF SYMBOLS (cont.)

<u>Symbol</u>	<u>Description</u>	<u>Page</u> <u>First Used</u>
$C_a$	Matrix partition of $B^T W \underline{d_m}$ + $V_A^{-1} (\underline{x}^{(n)} - \underline{x}_A)$ associated with $\underline{a}$	2.10-11
$C_i$	Computed measurement value corresponding to $\underline{o}_i$	2.2-5
$C_i$	Coefficients of spheroid height polynomial for natural log of density, themselves polynomials in exospheric temperature	2.8-56
$C_k$	Matrix partition of $(B^T W \underline{d_m} + V_A^{-1} (\underline{x}^{(n)} - \underline{x}_A))$ associated with $\underline{k}$	2.10-11
$C_{nm}$	Gravitational harmonic coefficient of degree $n$ , order $m$	2.6-22
$C_r$	Matrix partition of $C_a$ associated with the $r^{\text{th}}$ arc	2.10-14
$C_{t+\Delta t}$	The computed observation at time $t+\Delta t$	2.6-1
$c$	Velocity of light	2.7-10
$D$	Mean elongation of the Moon from the Sun	2.3-9
$D_r$	Matrix containing $\frac{\partial \bar{A}_D}{\partial \bar{x}_t}$	2.8-8

GLOSSARY OF SYMBOLS (Cont.)

<u>Symbols</u>	<u>Description</u>	<u>Page</u> <u>First Used</u>
$d_{0_i}$	Error of observation associated with $0_i$	2.2-5
$\underline{da}$	Partition of $\underline{dx}^{(n+1)}$ associated with $\underline{a}$ (correction vector for arc parameters)	2.10-11
$\underline{da}_r$	Partition of $\underline{da}$ associated with the $r^{\text{th}}$ arc (correction vector for the $r^{\text{th}}$ arc parameters)	2.10-15
$\underline{da}_r'$	Correction vector to $r^{\text{th}}$ arc parameters not including common parameter solution effects	2.10-16
$\underline{dk}$	Partition of $\underline{dx}^{(n+1)}$ associated with the common parameters $\underline{k}$	2.10-11
$\underline{dm}$	Vector of residuals (O-C) from the $n^{\text{th}}$ approximation to $\hat{\underline{x}}$ (same as $\underline{d}_z^{(n)}$ )	2.10-8
$\underline{dx}^{(n+1)}$	Vector of corrections to the parameters $\underline{x}$	2.10-7
$\underline{d}_z^{(n)}$	Vector of residuals (O-C) from the $n^{\text{th}}$ approximation (same as $\underline{dm}$ )	2.10-7
$\dot{E}$	Eccentric anomaly of the orbit	2.11-16
$\hat{\underline{E}}$	East baseline vector in the topocentric horizon coordinate system	2.5-14

## GLOSSARY OF SYMBOLS (Cont.)

<u>Symbols</u>	<u>Description</u>	<u>Page</u> <u>First Used</u>
$E( )$	Expected value	2.11-13
$E_M$	Input multiplier for editing criterion	2.10-20
$E_R$	Weighted RMS of previous outer iteration. Input for first outer iteration	2.10-20
$E_\alpha$	Elevation of the satellite (measurement type)	2.6-15
$e$	Eccentricity of the reference ellipsoid	2.5-3
$e$	Eccentricity of the orbit	2.11-16
$\bar{e}$	Constant of integration - a vector of a magnitude equal to the eccentricity of the orbit and pointing toward perihelion	2.11-20
$F$	Mean angular distance of the Moon from the Sun	2.3-19
$F$	Matrix containing $\frac{\partial \ddot{r}}{\partial \ddot{\beta}}$ (same as $\ddot{Y}$ )	2.8-8
$F_B$	Base frequency for Doppler measurements	2.7-10
$F_M$	Measured frequency for Doppler observations	2.7-10
$F_{10.7}$	Mean of the 10.7 cm. solar flux values for a given day	2.8-45

GLOSSARY OF SYMBOLS (Cont.)

<u>Symbols</u>	<u>Description</u>	<u>Page First Used</u>
$\bar{F}_{10.7}$	Average 10.7 cm. solar flux value over 2 or 3 solar rotations	2.8-44
	Flattening of the Earth	2.5-3
	Matrix containing the direct partial derivatives of $\bar{x}_t$ with respect to $\bar{\beta}$	2.8-8
$f$	The true anomaly of the orbit	2.11-16
$f_t$	The geometric relationship defined by the observation type at time 't'.	2.6-1
$G$	The universal gravitational constant	2.6-22
$g$	Mean anomaly of the Moon	2.3-19
$g'$	Mean anomaly of the Sun	2.3-19
$H$	Hour angle of the Sun	2.8-49
$H_{alt}$	Altimeter height (measurement type)	2.6-9
$h$	Spheroid height	2.5-3
$h_s$	Hour angle of the satellite	2.7-6
$I$	Identity matrix	2.9-5
$i$	Inclination of the orbit	2.11-16

GLOSSARY OF SYMBOLS (Cont.)

<u>Symbols</u>	<u>Description</u>	<u>Page</u> <u>First Used</u>
J	Julian Ephemeris Date of desired nutation calculation	2.3-18
$J_0$	Julian Ephemeris Date corresponding to 1900 January 0.5 Ephemeris Time	2.3-18
K	Partition of $(B^T WB + V_A^{-1})$ associated with $\underline{k}$	2.10-11
$\underline{k}$	Vector of parameters common to all arcs; partition of $\underline{x}$	2.10-9
$L_j(\cdot)$	Lagrange polynomial	2.9-11
$\ell$	Direction cosine (measurement type)	2.6-13
M	Mass of the Earth	2.6-22
M	Number of parameters in $\underline{x}$	2.10-2
M	Mean anomaly of the orbit	2.11-16
m	Direction cosine (measurement type)	2.6-13
$m_d$	Mass of the disturbing body for third body perturbations	2.8-26
$m_i$	Computed equivalent of the $i^{\text{th}}$ measurement (see $C_i$ and $C_{t+\Delta t}$ )	2.10-9

## GLOSSARY OF SYMBOLS (Cont.)

<u>Symbols</u>	<u>Description</u>	<u>Page Used First</u>
$m_s$	Mass of the satellite	2.8-28
$N$	Number of observations in $\underline{z}$	2.10-2
$\hat{\mathbf{n}}$	North baseline unit vector in the topocentric horizon coordinate system	2.5-14
$n$	Direction cosine (measurement type)	2.6-13
$n_s$	Surface index of refraction	2.7-8
$o_i$	The $i^{\text{th}}$ observed measurement value	2.2-5
$\bar{\mathbf{P}}$	Vector of parameters to be determined (same as $\underline{x}$ )	2.2-5
$P(t)$	Hermite polynomial	2.9-10
$P_a$	Parallactic angle	2.7-6
$P_m^n$ ( )	Legendre polynomial	2.6-22
$P_s$	Solar radiation pressure in the vicinity of the Earth	2.8-28
$p(\underline{x})$	Joint probability density function for $\underline{x}$	2.10-2
$p(\underline{z})$	Joint probability density function for $\underline{z}$	2.10-2

GLOSSARY OF SYMBOLS (Cont.)

<u>Symbols</u>	<u>Description</u>	<u>Page First Used</u>
$p(\underline{x} \underline{z})$	Joint conditional probability density function for $\underline{x}$ , given that $\underline{z}$ has occurred	2.10-2
$p(\underline{z} \underline{x})$	Joint conditional probability density function for $\underline{z}$ given that $\underline{x}$ has occurred	2.10-2
$R_d$	Third body disturbing potential	2.8-26
$R_i$	Residual value ( $dm_i$ )	2.11-12
$\bar{r}$	Geocentric satellite position vector	2.5-11
$\bar{r}_d$	True of date position vector of third body for third body gravitational effects	2.8-26
$r_{ij}$	Aitken-Neville factors for integrator starting scheme	2.9-9
$\bar{r}_{ob}$	Geocentric position vector of a tracking station	2.2-8
$\hat{r}_s$	True of date unit vector pointing to the Sun	2.8-28
$S$	The cosine of the enclosed angle between $\bar{r}$ and $\bar{r}_d$	2.8-26

GLOSSARY OF SYMBOLS (Cont.)

<u>Symbols</u>	<u>Description</u>	<u>Page First Used</u>
$S_{nm}$	Gravitational harmonic coefficient of degree $n$ , order $m$	2.8-4
$s^2$	Sample variance	2.11-13
$T$	Exospheric temperature	2.8-48
$T_0$	Global nighttime minimum temperature corrected for semi-annual variation	2.8-46
$T'_0$	Global nighttime minimum temperature for a given day	2.8-45
$\bar{T}_0$	Average global nighttime minimum temperature for a given period	2.8-44
$U$	Geopotential field of the Earth	2.6-22
$U_{2C}$	Matrix containing the second partial derivatives of the gravitational potentials with respect to the true of date position coordinates	2.8-8
$u$	Central angle between the satellite vector and a vector pointing toward the ascending node of the orbit	2.11-21
$\hat{u}$	Unit vector in the direction of $\bar{\rho}$	2.6-8
$V$	Covariance matrix of $\hat{x}$	2.10-6

GLOSSARY OF SYMBOLS (Cont.)

<u>Symbols</u>	<u>Description</u>	<u>Page</u> <u>First Used</u>
$V_A$	$\underline{\text{a priori}}$ covariance matrix associated with $\bar{x}_A$ ; same as $\Sigma_A^{-1}$	2.10-8
$V_a$	Matrix partition of $V_A$ ; $\underline{\text{a priori}}$ covariance matrix associated with $\underline{a}$	2.10-10
$V_k$	Matrix partition of $V_A$ ; $\underline{\text{a priori}}$ covariance matrix associated with $\underline{k}$	2.10-10
$V_r$	Matrix partition of $V_a$ associated with the $r^{\text{th}}$ arc	2.10-13
$W$	Weighting matrix for observations; same as $\Sigma_z^{-1}$	2.10-8
$X$	Coordinate system direction:	2.2-4
	a) Direction in the equatorial plane pointing toward the Greenwich meridian (Earth-fixed system)	
	b) In the direction of the true equinox of date at $0^{\text{h}} 0^{\text{m}}$ of the epoch day (inertial system)	
	c) In the direction of the true equinox of date (true of date system)	
$X(t)$	Position, velocity, and variational partials at time $t$	2.9-10

GLOSSARY OF SYMBOLS (Cont.)

<u>Symbols</u>	<u>Description</u>	<u>Page</u> <u>First Use</u>
$x^{(i)}(t)$	$i^{\text{th}}$ derivative of $X(t)$	2.9-10
$X_a$	The $X$ angle of the satellite (measurement type)	2.6-15
$X_e$	Earth-fixed position component	2.3-3
$X_i$	True of date position component	2.3-3
$X_m$	Matrix containing the variational partials	2.8-8
$x$	True of date $X$ position component of the satellite	2.2-8
$\chi$	Rotation angle for polar motion	2.5-22
$\underline{x}$	Vector of $M$ parameters	2.10-2
$\hat{\underline{x}}$	The "best" estimate of $\underline{x}$	2.10-3
$\hat{\underline{x}}^{(n)}$	The $n^{\text{th}}$ approximation to $\hat{\underline{x}}$	2.10-3
$\underline{x}_A$	The <u>a priori</u> estimate of $\underline{x}$	2.10-3
$\bar{\underline{x}}_t$	The vector describing the true of date position and velocity of the satellite	2.2-8

GLOSSARY OF SYMBOLS (Cont.)

<u>Symbols</u>	<u>Description</u>	<u>Page First Used</u>
Y	Coordinate system direction (associated with the X and Z directions)	2.2-4
Y	Partition of $X_m$ ; a matrix containing $\frac{\partial \dot{r}}{\partial \beta}$	2.9-4
Y	Partition of $X_m$ ; a matrix containing $\frac{\partial \dot{r}}{\partial \beta}$	2.9-4
Y	Matrix containing $\frac{\partial \ddot{r}}{\partial \beta}$ ; same as matrix F	2.9-4
$Y_a$	The Y angle of the satellite (measurement type)	2.6-13
$Y_e$	Earth-fixed position component	2.3-3
$Y_i$	True of date position component	2.3-3
y	True of date Y position component of the satellite	2.2-8
y	Rotation angle for polar motion	2.5-22
z	Direction of the spin axis of the Earth for Z direction of coordinate systems. (Taken at o. <sup>h</sup> o of epoch day for inertial coordinate system.) Compare X	2.2-3

GLOSSARY OF SYMBOLS (Cont.)

<u>Symbols</u>	<u>Description</u>	<u>Page</u> <u>First Used</u>
$\hat{z}$	The zenith baseline unit vector in the topocentric horizon coordinate system	2.5-14
$z_e$	Earth-fixed component; same as $z$	2.5-6
$z_o$	Observed zenith angle	
$z$	True of date $Z$ position coordinate of the satellite	2.2-8
$\zeta$	A precession angle	2.3-14
$\underline{z}$	A vector of $N$ independent observations	2.10-2

## GLOSSARY OF SYMBOLS (Cont.)

<u>Symbols</u>	<u>Description</u>	<u>Page</u> <u>First Used</u>
$\alpha$	Topocentric right ascension of the satellite (measurement, type)	2.6-11
$\bar{\alpha}$	The set of parameters not affecting the dynamics of satellite motion	2.2-7
$\bar{\beta}$	The set of parameters affecting the dynamics of satellite motion	2.2-7
$\beta_{qp}, \beta_{qp}^*$ $\gamma_{qp}, \gamma_{qp}^*$	Cowell integration scheme coefficients	2.9-2
$\Delta\ell$	Correction to measurement of direction cosine $\ell$	2.7-9
$\Delta m$	Correction to measurement of direction cosine $m$	2.7-9
$\Delta R$	Differential refraction	2.7-7
$\Delta T$	Geomagnetic heating correction to $T$	2.8-50
$\Delta t$	Measurement timing bias	2.6-2
$\Delta X_a$	Correction to measured X angle	2.7-10
$\Delta Y_a$	Correction to measured Y angle	2.7-10

GLOSSARY OF SYMBOLS (Cont.)

<u>Symbols</u>	<u>Description</u>	<u>Page First Used</u>
$\Delta\alpha$	Equation of the equinoxes	2.3-7
$\Delta\alpha$	Right ascension measurement correction	2.7-5
$\Delta\delta$	Declination measurement correction	2.7-5
$\Delta\epsilon$	Nutation in obliquity	2.3-19
$\Delta\rho$	Correction to range measurement	2.7-4
$\Delta\psi$	Nutation in longitude	2.3-16
$\delta$	Topocentric declination of satellite (measurement type)	2.6-11
$\delta_{\odot}$	Declination of the Sun	2.8-49
$\epsilon_T$	True obliquity of date	2.3-16
$\epsilon_M$	Mean obliquity of date	2.3-16
$\zeta$	Precession angle	2.3-14
$\theta$	Precession angle	2.3-14
$\theta_g$	Greenwich hour angle	2.2-4
$\lambda$	East longitude	2.5-2
$\mu_c$	Mean of residuals	2.11-12

GLOSSARY OF SYMBOLS (Cont.)

<u>Symbols</u>	<u>Description</u>	<u>Page First Used</u>
$v$	Satellite eclipse factor	2.8-28
$\bar{p}$	The station-satellite vector	2.6-8
$\rho_D$	Atmospheric density at the satellite position	2.8-30
$\rho_s$	Specular reflectivity of the satellite	2.8-29
$\Sigma_A$	<u>a priori</u> covariance matrix associated with the <u>a priori</u> parameter vector $\underline{x}_A$	2.10-4
$\Sigma_z$	Covariance matrix associated with the observations $\underline{z}$	2.10-5
$\sigma$	Standard deviation	2.11-13
$\underline{\sigma}$	Vector of noise on the observations $\underline{z}$	2.10-2
$\phi$	Geodetic latitude	2.5-2
$\phi'$	Geodetic longitude	2.5-2
$\Omega$	Longitude of the ascending node of the Moon's orbit	2.3-19
$\Omega$	Longitude of the ascending node of a satellite orbit	2.11-16
$\omega$	Argument of perigee of a satellite orbit	2.11-16

SECTION 1.0  
INTRODUCTION TO THE  
NONAME ORBIT DETERMINATION SYSTEM

The NONAME Orbit Determination and Geodetic Parameter Estimation System consists of a set of computer programs designed to determine and analyze definitive satellite orbits and their associated geodetic and measurement parameters.

The heart of the system is the NONAME program itself, which possesses the capability of estimating that set of orbital elements, station positions, measurement biases, and a set of force model parameters such that the orbital tracking data from multiple arcs of multiple satellites best fits the entire set of estimated parameters. In any given run, little or all of this capability may be exercised according to the type of orbit, the amount and type of data available, and the purpose for which the run is being made.

NONAME ancillary analysis programs may be grouped into three different categories according to the function which they perform:

1: Orbit Comparisons

The DELTA program performs the function of differencing satellite orbits and transforming the differences in position and velocity into the more physically meaningful along track, cross track, and radial components. This program is useful for

comparing orbits generated using different data sets, using different gravity models, using different modes of data reduction, etc.

2. Data Analysis using Reference Orbits

The GEORGE program is used to analyze residuals from measurements not used in an orbita solution, but computed on the basis of a reference orbit determined by measurements of known quality. Measurement biases and timing errors are computed on a pass by pass basis. The results of this analysis may be given different interpretations, depending upon the quality of the unweighted data and the quality of the reference orbit.

3. Pass Geometry Computation

The GROUND TRACK program plots the sub-satellite points of orbits at station mea-surcment times. A graph is produced for each station giving the total geometric coverage achieved during a spccified data period.

All the above three programs use one or more tapes written by the NONAME program in either a data reduction or orbit generator run. Although it is not necessary, these programs are generally run immediately following the associated NONAME run, thus minimizing tape handling problems. In addition all three programs usc the WRDC PLOT PACKAGE and can produce a graphical depiction of their results both on printer plots and on SC4020 micro-film or hardcopy plots.

In addition to the above analysis programs, the NONAME System contains three data management routines:

1. SORT-MERGE Programs

a. NGSP Format

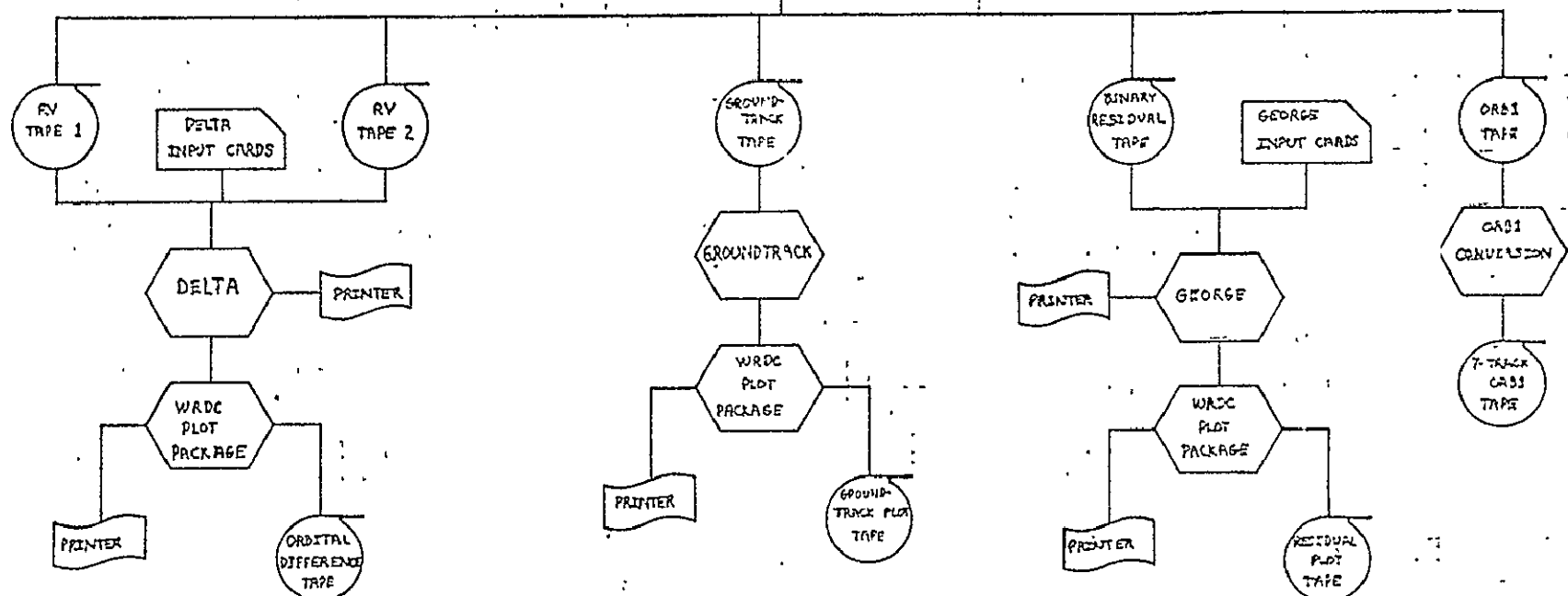
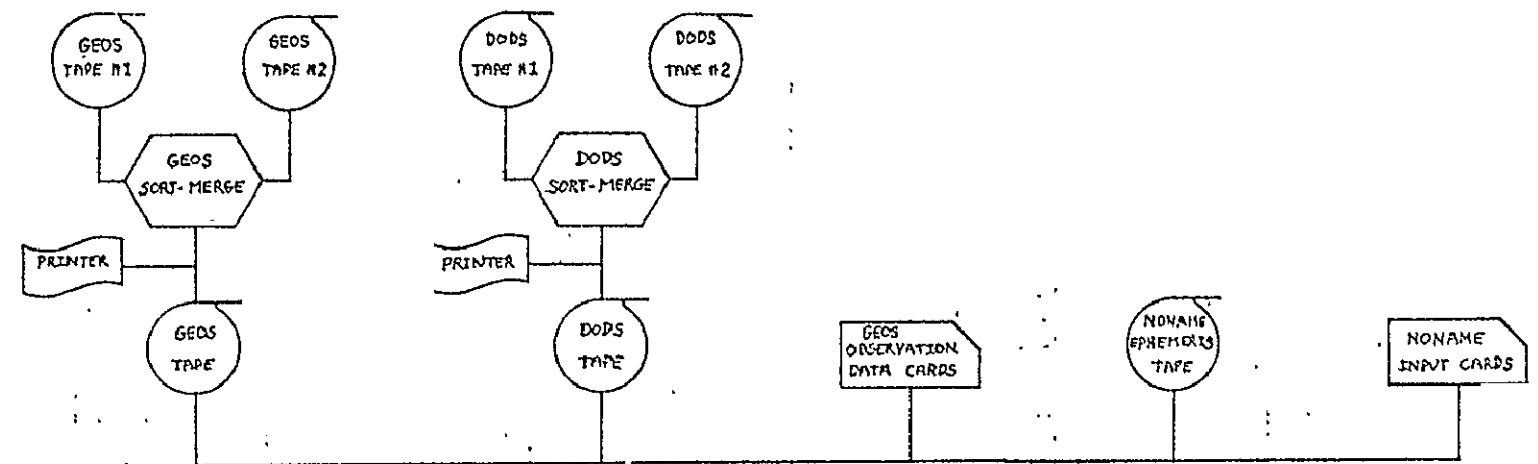
b. DODS Format

There are two programs for merging multiple data tapes, which may not be in time order, and producing a single tape with the data in time order. These two programs differ only in the format of the data tapes.

2. 9-7 TRACK Conversion Program

This program converts a 9-track ORB1 tape written by the IBM System 360 computers into a 7-track tape which can be read by the GSFC 7094 computer.

1.0-4



NOT REPRODUCIBLE

NONAME SYSTEM FLOWCHART

## SECTION 2.0

### THE NONAME PROGRAM

The original version of the NONAME Program was written for GSFC by WOLF in 1967. Since that time NONAME has undergone extensive development to enhance its capability, accuracy, and versatility.

NONAME has become one of the most widely used orbit and geodetic parameter estimation programs in the world. It is currently operational at GSFC on the IBM 360 '95, '91, and '75; at the Goddard Institute for Space Studies in New York on an IBM 360 '95; at Wallops Island on the GE 625; and at the Institut für Physik und Plasmaphysik, Garching, West Germany on an IBM 360 '91.

NONAME has been used for

- determination of definitive orbits
- tracking instrument calibration
- satellite operational predictions
- geodetic parameter estimation

and many other items relating to applied research in satellite geodesy using virtually all types of satellite tracking data.

## SECTION 2.1

### INTRODUCTION TO THE NONAME PROGRAM

The NONAME Program is an orbit and geodetic parameter estimation program utilizing the Bayesian least squares process for determining the set of parameters which makes the measurements most consistent with the satellite orbits. Multiple arcs of multiple satellites may be used in a simultaneous solution when adjustments are desired for geodetic parameters.

The NONAME Program is designed around the concept that the determination of definitive satellite orbits will be affected by small errors from three different sources: measurement errors (biases, etc.), station position errors, and force model errors. Accordingly, the program has the capability of adjusting these types of parameters along with the satellite orbital elements. In general, this process leads to an improved orbit and improved values for the measurement and geodetic parameters.

The parameter adjustment features of NONAME provide a large number of options and thus great flexibility in the use of the program. The manner in which independent parameters are assigned is based upon the physical and statistical independence expected, with some latitude left to the user for certain parameters. The types of parameters, along with limitations (through program dimensioning) on the number of each are:

A. Individual arc parameters.

1. Orbit elements - one set of six for each arc which must always be adjusted (a priori information can be used to effectively constrain them if no adjustment is desired).
2. Measurement biases - limit of 50, optionally applied with assignments normally made on a pass by pass basis. The same bias may be applied for any period of time up to the length of the arc.
3. Station timing errors - same as for measurement biases. The limit of 50 applies to the sum of measurement and timing biases.
4. Atmospheric drag coefficient - optionally, one drag coefficient per arc may be adjusted.
5. Solar radiation pressure reflectivity - optionally, one reflectivity parameter may be adjusted.

B. Parameters common to all arcs

1. Station positions - optionally, up to 21 independent stations may be adjusted. In addition, any number of stations in the tracking complement may be constrained to move with a fixed relative location to one of the independent stations.

2. Geopotential coefficients - limit of 20, with the adjustment of any coefficient whose degree is less than or equal to the maximum degree coefficient used in the orbit integration.

In addition to the above restrictions, the following overall parameter limitations must be observed:

1. The total number of adjusted parameters affecting any one arc may not exceed 70.
2. The total number of force model parameters affecting any one arc may not exceed 20.

The NONAME program is configured to iterate on the adjustment of orbital elements with fixed station positions and geopotential model. After this iteration process has converged, the common parameters of station positions and geopotential parameters are adjusted and the process is repeated.

Many features are designed into NONAME to facilitate ease of usage and to assist in interpretation of the results. These features are discussed as a part of the detailed program description in this volume and in the Operations Manual.

SECTION 2.2  
THE ORBIT AND GEODETIC PARAMETER ESTIMATION PROBLEM

The purpose of this section is to provide an understanding of the relationship between the various elements in the solution to the orbit and geodetic parameter estimation problem. As such, it is a general statement of the problem and serves to coordinate the detailed solutions to each element in the problem presented in the sections which follow.

The problem is divided into two parts:

- the orbit prediction problem, and
- the parameter estimation problem.

The solution to the first of these problems corresponds to NONAME's orbit generation mode. The solution to the latter corresponds to NONAME's data reduction mode and of course is based on the solution to the former.

The reader should note that there are two key choices which dramatically affect the NONAME solution structure:

- Cowell's method for integrating the orbit, and
- a Bayesian least squares statistical estimation procedure for the parameter estimation problem.

### 2.2.1 The Orbit Prediction Problem

There are a number of approaches to orbit prediction. The NONAME approach is to use Cowell's method, which is the direct numerical integration of the satellite equations of motion in rectangular coordinates. The initial conditions for these differential equations are the epoch position and velocity; the accelerations of the satellite must be evaluated.

The acceleration producing forces which are currently modelled in NONAME are the effects of

- the geopotential,
- the luni-solar potentials,
- radiation pressure, and
- atmospheric drag

Perhaps the most outstanding common feature of these forces is that they are functions of the position of the satellite relative to either the Earth, Sun, or Moon. Only atmospheric drag is a function of any additional quantity,\* specifically, the relative velocity of the satellite with respect to the atmosphere.

The accurate evaluation of the acceleration of a satellite therefore involves the solution to two concomitant problems:

\*Not to be confused with the "fixed" parameters in the models.

- the accurate modeling of each force on the satellite - Earth - Sun - Moon relationship, and
- the precise modeling of the motions of the Earth, Sun, and Moon.

The specific details for each model in these solutions are given elsewhere in Sections 2.3, 2.4, and 2.8. The question of how these models fit together is in effect the question of appropriate coordinate systems.

The key factor in the selection of coordinate systems for the satellite orbit prediction problem is the motion of the Earth. For the purposes of NONAME, this motion consists of:

- precession and nutation, and
- rotation.

We are considering here the motion of the solid body of the Earth, as versus the slippage in the Earth's crust (polar motion) which just affects the position of the observer.

The precession and nutation define the variation in

- the direction of the spin axis of the Earth (+ Z), and

- the direction of the true equinox of date (+ X).

These directions define the (geocentric) true of date coordinate system.

The rotation rate of the Earth is the time rate of change of the Greenwich hour angle  $\theta_g$  between the Greenwich meridian and the true equinox of date. Thus the Earth-fixed system differs from the true of date system according to the rotation angle  $\theta_g$ .

The equations of motion for the satellite must be integrated in an inertial coordinate system. The NONAME inertial system is defined as the true of date system corresponding to 0<sup>h</sup>0 of the day of epoch.

The coordinate systems in which the accelerations due to each physical effect are evaluated should be noted. The geopotential effects are evaluated in the Earth-fixed system, and then transformed to true of date to be combined with the other effects. The others are evaluated in the true of date system. The total acceleration is then transformed to the inertial system for use in the integration procedure.

The integration procedure used in NONAME is a predictor-corrector type with a fixed time step. There is an optional variable step procedure which will halve or double the step size. As the integration algorithms used provide for output on an even step, an interpolation procedure is required.

### 2.2.2 The Parameter Estimation Problem

Let us consider the relationships between the observations  $O_i$ , their corresponding computed values  $C_i$  and  $\bar{P}$ , the vector of parameters to be determined. These relationships are given by

$$O_i - C_i = \sum_j \frac{\partial C_i}{\partial P_j} dP_j + dO_i \quad (1)$$

where

$i$  denotes the  $i^{\text{th}}$  observation or association with it,

$dP_j$  is the correction to the  $j^{\text{th}}$  parameter, and

$dO_i$  is the error of observation associated with the  $i^{\text{th}}$  observation.

The basic problem of parameter estimation is to determine a solution to these equations.

The role of data preprocessing is quite apparent from these equations. First, the observation and its computed equivalent must be in a common time and spatial reference system. Second, there are certain physical effects such as atmospheric refraction which do not significantly vary by any likely change in the parameters represented by  $\bar{P}$ .

These computations and corrections may equally well be applied to the observations as to their computed

values. Furthermore, the relationship between the computed value and the model parameters  $\bar{P}$  is, in general, nonlinear, and hence the computed values may have to be evaluated several times in the estimation procedure. Thus a considerable increase in computational efficiency may be attained by applying these computations and corrections to the observations; i.e., to preprocess the data.

The preprocessed observations used by NONAME are directly related to the position and/or velocity of the satellite relative to the observer at the given observation time. These relationships are geometric, hence computed equivalents for these observations are obtained by applying these geometric relationships to the computed values for the positions and velocities of the satellite and the observer at the desired time.

Associated with each measurement from each observing station is a (known) statistical uncertainty. This uncertainty is a statistical property of the noise on the observations. This uncertainty is the reason a statistical estimation procedure is required for the NONAME parameter determination.

It should be noted that  $d_{0_i}$ , the measurement error, is not the same as the noise on the observations. The  $d_{0_i}$  account for all of the discrepancy  $(0_i - C_i)$  which is not accounted for by the corrections to the parameters  $\bar{P}$ . These  $d_{0_i}$  represent both

- the contribution from the noise on the observation, and
- the incompleteness of the mathematical model represented by the parameters  $\bar{P}$ .

By this last we mean either that the parameter set being determined is insufficient or that the functional form of the model is inadequate.

NONAME has two different ways of dealing with these errors of observation:

1. The measurement model includes both a constant bias and a timing bias which may be determined.
2. There is an automatic editing procedure to delete bad (statistically unlikely) measurements.

The nature of the parameters to be determined has a significant effect on the functional structure of the solution. In NONAME, these parameters are:

- the position and velocity of the satellite at epoch. These are the initial conditions for the equations of motion.
- force model parameters. These affect the motion of the satellite.
- station positions and biases for station measurement types. These do not affect the motion of the satellite.

Thus, the parameters to be determined are implicitly partitioned into a set  $\bar{\alpha}$ , which are not concerned with the dynamics of the satellite motion and a set  $\bar{\beta}$  which are.

The computed value  $C_i$  for each observation  $O_i$  is a function of  $\bar{r}_{ob}$ ,  $\bar{x}_t$ , and  $\bar{B}$ .

$\bar{r}_{ob}$ : the Earth-fixed position vector of the station, and

$\bar{x}_t$ : the true of date position and velocity vector of the satellite  $\{x, y, z, \dot{x}, \dot{y}, \dot{z}\}$

at the desired observation time. When measurement biases are used,  $C_i$  is also a function of  $\bar{B}$ , the biases associated with the particular station measurement type.

Let us consider the effect of the given partitioning on the required partial derivatives in the observational equations. The  $\frac{\partial C_i}{\partial P}$  become

$$\frac{\partial C_i}{\partial \alpha} = \left\{ \frac{\partial C_i}{\partial \bar{r}_{ob}}, \frac{\partial C_i}{\partial \bar{B}} \right\} \quad (2)$$

$$\frac{\partial C_i}{\partial \beta} = \frac{\partial C_i}{\partial \bar{x}_t} \frac{\partial \bar{x}_t}{\partial \beta} \quad (3)$$

The partial derivatives  $\frac{\partial \bar{x}_t}{\partial \beta}$  are called the variational partials. While the other partial derivatives on the right-hand side of the equations above are computed from the measurement model at the given time, the variational partials must be obtained by integrating the variational equations. As will be shown in Section 2.8, these equations are similar to the equations of motion.

The need for the above mentioned variational partials obviously has a dramatic effect on any solution to the observational equations. In addition to integrating the equations of motion to generate an orbit, the solution requires that the variational equations be integrated.

We have heretofore discussed the elements of the observational equations; we shall now discuss the solution of these equations; i.e., the statistical estimation scheme.

There are a number of estimation schemes that can be used. The method used in NONAME is a batch scheme that uses all observations simultaneously to estimate the parameter set. The alternative would be a sequential scheme that uses the observations sequentially to calculate an updated set of parameters from each additional observation. Although batch and sequential schemes are essentially equivalent, practical numerical problems often occur with sequential schemes, especially when processing highly accurate observations. Therefore, a batch scheme was chosen.

The particular method selected for NONAME is a partitioned Bayesian least squares method as detailed in Section 2.10. A Bayesian method was selected because such a scheme utilizes meaningful a priori information. The partitioning is such that the arrays which must be simultaneously in core are arrays associated with parameters common to all satellite arcs, and arrays pertaining to the arc being processed. Its purpose is to dramatically reduce the core storage requirements of the program without any significant cost in computation time.

There is an interesting aside related to the use of a priori information in practice. The use of a priori information for the parameters guarantees that the estimation procedure will mechanically operate (but not necessarily converge). The user must ensure that his data contains information relating to the parameters he wishes determined.

## SECTION 2.3

### THE MOTION OF THE EARTH AND RELATED COORDINATE SYSTEMS

The major factor in satellite dynamics is the gravitational attraction of the Earth. Because of the (usual) closeness of the satellite and its primary, the Earth cannot be considered a point mass, and hence any model for the dynamics must contain at least an implicit mass distribution. The concern of this section is the motion of this mass distribution and its relation to coordinate systems.

We will first consider the meaning of this motion of the Earth in terms of the requisite coordinate systems for the orbit prediction problem.

The choice of appropriate coordinate systems is controlled by several factors:

- In the case of a satellite moving in the Earth's gravitational field, the most suitable reference system for orbit computation is a system with its origin at the Earth's center of mass, referred to as a geocentric reference system.
- The satellite equations of motion must be integrated in an inertial coordinate system.
- The Earth is rotating at a rate  $\dot{\theta}_g$ , which is the time rate of change of the Greenwich hour angle. This angle is the hour angle of the true equinox of date with respect to the Greenwich meridian as measured in the equatorial plane.

- The Earth both precesses and nutates, thus changing the directions of both the Earth's spin axis and the true equinox of date in inertial space.

The motions of the Earth referred to here are of course those of the "solid body" of the Earth, the motion of the primary mass distribution. The slippage of the Earth's crust is considered elsewhere in Section 2.5.4 (polar motion).

### 2.3.1 The True of Date Coordinate System

Let us consider that at any given time, the spin axis of the Earth (+ Z) and the direction of the true equinox of date (+ X) may be used to define a right-handed geocentric coordinate system. This system is known as the true of date coordinate system. The coordinate systems of NONAME will be defined in terms of this system.

### 2.3.2 The Inertial Coordinate System

The inertial coordinate system of NONAME is the true of date coordinate system defined at  $0^h 0^m$  of the epoch day for each satellite. This is the system in which the satellite equations of motion are integrated.

This is a right-handed, Cartesian, geocentric coordinate system with the X axis directed along the true equinox of  $0^h 0^m$  of the epoch day and with the Z axis directed along the Earth's spin axis toward north at the same time. The Y axis is of course defined so that the coordinate system is orthogonal.

It should be noted that the inertial system differs from the true of date system by the variation in time of the directions of the Earth's spin axis and the true equinox of date. This variation is described by the effects of precession and nutation.

### 2.3.3 The Earth-fixed Coordinate System

The Earth-fixed coordinate system is geocentric, with the Z axis pointing north along the axis of rotation and with the X axis in the equatorial plane pointing toward the Greenwich meridian. The system is orthogonal and right-handed; thus the Y axis is automatically defined.

This system is rotating with respect to the true of date coordinate system. The Z axis, the spin axis of the Earth, is common to both systems. The rotation rate is equal to the Earth's angular velocity. Consequently, the hour angle  $\theta_g$  of the true equinox of date with respect to the Greenwich meridian (measured westward in the equatorial plane) is changing at a rate  $\dot{\theta}_g$  equal to the angular velocity of the Earth.

### 2.3.4 Transformation Between Earth-fixed and True of Date Coordinates

The transformation between Earth-fixed and true of date coordinates is a simple rotation. The Z axis is common to both systems. The angle between  $x_i$ , the true of date X component vector, and  $x_e$ , the Earth-fixed component vector, is  $\theta_g$ , the Greenwich hour angle. The Y component vectors are similarly related. These transformations for  $x_e$ ,  $y_e$ ,  $x_i$ ,  $y_i$  which are accomplished in

XEFIX  
YEFIX  
XINERT  
YINERT  
GRIIRAN

NONAME by the functions XEFIX, YEFIX, XINERT, and YINERT      GRHRAN  
are:

$$\bullet \quad X_c = X_i \cos \theta_g + Y_i \sin \theta_g \quad \text{XEFIX}$$

$$\bullet \quad Y_c = X_i \sin \theta_g + Y_i \cos \theta_g \quad \text{YEFIX}$$

$$\bullet \quad X_i = X_e \cos \theta_g - Y_e \sin \theta_g \quad \text{XINERT}$$

$$\bullet \quad Y_i = X_e \sin \theta_g + Y_e \cos \theta_g \quad \text{YINERT}$$

The transformation of velocities requires taking into account the rotational velocity,  $\theta_g$ , of the Earth-fixed system with respect to the true of date reference frame. The following relationships should be noted:

$$\frac{\partial X_e}{\partial \theta_g} = Y_e \quad \frac{\partial Y_c}{\partial \theta_g} = -X_e \quad (1)$$

$$\frac{\partial X_i}{\partial \theta_g} = -Y_i \quad \frac{\partial Y_i}{\partial \theta_g} = X_i \quad (2)$$

The velocity transformations are then

OBS DOT

PREDICT

$$\dot{X}_e = [\dot{X}_i \cos \theta_g + \dot{Y}_i \sin \theta_g] + \dot{Y}_c \dot{\theta}_g$$

$$\dot{Y}_e = [-\dot{X}_i \sin \theta_g + \dot{Y}_i \cos \theta_g] - \dot{X}_c \dot{\theta}_g$$

$$\dot{X}_i = [\dot{X}_e \cos \theta_g - \dot{Y}_e \sin \theta_g] - \dot{Y}_i \dot{\theta}_g$$

$$\dot{Y}_i = [\dot{X}_e \sin \theta_g + \dot{Y}_e \cos \theta_g] + \dot{X}_i \dot{\theta}_g$$

The brackets denote the part of each transform which is a transformation identical to its coordinate equivalent.

These same transformations are used in the transformation of partial derivatives from the Earth-fixed system to true of date. For the  $k^{\text{th}}$  measurement,  $C_k$ , the partial derivative transformations are explicitly:

PREDICT

$$\frac{\partial C_k}{\partial X_i} = \left[ \frac{\partial C_k}{\partial X_e} \cos \theta_g - \frac{\partial C_k}{\partial Y_e} \sin \theta_g \right] \quad (3)$$

$$+ \left[ \frac{\partial C_k}{\partial X_e} \sin \theta_g - \frac{\partial C_k}{\partial Y_e} \cos \theta_g \right] \dot{\theta}_g$$

$$\frac{\partial C_k}{\partial Y_i} = \left[ \frac{\partial C_k}{\partial X_e} \sin \theta_g + \frac{\partial C_k}{\partial Y_e} \cos \theta_g \right] . \quad (4)$$

$$+ \left[ \frac{\partial C_k}{\partial X_e} \cos \theta_g - \frac{\partial C_k}{\partial Y_e} \sin \theta_g \right] \dot{\theta}_g$$

$$\frac{\partial C_k}{\partial X_i} = \left[ \frac{\partial C_k}{\partial X_e} \cos \theta_g - \frac{\partial C_k}{\partial Y_e} \sin \theta_g \right] \quad (5)$$

$$\frac{\partial C_k}{\partial Y_i} = \left[ \frac{\partial C_k}{\partial X_e} \sin \theta_g + \frac{\partial C_k}{\partial Y_e} \cos \theta_g \right] \quad (6)$$

The brackets have the same meaning as before.

These above transforms are used or computed using the functions XEFIX, YEFIX, XINERT, or YINERT in three NONAME subroutines: GRIIRAN, OBSDOT, and PREDCT.

XEFIX

YEFIX

XINERT

YINERT

GRIIRAN

OBSDOT

PREDCT

### 2.3.5 Computation of $\theta_g$

The computation of the Greenwich hour angle is quite important because it provides the orientation of the Earth relative to the true of date system. The additional effects; i.e., to transform from true of date to inertial, of precession and nutation are sufficiently small that early orbit analysis programs neglected them. Thus, this angle is the major variable in relating the Earth-fixed system to the inertial reference frame in which the satellite equations of motion are integrated.

GRIIRAN

F

The evaluation of  $\theta_g$  is discussed in detail in the Explanatory Supplement, Reference 1.  $\theta_g$  is computed in subroutines GRIRAN and F from the expression:

GRIRAN  
F

$$\theta_g = \theta_{g_0} + \Delta t_1 \dot{\theta}_1 + \Delta t_2 \dot{\theta}_2 + \Delta\alpha \quad (1)$$

where

$\Delta t_1$  is the integer number of days since January 0.0 of the reference year,

$\Delta t_2$  is the fractional part of a day for the time of interest,

$\theta_{g_0}$  is the Greenwich hour angle on January 0.0 of the reference year,

$\dot{\theta}_1$  is the mean advance of the Greenwich hour angle per mean solar day,

$\dot{\theta}_2$  is the mean daily rate of advance of Greenwich hour angle ( $2\pi + \dot{\theta}_1$ ), and

$\Delta\alpha$  is the equation of equinoxes (nutation in right ascension).

The initial  $\theta_g$  is obtained from a table of values containing the  $\theta_{g_0}$  Greenwich hour angle on January 0.0 for each year. This table is in Common Block CGEOS and is accessed in JANTHG.

JANTHG

The equation of equinoxes,  $\Delta\alpha$ , is obtained from subroutine EPHEM, which calculates the quantity from the ephemeris tape data according to the Everett fifth-order interpolation scheme used for the lunar and solar ephemerides.

GRIHAN  
F  
EPHEM

### 2.3.6 Precession and Nutation

EQN  
EQUATR  
NUTATE  
PRECES  
REFCOR

The inertial coordinate system of NONAME, in which the equations of motion are integrated, is defined by the true equator and equinox of date for 0<sup>h</sup>0 of the day of epoch. However, the Earth-fixed coordinate system is related to the true equator and equinox of date at any given instant. Thus, it is necessary to consider the effects which change the orientation in space of the equatorial plane and the ecliptic plane.

These phenomena are

- the combined gravitational effect of the moon and the sun on the Earth's equatorial bulge, and
- the effect of the gravitational pulls of the various planets on the Earth's orbit.

The first of these affects the orientation of the equatorial plane; the second affects the orientation of the ecliptic plane. Both affect the relationship between the inertial and Earth-fixed reference systems of NONAME.

The effect of these phenomena is to cause precession and nutation, both for the spin axis of the Earth and for the ecliptic pole. This precession and nutation provides the relationship between the inertial system defined by the true equator and equinox of date for epoch and the "instantaneous" inertial system defined by the true equator and equinox of date at any

given instant. Let us consider the effect of each of these phenomena in greater detail.

EQN  
EQUATR  
NUTATE  
PRECES  
REFCOR

The luni-solar effects cause the Earth's axis of rotation to precess and nutate about the ecliptic pole. This precession will not affect the angle between the equatorial plane and the ecliptic (the "obliquity of the ecliptic") but will affect the position of the equinox in the ecliptic plane. Thus the effect of luni-solar precession is entirely in celestial longitude. The nutation will affect both, consequently we have nutation in longitude and nutation in obliquity.

The effect of the planets on the Earth's orbit will cause both secular and periodic deviations. However, the ecliptic is defined to be the mean plane of the Earth's orbit. Periodic effects are not considered to be a change in the orientation of the ecliptic; they are considered to be a perturbation of the Earth's celestial latitude. (See Reference 1.)

The secular effect of the planets on the ecliptic plane is separated into two parts: planetary precession and a secular change in obliquity. The effect of planetary precession is entirely in right ascension.

In summary, the secular effects on the orientations of the equatorial plane are:

- lunisolar precession, EQN
- planetary precession, and EQUATR
- a secular change in obliquity. NUTATE

PRECES

REFCOR

As is the convention, all of these secular effects are considered under the heading, "precession." The periodic effects are

- nutation in longitude, and
- nutation in obliquity.

In terms of the NONAME system, subroutine PRECES determines the secular effects; i.e., the rotation matrix which will transform coordinates from the mean equator and equinox of date to the mean equator and equinox of 1950.0.

PRECES

Subroutine NUTATE determines the rotation matrix to transform from true equator and equinox of date to mean equator and equinox of date. This accounts for the periodic effects.

NUTATE

NONAME has two different routines for transforming from one epoch to another. These are EQUATR and REFCOR. Both will take either mean or true coordinate input and output in mean or true coordinates as requested. The same general algorithm is used in both:

EQUATR  
REFCOR

- Rotate from true to mean equator and equinox of input date if required.

- Rotate from mean of input date to mean of 1950.0.
- Rotate from mean of 1950.0 to mean of output date.
- Rotate from mean to true of output date if required.

EQUATR  
REFCOR

All of these rotations are of course done with rotation matrices.

Subroutine REFCOR will transform between any time of day and  $0^h$  on a given reference day. This reference day and time are the epoch of the inertial coordinate system of NONAME. It performs this transform by interpolating linearly between the rotation matrices for the day of the input and that day plus one.

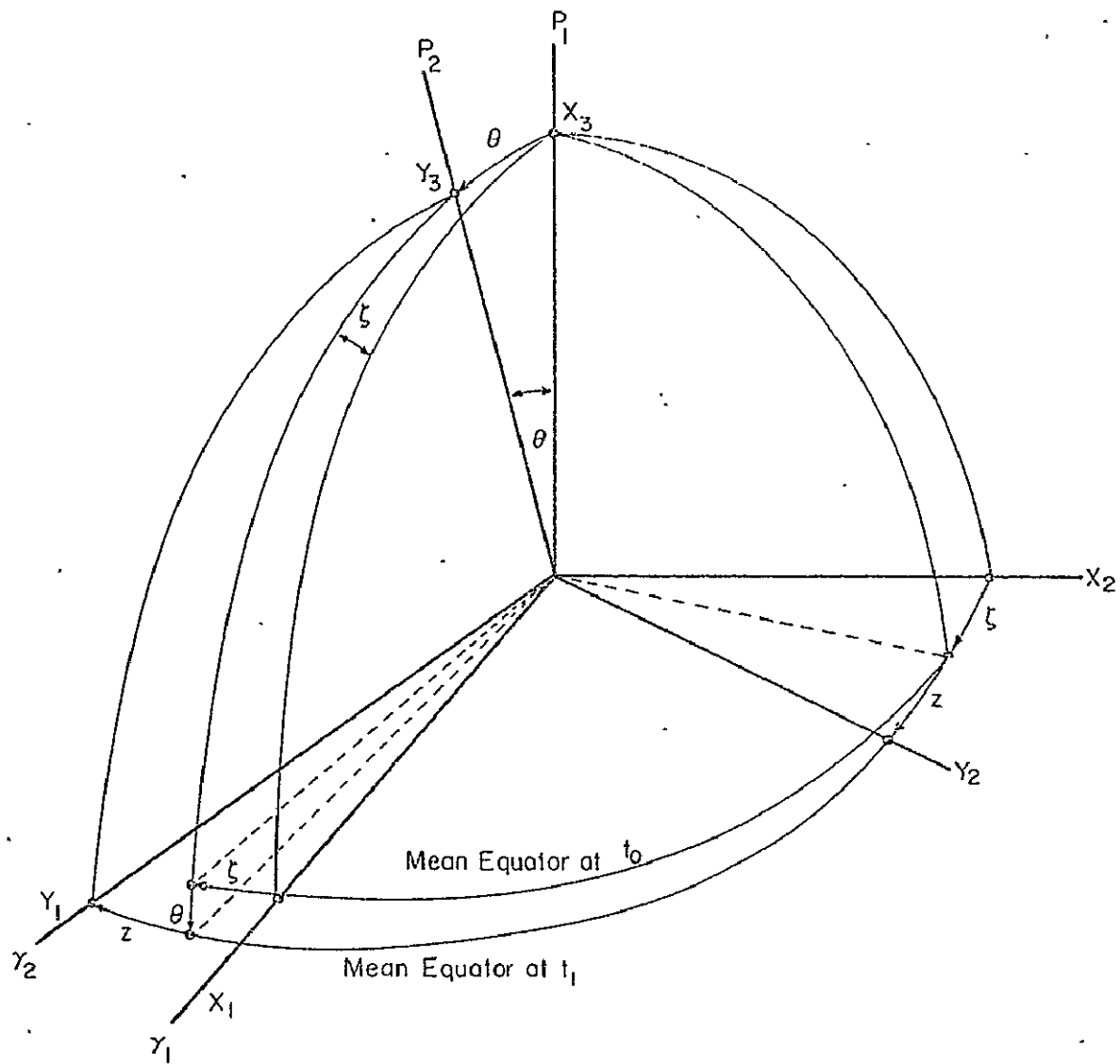
REFCOR

### 2.3.6.1 Precession

The precession of coordinates from the mean equator and equinox of one epoch  $t_0$  to the mean equator and equinox of  $t_1$  is accomplished very simply. Examine Figure 1 and consider a position described by the vector  $\bar{X}$  in the  $X_1, X_2, X_3$  coordinate system which is

PRECES

## PRECESSION



$P_1$  = Direction of Mean Axis of Motion at  $t_0$

$P_2$  = Direction of Mean Axis of Motion at  $t_1$

$Y_1$  = Direction of Mean Equinox at  $t_0$

$Y_2$  = Direction of Mean Equinox at  $t_1$

Fig.1: Rotation Between Mean Equator & Equinox of Epoch  $t_0$   
and  
Mean Equator & Equinox of Epoch  $t_1$

defined by the mean equator and equinox of  $t_0$ . Likewise, consider the same position as described by the vector  $Y$  in the  $Y_1, Y_2, Y_3$  system defined by the mean equator and equinox of  $t_1$ . The expression relating these vectors,

PRICES

$$Y = R_3(-z) R_2(0) R_3(-\zeta) X, \quad (1)$$

follows directly from inspection of Figure 1.

It should be observed that  $90^\circ - \zeta$  is the right ascension of the ascending node of the equator of epoch  $t_0$  reckoned from the equinox of  $t_0$ ,  $90^\circ = z$  is the right ascension of the node reckoned from the equinox of  $t_1$  and 0 is the inclination of the equator of  $t_1$  to the epoch of  $t_0$ .

Numerical expressions for these rotation angles  $z, \theta, \zeta$  were derived by Simon Newcomb, based partly upon theoretical considerations but primarily upon actual observation. (See References for the derivations.) The formulae used in NONAME are relative to an initial epoch of 1950.0:

$$\begin{aligned} \zeta &= .305\ 953\ 204\ 65 \times 10^{-6}d + .109\ 749\ 2 \times 10^{-14}d^2 \\ &+ .178\ 097 \times 10^{-20}d^3 \end{aligned} \quad (2)$$

$$\begin{aligned} z &= .305\ 953\ 204\ 65 \times 10^{-6}d + .397\ 204\ 9 \times 10^{-14}d^2 \\ &+ .191\ 031 \times 10^{-20}d^3 \end{aligned} \quad (3)$$

$$\theta = \frac{R}{266039} 997.54 \times 10^{-6} d - \frac{R}{154811} 8 \times 10^{-14} d^2 - \frac{R}{413902} 20 d^3 \quad (4) \quad \text{PRECES}$$

The angles are in radians. The quantity  $d$  is the number of elapsed days since 1950.0.

The nutation of coordinates between mean and true equator and equinox of date is readily accomplished using rotation matrices. Examine Figure 1 and consider a position described by the vector  $\bar{X}$  in the  $X_1, X_2, X_3$  system which is described by the mean equator and equinox of date. Likewise, consider the same position as described by the vector  $\bar{Z}$  in the  $Z_1, Z_2, Z_3$  system defined by the true equator and equinox of date. The expression relating these vectors,

$$\bar{Z} = R_1(-\varepsilon_T) R_3(-\Delta\psi) R_1(\varepsilon_m) \bar{X}, \quad (1)$$

follows directly from inspection of Figure 1.

The definition of these angles are:

$\varepsilon_T$  - true obliquity of date

$\varepsilon_m$  - mean obliquity of date

$\Delta\psi$  - nutation in longitude

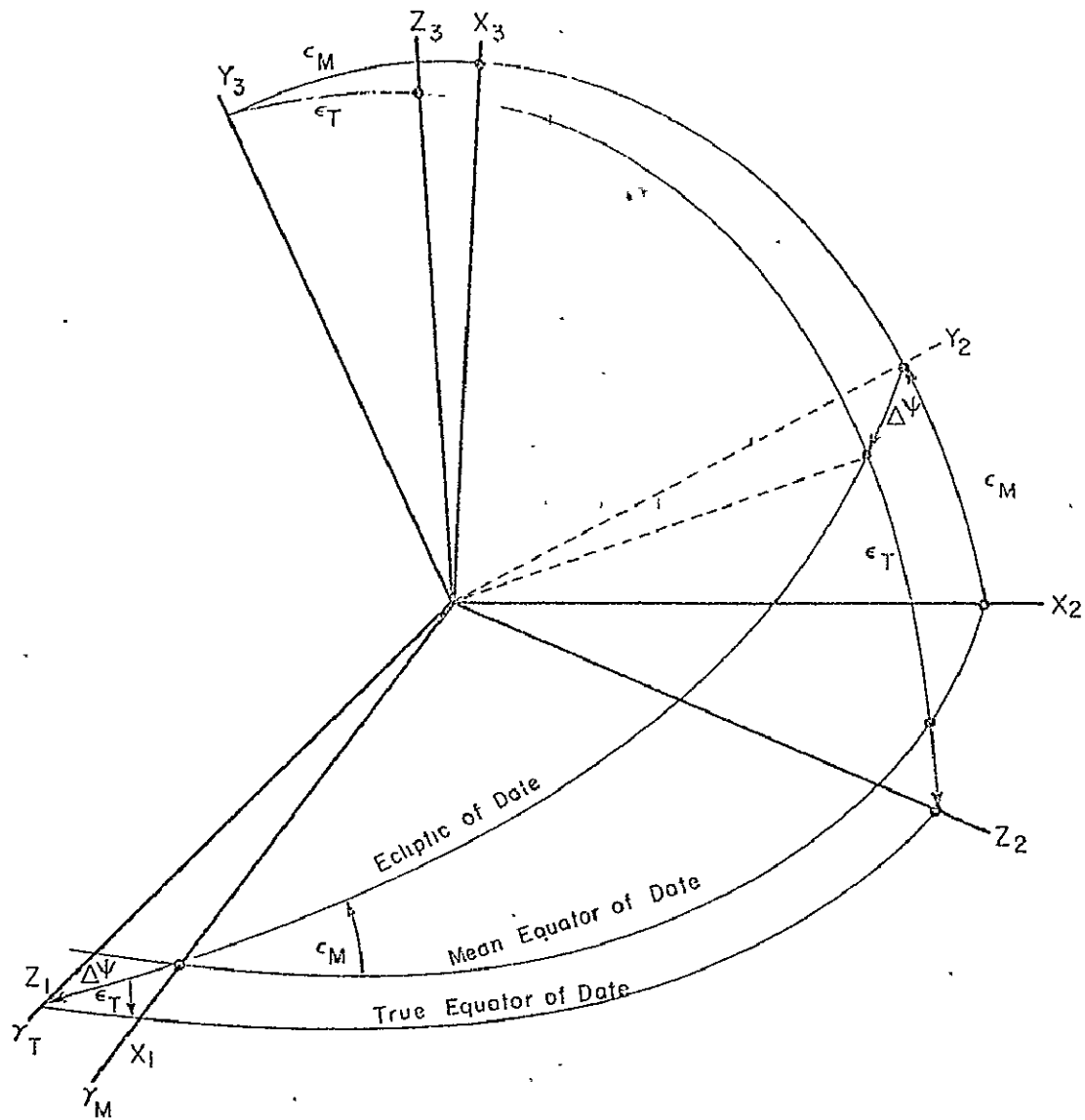
Note that  $\varepsilon_T - \varepsilon_m$  is the nutation in obliquity.

The remaining problem is to compute the nutations in longitude and obliquity. The algorithm used in NONAME was developed by Woolard and is coded in subroutine EQN.

NUTATE

EQN

# NUTATION



$\epsilon_M$  = Mean Obliquity of Date

$\epsilon_T$  = True Obliquity of Date

$\gamma_M$  = Direction of Mean Equinox of Date

$\gamma_T$  = Direction of Time Equinox of Date

Figure 1: Rotation Between Mean Equator & Equinox of Date  
and  
True Equator & Equinox of Date

Woolard's solution as it appears in references J through 4 is reproduced in Tables 1a, 1b, and 1c. The periodic terms have been rearranged in descending order of magnitude. The subprogram EQN computes the nutation in longitude and obliquity by using the algorithm in Tables 2a, 2b, and 2c. In Table 2a the angular units of the fundamental arguments have been changed to radians and the time units have been changed to days. Tables 2b and 2c are identical to Tables 1b and 1c often neglecting all periodic terms with coefficients less than .001 and all secular portions of the coefficient which are less than .001. The expressions for true obliquity of date and nutation in right ascension appear in Table 2d.

EQN

The definitions of the variables used in these solutions and additional notation are as follows:

$J$  = Julian Ephemeris Date of desired calculation

$J_0$  = 241 5020.5 (Julian Ephemeris Date corresponding to 1900 January 0.5 Ephemeris Time)

$T$  =  $(J - J_0)/36525$  = Julian ephemeris centuries of 36525 Ephemeris Days elapsed from  $J_0$  to  $J$

$d$  =  $J - J_0$  = Ephemeris Days elapsed from  $J$  to  $J_0$

COORDINATE SYSTEM: Geocentric, ecliptic and mean equinox of date:

$g$  = mean anomaly - Moon

$g'$  = mean anomaly - Sun

$F$  = mean angular distance of the Moon from its ascending node

$D$  = mean elongation of the Moon from the Sun

$\Omega$  = longitude of the mean ascending node of the Moon's orbit

$\varepsilon_M$  = mean obliquity of date

$\varepsilon_T$  = true obliquity of date

$\Delta\varepsilon$  = nutation in obliquity

$\Delta\psi$  = nutation in longitude

$\Delta\alpha$  = nutation in right ascension  
(equation of the equinoxes)

TABLE 1a FUNDAMENTAL ARGUMENTS

$g = 296^\circ 06' 16'' 59 + 1325^r 198^\circ 50' 56'' 79 T + 33'' 09 T^2 + 00518 T^3$
$g' = 3358^\circ 28' 33'' 00 + 99^r 359^\circ 02' 59'' 10 T - 59'' T^2 - 00120 T^3$
$F = 11^\circ 15' 03'' 20 + 1342^r 82^\circ 01' 30'' 54 T - 11'' 56 T^2 - 00012 T^3$
$D = 350^\circ 44' 14'' 95 + 1236^r 307^\circ 06' 51'' 18 T - 5'' 17 T^2 - 00068 T^3$
$\Omega = 259^\circ 10' 59'' 79 - 5^r 134^\circ 08' 31'' 23 T + 7'' 48 T^2 + 00080 T^3$
$\epsilon_M = 23^\circ 27' 08'' 26 - 46'' 845 T - 00059 T^2 + 00080 T^3$

TABLE 1b NUTATION IN OBLIQUITY

		Series No.
$\Delta\epsilon = + (0.00091 T + 9.2100) \cos ($	$+ \Omega)$	1
$+ (-0.00029 T + 0.5522) \cos ($	$+ 2F - 2D + 2\Omega)$	2
$+ (0.00004 T - 0.0904) \cos ($	$+ 2\Omega)$	3
$+ (-0.00005 T + 0.0884) \cos ($	$+ 2F + 2\Omega)$	4
$+ (-0.00006 T + 0.0216) \cos ($	$+ g' + 2F - 2D + 2\Omega)$	5
$+ 0.0183 \cos ($	$+ 2F + \Omega)$	6
$+ (-0.00001 T + 0.0113) \cos (+ g$	$+ 2F + 2\Omega)$	7
$+ (0.00003 T - 0.0093) \cos (- g' + 2F - 2D + 2\Omega)$		8
$- 0.0066 \cos ($	$+ 2F - 2D + \Omega)$	9
$- 0.0050 \cos (- g$	$+ 2F + 2\Omega)$	10
$- 0.0031 \cos (+ g$	$+ \Omega)$	11
$+ 0.0030 \cos (- g$	$+ \Omega)$	12
$- 0.0024 \cos (- 2g$	$+ 2F + \Omega)$	13
$+ 0.0023 \cos (+ g$	$+ 2F + \Omega)$	14
$+ 0.0022 \cos (- g$	$+ 2F - 2D + 2\Omega)$	15
$+ 0.0014 \cos ($	$+ 2F + 2D + 2\Omega)$	16
$- 0.0011 \cos (+ g$	$+ 2F - 2D + 2\Omega)$	17
$+ 0.0011 \cos (+ 2g$	$+ 2F + 2\Omega)$	18
$- 0.0010 \cos (- g$	$+ 2F + \Omega)$	19
$+ 0.0008 \cos ( + g'$	$+ \Omega)$	20
$- 0.0007 \cos (- g$	$+ D + \Omega)$	21

TABLE 1b (Cont.)

		Series No.
-	0.0007 cos (- g	- 2D + Ω) 22
+	0.0007 cos (+ g + 2g' + 2F - 2D + 2Ω)	23
+	0.0005 cos (- - g'	+ Ω) 24
+	0.0005 cos (- g + 2F + 2D + Ω)	25
-	0.0003 cos (+ + g' + 2F + 2D + 2Ω)	26
+	0.0003 cos (- - g' + 2F + 2D + 2Ω)	27
+	0.0003 cos (+ g + 2F + 2D + 2Ω)	28
+	0.0003 cos (- - + 2D + Ω)	29
+	0.0003 cos (-2g + 2D + Ω)	30
+	0.0003 cos (- - g' + 2F - 2D + Ω)	31
-	0.0003 cos (+ g + 2F - 2D + Ω)	32
+	0.0003 cos (- - - 2D + Ω)	33
+	0.0003 cos (- + 2F + 2D + Ω)	34
-	0.0002 cos (+2g + 2F - 2D + 2Ω)	35
+	0.0002 cos (- - 2g' + 2F - 2D + Ω)	36
-	0.0002 cos (+2g - 2D + Ω)	37
+	0.0002 cos (+2g + 2F + Ω)	38
-	0.0002 cos (- + g' + 2F - 2D + Ω)	39
+	0.0002 cos (-2g + 2F + 2Ω)	40

TABLE 1c NUTATION IN LONGITUDE

		Series No.
$\Delta\psi = + (-0^{\text{h}}01737 T - 17^{\text{m}}2327) \sin ($	$+ \Omega)$	1
$+ (-0.00013 T - 1.2729) \sin ($	$+ 2F - 2D + 2Ω)$	2
$+ (+0.00002 T + 0.2008) \sin ($	$+ 2Ω)$	3
$+ (-0.00002 T - 0.2037) \sin ($	$+ 2F + 2Ω)$	4
$+ (-0.00031 T + 0.1261) \sin ( + g'$	$)$	5
$+ (+0.00001 T + 0.0675) \sin (+ g$	$)$	6
$+ (+0.00012 T - 0.0497) \sin ( g' + 2F - 2D + 2Ω)$		7
$+ (-0.00004 T - 0.0342) \sin ( + 2F + 2Ω)$		8

TABLE Ic (Cont.)

					Series No.
-	0.0261	sin (+ g			Ω) 9
+	(-0.00005 T	+ 0.0214) sin (- g' + 2F - 2D + 2Ω)			10
-	0.0149	sin (+ g		- 2D	) 11
+	(+0.00001 T	+ 0.0124) sin (- g' + 2F - 2D + Ω)			12
+	0.0114	sin (- g	+ 2F	+ 2D + 2Ω)	13
+	0.0060	sin (- g		+ 2D	) 14
+	0.0058	sin (+ g		+ Ω)	15
-	0.0057	sin (- g		+ Ω)	16
-	0.0052	sin (- g	+ 2F + 2D + 2Ω)		17
+	0.0045	sin (- 2g	+ 2F	+ Ω)	18
+	0.0045	sin (+ 2g		- 2D	) 19
-	0.0044	sin (+ g	+ 2F	+ Ω)	20
-	0.0032	sin (- g	+ 2F + 2D + 2Ω)		21
+	0.0028	sin (+ 2g			) 22
+	0.0026	sin (+ g	+ 2F - 2D + 2Ω)		23
-	0.0026	sin (+ 2g	+ 2F	+ 2Ω)	24
+	0.0025	sin (- g	+ 2F		) 25
-	0.0021	sin (- g	+ 2F - 2D		) 26
+	0.0019	sin (- g	+ 2F	+ Ω)	27
+	(-0.00001 T	+ 0.0016) sin (+ 2g'			) 28
+	(+0.00001 T	- 0.0015) sin (+ 2g' + 2F - 2D + 2Ω)			29
-	0.0015	sin (+ g'		+ Ω)	30
+	0.0014	sin (- g		+ 2D + Ω)	31
-	0.0013	sin (+ g		- 2D + Ω)	32
-	0.0010	sin (- g'		+ Ω)	33
+	0.0010	sin (+ 2g	- 2F		) 34
-	0.0009	sin (- g	+ 2F + 2D + Ω)		35
+	0.0007	sin (+ g' + 2F		+ 2Ω)	36
-	0.0007	sin (+ g + g'		- 2D	) 37
+	0.0006	sin (+ g		+ 2D	) 38

TABLE 1c (Cont.)

-	0.0006	$\sin ( - g' + 2F + 2D + 2\Omega )$	59
-	0.0006	$\sin ( + g + 2F + 2D + 2\Omega )$	40
+	0.0006	$\sin ( + 2g + 2F - 2D + 2\Omega )$	41
-	0.0006	$\sin ( - g + 2F + 2D + \Omega )$	42
-	0.0005	$\sin ( - 2g + 2D + \Omega )$	43
-	0.0005	$\sin ( - g' + 2F - 2D + \Omega )$	44
+	0.0005	$\sin ( g + 2F - 2D + \Omega )$	45
-	0.0005	$\sin ( - g + 2F - 2D + \Omega )$	46
-	0.0005	$\sin ( - g + 2F + 2D + \Omega )$	47
-	0.0004	$\sin ( - 2g' + 2F - 2D + \Omega )$	48

TABLE 2a FUNDAMENTAL ARGUMENTS

$g$	$=$	$5.168\ 000\ 345\ 745 + .228\ 027\ 134\ 959\ 576\ d + .120\ 251\ 689 \times 10^{-12}\ d^2 + 5.153\ 876 \times 10^{-21}\ c$
$g'$	$=$	$6.256\ 583\ 580\ 497 + .017\ 201\ 969\ 766\ 646\ d - .001\ 966\ 037 \times 10^{-12}\ d^2 - 1.193\ 948 \times 10^{-21}\ c$
$F$	$=$	$.196\ 365\ 054\ 887 + .230\ 895\ 723\ 235\ 372\ d - .042\ 009\ 958 \times 10^{-12}\ d^2 - .119\ 595 \times 10^{-21}\ c$
$D$	$=$	$6.121\ 523\ 942\ 807 + .212\ 768\ 711\ 675\ 140\ d - .018\ 788\ 191 \times 10^{-12}\ d^2 + .676\ 571 \times 10^{-21}\ c$
$\Omega$	$=$	$4.523\ 601\ 514\ 852 - .000\ 924\ 220\ 294\ 225\ d + .027\ 182\ 914 \times 10^{-12}\ d^2 + .795\ 965 \times 10^{-21}\ c$
$\epsilon_m$	$=$	$.409\ 319\ 755\ 205 - .000\ 000\ 006\ 217\ 959\ d - .000\ 021\ 441 \times 10^{-12}\ d^2 + .180\ 087 \times 10^{-21}\ c$

TABLE 2b NUTATION IN OBLIQUITY

Series No.				
$\Delta\epsilon = + 9112100 \cos ($		$\dots + \Omega)$	1	
$+ 0.5522 \cos ($	$\dots + 2F - 2D + 2\Omega)$		2	
$- 0.0904 \cos ($		$\dots + 2\Omega)$	3	
$+ 0.0884 \cos ($	$\dots + 2F$	$\dots + 2\Omega)$	4	
$+ 0.0216 \cos ($	$+ g'$	$\dots + 2F - 2D + 2\Omega)$	5	
$+ 0.0183 \cos ($		$\dots + 2F$	$\dots + \Omega)$	6
$+ 0.0113 \cos ($	$+ g'$	$\dots + 2F$	$\dots + 2\Omega)$	7
$- 0.0093 \cos ($	$- g'$	$\dots + 2F - 2D + 2\Omega)$	8	
$- 0.0066 \cos ($		$\dots + 2F - 2D + \Omega)$	9	
$- 0.0050 \cos (- g$		$\dots + 2F$	$\dots + 2\Omega)$	10
$- 0.0031 \cos (+ g$			$\dots + \Omega)$	11
$+ 0.0030 \cos (- g$			$\dots + \Omega)$	12
$- 0.0024 \cos (-2g$		$\dots + 2F$	$\dots + \Omega)$	13
$+ 0.0023 \cos (+ g$		$\dots + 2F$	$\dots + \Omega)$	14
$+ 0.0022 \cos (- g$		$\dots + 2F + 2D + 2\Omega)$	15	
$+ 0.0014 \cos ($		$\dots + 2F + 2D + 2\Omega)$	16	
$- 0.0011 \cos (+ g$		$\dots + 2F - 2D + 2\Omega)$	17	
$+ 0.0011 \cos (+2g$		$\dots + 2F$	$\dots + 2\Omega)$	18
$- 0.0010 \cos (- g$		$\dots + 2F$	$\dots + \Omega)$	19

TABLE 2C NUTATION IN LONGITUDE

		Series No.
$\Delta\psi = + (-0^\circ 01' 37'' T - 17^\circ 23' 27'')$	$\sin ($	$+ \Omega)$ 1
- 1.2729)	$\sin ($	$+ 2F - 2D + 2\Omega)$ 2
+ 0.2008)	$\sin ($	$+ 2\Omega)$ 3
- 0.2037)	$\sin ($	$+ 2F + 2\Omega)$ 4
+ 0.1261)	$\sin ($	$+ g^1$ ) 5
+ 0.0675)	$\sin ($	$+ g$ ) 6
- 0.0497)	$\sin ($	$g^1 + 2F - 2D + 2\Omega)$ 7
- 0.0342)	$\sin ($	$+ 2F + 2\Omega)$ 8
- 0.0261	$\sin ($	$+ g + 2F$ ) 9
+ 0.0214)	$\sin ($	$- g^1 + 2F - 2D + 2\Omega)$ 10
- 0.0149	$\sin ($	$+ g - 2D$ ) 11
+ 0.0124)	$\sin ($	$+ 2F - 2D + \Omega)$ 12
+ 0.0114	$\sin ($	$- g + 2F + 2\Omega)$ 13
+ 0.0060	$\sin ($	$+ 2D$ ) 14
+ 0.0058	$\sin ($	$+ g + \Omega)$ 15
- 0.0057	$\sin ($	$- g + \Omega)$ 16
- 0.0052	$\sin ($	$- g + 2F + 2D + 2\Omega)$ 17
+ 0.0045	$\sin ($	$- 2g + 2F + \Omega)$ 18
+ 0.0045	$\sin ($	$+ 2g - 2D$ ) 19
- 0.0044	$\sin ($	$+ g + 2F + \Omega)$ 20
- 0.0032	$\sin ($	$+ 2F + 2D + 2\Omega)$ 21
+ 0.0028	$\sin ($	$+ 2g + 2\Omega)$ 22
+ 0.0026	$\sin ($	$+ g + 2F - 2D + 2\Omega)$ 23
- 0.0026	$\sin ($	$+ 2g + 2F + 2\Omega)$ 24
+ 0.0025	$\sin ($	$+ 2F$ ) 25
- 0.0021	$\sin ($	$+ 2F - 2D$ ) 26
+ 0.0019	$\sin ($	$- g + 2F + \Omega)$ 27
+ 0.0016)	$\sin ($	$+ 2g^1$ ) 28

TABLE 2C (Cont.)

-	0.0015j	$\sin ( + 2g' + 2f - 2D + 2\Omega)$	29
-	0.0015	$\sin ( + g' + \Omega)$	30
+	0.0014	$\sin (-g + 2D + \Omega)$	31
-	0.0013	$\sin (+g - 2D + \Omega)$	32
-	0.0010	$\sin (-g + \Omega)$	33
+	0.0010	$\sin (+2g - 2f + \Omega)$	34

Note: To change time units for coefficient of 1st term, use  
 $.475565 \times 10^{-6}d = .01737 T$

Table 2d: True obliquity of Date and Nutation in right ascension

$$\varepsilon_T = \varepsilon_M + \Delta\varepsilon$$

$$\Delta\alpha = \Delta\psi \cos \varepsilon_T$$

SECTION 2.4  
LUNI-SOLAR EPHemerides

<sup>1</sup> NONAME uses precomputed equi-spaced ephemeris data in true of date coordinates for both the Sun and the Moon. The actual ephemerides are computed using Everett's fifth-order interpolation formula. The interval between ephemerides; i.e., the tabular interval  $h$ , is 0.5 days. EPHEM

<sup>1</sup> The NONAME ephemeris tape contains the lunar and solar ephemerides in true of date coordinates and the equation of equinox. The format of this tape is presented in Volume III of the NONAME System Documentation.

This ephemeris tape was prepared from a JPL planetary ephemeris tape corresponding to "JPL Development Ephemeris Number 19," Reference 1. JPL provided subroutines READE and GETTAP which obtain the ephemerides from the JPL tape. NONAME subroutine EQUATR was used to precess and nutate the ephemerides to the true of date system. The interpolation differences  $d_j$  were also recomputed, using the equations given on page 6 of the above report.

The formulation for Everett's fifth-order interpolation is

$$y(t_j + sh) = y_j F_0(1-s) + d_j^2 F_2(1-s) \quad (1)$$

$$+ d_j^4 F_4(1-s)$$

$$+ y_{j+1} F_0(s) + d_{j+1}^2 F_2(s)$$

$$+ d_{j+1}^4 F_4(s)$$

where

EPHEM

$$F_0(s) = s$$

$$F_2(s) = [(s-1)(s)(s+1)]/6$$

$$F_4(s) = [(s-2)(s-1)(s)(s+1)(s+2)]/120$$

The quantity  $s$  is of course the fractional interval for the interpolation. The quantities  $d_j$  are obtained from the ephemeris tape.

## SECTION 2.5

### THE OBSERVER

This section is concerned with the position and coordinate systems of the observer. Thus it will cover

- geodetic station position coordinates,
- topocentric coordinate systems,
- time reference systems, and
- polar motion.

The geodetic station position coordinates are a convenient and quite common way of describing station positions. Consequently, NONAME contains provisions for converting to and from these coordinates, including the transformation of the covariance matrix for the determined Cartesian station positions.

The topocentric coordinate systems are coordinate systems to which the observer references his observations.

The time reference systems are the time systems in which the observer specifies his observations. The transformations between time reference systems are also given. These latter are used both to convert the observation times to Al time, which is the independent variable in the equations of motion, and to convert the NONAME output to UTC time, which is the generally recognized system for output.

The positions of the observers in NONAME are referred to an Earth-fixed system defined by the mean pole of 1900.5 and Greenwich. They are rotated into the Earth-fixed system of date at each observation time by applying "polar motion", which is considered to be slippage of the Earth's crust.

### 2.5.1 Geodetic Coordinates

Frequently, it is more convenient to define the station positions in a spherical coordinate system. The spherical coordinate system uses an oblate spheroid or an ellipsoid of revolution as a model for the geometric shape of the Earth. The Earth is flattened slightly at the poles and bulges a little at the equator; thus, a cross section of the Earth is approximately an ellipse. Rotating an ellipse about its shorter axis forms an oblate spheroid.

An oblate spheroid is uniquely defined by specifying two dimensions, conventionally, the semi-major axis and the flattening,  $f$ , where  $f = \frac{a-b}{a}$ . (See Figure 1)

This model is used in the NONAME system. The spherical coordinates utilized are termed geodetic coordinates and are defined as follows:

- $\phi$  is geodetic latitude, the acute angle between the semi-major axis and a line through the observer perpendicular to the spheroid.

- $\lambda$  is east longitude, the angle measured eastward in the equatorial plane between the Greenwich meridian and the observer's meridian.
- $h$  is spheroid height, the perpendicular height of the observer above the reference spheroid.

Consider the problem of converting from  $\phi$ ,  $\lambda$ , and  $h$  to  $X_e$ ,  $Y_e$ , and  $Z_e$ , the Earth-fixed Cartesian coordinates. SQUANT

The geometry for an X-Z plane is illustrated in Figure 1. The equation for this ellipse is

$$x^2 + \frac{z^2}{(1-e^2)} = a^2, \quad (1)$$

where the eccentricity has been determined from the flattening by the familiar relationship

$$e^2 = 1 - (1-f)^2. \quad (2)$$

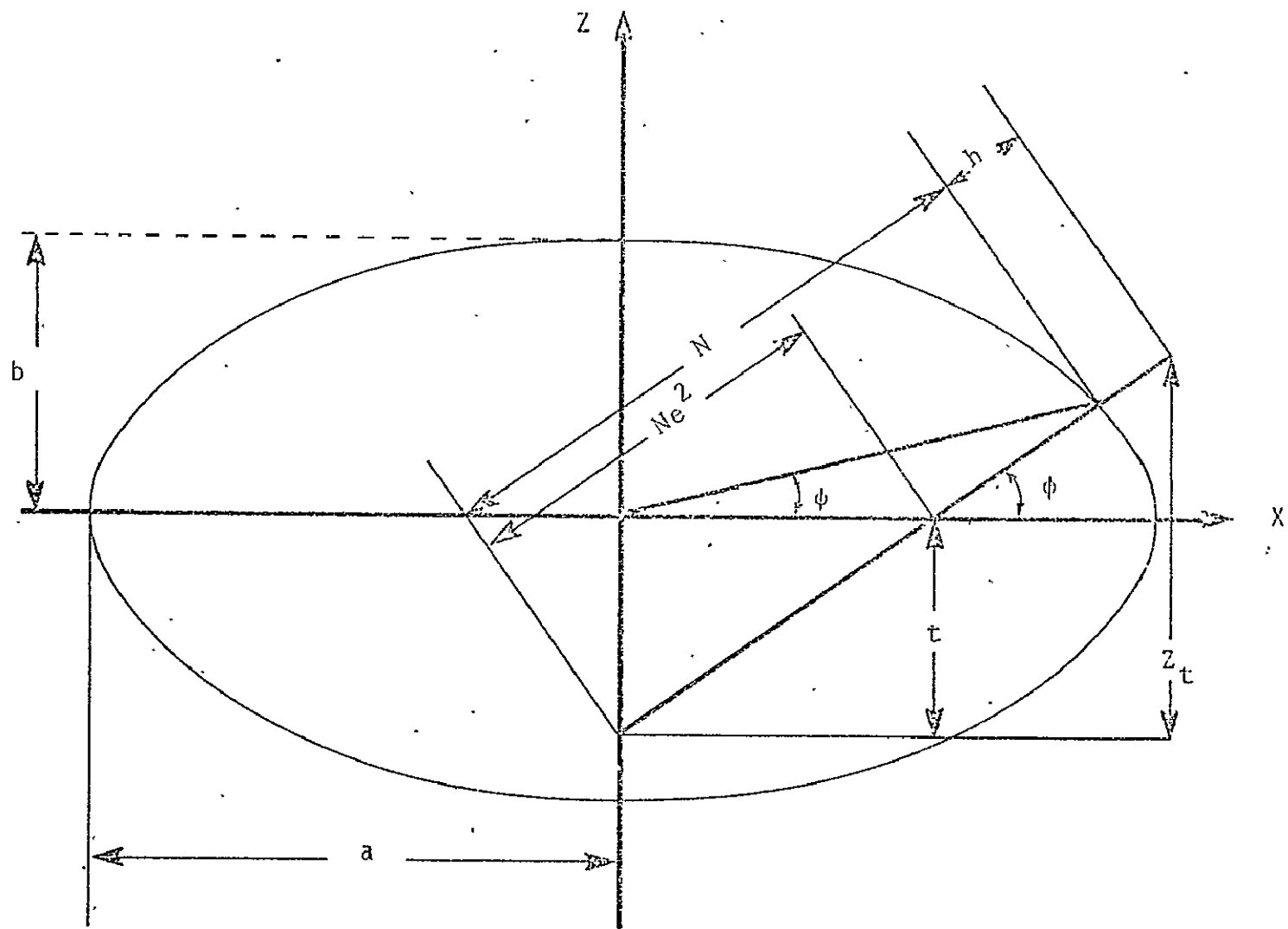


Figure 1: Diagram of Geodetic and Geocentric Latitudes

The equation for the normal to the surface of the ellipse yields

SEQUANT

$$\tan \phi = - \frac{dx}{dz} \quad (3)$$

By taking differentials on equation (1) and applying the result in equation (3), we arrive at

$$\frac{z}{x} = (1-e^2) \tan \phi \quad (4)$$

The simultaneous solution of equations (1) and (4) for  $x$  yields

$$x = \frac{a \cos \phi}{\sqrt{1-e^2 \sin^2 \phi}} \quad (5)$$

From inspection of Figure 1 we have:

$$\cos \phi = \frac{x}{N}; \quad (6)$$

and hence, applying equation (5),

$$N = \frac{a}{\sqrt{1-e^2 \sin^2 \phi}} \quad (7)$$

For an observer at a distance  $h$  from the reference ellipsoid, the observer's coordinates  $(X, Z)$  become

SQUANT

$$X = N \cos \phi + h \cos \phi \quad (8)$$

and

$$Z = N (1 - c^2) \sin \phi + h \sin \phi. \quad (9)$$

The conversion of  $\phi$ ,  $\lambda$ , and  $h$  to  $X_e$ ,  $Y_e$ , and  $Z_e$  is then

$$\begin{bmatrix} X_e \\ Y_e \\ Z_e \end{bmatrix} = \begin{bmatrix} (N+h) \cos \phi \cos \lambda \\ (N+h) \cos \phi \sin \lambda \\ (N+h - c^2 N) \sin \phi \end{bmatrix} \quad (10)$$

In the NONAME system this conversion is performed in subroutine SQUANT.

The problem of converting from  $X_e$ ,  $Y_e$ , and  $Z_e$  to  $\phi$ ,  $\lambda$ , and  $h$  is more complex as we cannot start with a point on the reference ellipsoid. For this reason the determination of accurate values for  $\phi$  and  $h$  requires an iterative technique.

### Conversion to Geodetic Coordinates

For the problem of converting station coordinates in  $X_e$ ,  $Y_e$ , and  $Z_e$  to  $\phi$ ,  $\lambda$ , and  $h$  we know that  $N$  is on the order of magnitude of an Earth radius, and  $h$  is a few meters. Hence

$$h \ll N \quad (11)$$

The Earth is approximately a sphere, hence

$$e \ll 1. \quad (12)$$

Therefore, again working in our  $X$ - $Z$  plane (see Figure 1),

$$N \sin \phi \approx Z. \quad (13)$$

From Figure 1 (see also equation (9)) we have

$$t = Ne^2 \sin \phi, \quad (14)$$

or, for an initial approximation,

$$t \approx e^2 Z. \quad (15)$$

The series of calculations to be performed on each iteration is:

PLHOUT

$$z_t = z + t \quad (16)$$

$$N+h = \left( x_e^2 + y_e^2 + z_t^2 \right)^{1/2} \quad (17)$$

$$\sin \phi = z_t / (N+h) \quad (18)$$

$$N = a / \left( 1 - c^2 \sin^2 \phi \right)^{1/2} \quad (19)$$

$$t = N c^2 \sin \phi. \quad (20)$$

When  $t$  converges,  $\phi$  and  $h$  are computed from  $\sin \phi$  and  $(N+h)$ . The computation of  $\lambda$  is obvious; it being simply

$$\lambda = \tan^{-1} \left( y_e / x_e \right) \quad (21)$$

This procedure for determining  $\phi$ ,  $\lambda$ , and  $h$  is that coded in subroutine PLHOUT.

There is a different procedure in subroutine PREDCT for computing  $\phi$ ,  $\lambda$ , and  $h$  for a satellite. This is because the accuracy requirements are less stringent.

DRAG  
PREDCT

This different procedure is also used in subroutine DRAG to evaluate the satellite height for subroutine DENSTY.

Because  $c \ll 1$ , we may write an approximation to equation (9):

$$Z = (N+h) (1-e^2) \sin \phi = Z_c \quad (22)$$

From Figure 1,

$$X = (N+h) \cos \phi = \sqrt{X_c^2 + Y_c^2} \quad (23)$$

and by remembering equation (2),

$$\phi = \tan^{-1} \left[ \frac{Z_c}{(1-f)^2 \sqrt{X_c^2 + Y_c^2}} \right] \quad (24)$$

The equation for the ellipse, equation (1), yields the following formula for the radius of the ellipsoid:

$$r_{\text{ellipsoid}} = \sqrt{x^2 + z^2} = \frac{a(1-f)}{\sqrt{1 - (2f-f^2)(1-\sin^2 \phi')}} \quad (27)$$

where  $\phi'$  is the geocentric latitude. After applying the Binomial Theorem, we arrive at

$$r_{\text{ellipsoid}} = a \left[ 1 - \left( f + \frac{3}{2} f^2 \right) \sin^2 \phi' + \frac{3}{2} f^2 \sin^4 \phi' \right] \quad (28)$$

wherein terms on the order of  $f^3$  have been neglected. The (spheroid) height may then be calculated from  $r$ , the geocentric radius of the satellite:

$$h = r - r_{\text{ellipsoid}}, \text{ or} \quad (29)$$

$$h = \sqrt{x_e^2 + y_e^2 + z_e^2} - a + \left( af + \frac{3}{2} af^2 \right) \sin^2 \phi' - \frac{3}{2} af^2 \sin^4 \phi' \quad (30)$$

The sine of the geocentric latitude,  $\sin \phi'$ , is of course  $\frac{z_e}{r}$ .

Subroutine VIIVAL also requires the partial derivatives of  $h$  with respect to position for the drag variational partials computations:

$$\frac{\partial h}{\partial r_i} = \frac{r_i}{r} + 2 \sin \phi \left[ \left( af + \frac{3}{2} af^2 \right) - 3 af^2 \sin^2 \phi \right] \left[ -\frac{z_e r_i}{r^3} + \frac{1}{r} \frac{\partial z_c}{\partial r_i} \right] \quad (31)$$

where the

$r_i$  are the Earth-fixed components of  $\bar{r}$ ; i.e.,  $\{x_e, y_e, z_e\}$ .

In addition to the conversion of the coordinates themselves, NONAME also converts covariance matrices for the station positions to either the  $\phi, \lambda, h$  system or the Earth-fixed rectangular system. This is accomplished in INOUP, SQUANT, and PLHOUT by calling VCONV to compute

$$V_{OUT} = P^T V_{IN} P \quad (32) \quad VCONV$$

where  $V_{OUT}$  is the output covariance matrix,  $V_{IN}$  is the input covariance matrix, and  $P$  is the matrix of partials relating the coordinates in the output system to the coordinates in the input system.

These partial derivatives (in P) which NONAME requires are for  $X_e$ ,  $Y_e$ ,  $Z_e$  with respect to  $\phi$ ,  $\lambda$ ,  $h$  and vice versa. These partials are:

PLIOUT

$$\begin{aligned}
 \frac{\partial \phi}{\partial X_e} &= -X_e Z_e (1-e^2) / ((1-e^2)^2 (X_e^2 + Y_e^2) + Z_e^2) \quad (X_e^2 + Y_e^2)^{\frac{1}{2}} \\
 \frac{\partial \phi}{\partial Y_e} &= -Y_e Z_e (1-e^2) / ((1-e^2)^2 (X_e^2 + Y_e^2) + Z_e^2) \quad (X_e^2 + Y_e^2)^{\frac{1}{2}} \\
 \frac{\partial \phi}{\partial Z_e} &= (X_e^2 + Y_e^2) / (1-e^2)^2 \quad (X_e^2 + Y_e^2) + Z_e^2 \quad (X_e^2 + Y_e^2)^{\frac{1}{2}} \\
 \frac{\partial \lambda}{\partial X_e} &= -Y_e / (X_e^2 + Y_e^2) \\
 \frac{\partial \lambda}{\partial Y_e} &= X_e / (X_e^2 + Y_e^2) \\
 \frac{\partial \lambda}{\partial Z_e} &= 0 \\
 \frac{\partial h}{\partial X_e} &= \frac{\partial \phi}{\partial X_e} (-e^2 a (1-e^2) \sin \phi \cos \phi / (1-e^2 \sin^2 \phi)^{\frac{3}{2}} - Z_e \cos \phi / \sin^2 \phi) \\
 \frac{\partial h}{\partial Y_e} &= \frac{\partial \phi}{\partial Y_e} (-e^2 a (1-e^2) \sin \phi \cos \phi / (1-e^2 \sin^2 \phi)^{\frac{3}{2}} - Z_e \cos \phi / \sin^2 \phi) \\
 \frac{\partial h}{\partial Z_e} &= \frac{\partial \phi}{\partial Z_e} (-e^2 a (1-e^2) \sin \phi \cos \phi / (1-e^2 \sin^2 \phi)^{\frac{3}{2}} - Z_e \cos \phi / \sin^2 \phi)
 \end{aligned} \tag{33}$$

$$\frac{\partial X_e}{\partial \phi} = -\sin\phi \cos\lambda \left[ N+h - \frac{Ne^2 \cos^2 \phi}{1-e^2 \sin^2 \phi} \right]$$

SQUANT

$$\frac{\partial X_e}{\partial \lambda} = -(N+h) \cos\phi \sin\lambda$$

$$\frac{\partial X_e}{\partial h} = \cos\phi \cos\lambda$$

$$\frac{\partial Y_c}{\partial \phi} = -\sin\phi \sin\lambda \left[ N+h - \frac{Ne^2 \cos^2 \phi}{1-e^2 \sin^2 \phi} \right]$$

$$\frac{\partial Y_c}{\partial \lambda} = (N+h) \cos\phi \cos\lambda \quad (34)$$

$$\frac{\partial Y_c}{\partial h} = \cos\phi \sin\lambda$$

$$\frac{\partial Z_e}{\partial \phi} = \cos\phi \left[ h+N (1-e^2) \left( 1 + \frac{e^2 \sin^2 \phi}{1-e^2 \sin^2 \phi} \right) \right]$$

$$\frac{\partial Z_e}{\partial \lambda} = 0$$

$$\frac{\partial Z_e}{\partial h} = \sin\phi$$

The partials for converting from  $X_c, Y_c, Z_e$  to  $\phi, \lambda, h$  are computed in subroutine PLHOUT. Those for converting from  $\phi, \lambda, h$  to  $X_e, Y_c, Z_e$  are computed in subroutine SQUANT.

### 2.5.2 Topocentric Coordinate Systems

The observations of a spacecraft are usually referenced to the observer, and therefore an additional set of reference systems is used for this purpose. The origin of these systems, referred to as topocentric coordinate systems, is the observer on the surface of the earth.

Topocentric right ascension and declination are measured in an inertial system whose Z axis and fundamental plane are parallel to those of the geocentric inertial system. The X axis in this case also points toward the vernal equinox.

The other major topocentric system is the Earth-fixed system determined by the zenith and the observer's horizon plane. This is an orthonormal system defined by  $\hat{N}$ ,  $\hat{E}$ , and  $\hat{Z}$ , which are unit vectors which point in the same directions as vectors from the observer pointing north, east, and toward the zenith. Their definitions are:

$$\hat{N} = \begin{bmatrix} -\sin \phi \cos \lambda \\ -\sin \phi \sin \lambda \\ \cos \phi \end{bmatrix} \quad (1)$$

$$\hat{E} = \begin{bmatrix} -\sin \lambda \\ \cos \lambda \\ 0 \end{bmatrix} \quad (2)$$

$$\hat{Z} = \begin{bmatrix} \cos \phi \cos \lambda \\ \cos \phi \sin \lambda \\ \sin \phi \end{bmatrix} \quad (3)$$

where  $\phi$  is the geodetic latitude and  $\lambda$  is the east longitude of the observer (see Section 2.5.1).

SQUANT  
PREDCT  
OBSDOT

These  $\hat{N}$ ,  $\hat{E}$ , and  $\hat{Z}$  vectors are computed in SQUANT for use in PREDCT and OBSDOT.

This latter system is the one to which such measurements as azimuth and elevation, X and Y angles, and direction cosines are related.

It should be noted that the reference systems for range and range rate must be Earth-fixed, but the choice of origin is arbitrary. In NONAME, range and range rate are not considered to be topocentric, but rather geocentric.

### 2.5.3 Time Reference Systems

Three principal time systems are currently in use: ephemeris time, atomic time, and universal time.

Ephemeris time is the independent variable in the equations of motion of the sun; this time is the uniform mathematical time. The corrections that must be applied to universal time to obtain ephemeris time are published in the American Ephemeris and Nautical Almanac or alternatively by BIH, the "Bureau International de l'Heure."

Atomic time is a time based on the oscillations of cesium at zero field. In practice Al time is based on the mean frequency of oscillation of several cesium standards as compared with the frequency of ephemeris time. This is the time system in which the satellite equations of motion are integrated in NONAME.

Universal time is determined by the rotation of the Earth. UT1, the time reference system used in NONAME to position the Earth, is universal time that has been corrected for polar motion. UTC is the time of the transmitting clock of any of the synchronized transmitting time signals. The frequency of a UTC clock is pre-set to a predicted frequency of UT2 time, where UT2 time is universal time corrected for observed polar motion and extrapolated seasonal variation in the speed of the earth's rotation.

The reader who is unfamiliar with these time systems should refer to one of the annual reports of BIH.

#### 2.5.3.1 Time System Transformations

The time system transformations are between any combination of the A1, UT1, UT2, or UTC reference systems. These transformations are computed in the NONAME system by subroutine TDIF.

TDIF

The time transformation between any input time system and any output time system is formed by simple addition and subtraction of the following set of time differences:

- UT2 - UT1
- A1 - UT1
- A1 - UTC

The following equation is used to calculate (UT2-UT1) for any year:

TDIF

$$(UT2-UT1) = + .022 \sin 2\pi t - .012 \cos 2\pi t \quad (1)$$

$$- .006 \sin 4\pi t + .007 \cos 4\pi t$$

$t$  = fraction of the tropical year elapsed from the beginning of the Besselian year for which the calculation is made.

(1 tropical year = 365.2422 days)

This difference, (UT2-UT1), is also known by the name "seasonal variation."

The time difference (Al-UT1) is computed by linear interpolation from a table of values. The spacing for the table is every 10 days, which matches the increment for the "final time of emission" data published by the U.S. Naval Observatory in the bulletin, "Time Signals." The differences for this table are determined by

$$(Al - UT1) = (Al - UTC) - (UT1 - UTC)$$

The values for (UT1 - UTC) are obtained from "Circular D", BIH. The differences (Al - UTC) are determined according to the following procedure.

The computation of ( $\Delta t$ -UTC) is simple, but not so straightforward. UTC contains discontinuities both in epoch and in frequency because an attempt is made to keep the difference between a UTC clock and a UT2 clock less than  $\frac{1}{2}$  second. When adjustments are made, by international agreement they are made in steps of  $\frac{1}{100}$  second and only at the beginning of the month; i.e., at  $0^h 0^m 0^s$  UT of the first day of the month. The general formula which is used to compute ( $\Delta t$ -UTC) is

$$(\Delta t - \text{UTC}) = a_0 + a_1 (t - t_0) \quad (2)$$

Both  $a_0$  and  $a_1$  are recovered from tables. The values in the table for  $a_0$  are the values of ( $\Delta t$ -UTC) at the time of each particular step adjustment. The values in the table for  $a_1$  are the values for the new rates of change between the two systems after each step adjustment.

Values for  $a_0$  and  $a_1$  are published both by the U.S. Naval Observatory and BIH.

#### 2.5.4 Polar Motion

Consider the point P which is defined by the intersection of the Earth's axis of rotation at some time  $t$  with the surface of the Earth. At some time  $t + \Delta t$ , the intersection will be at some point P' which is different than P. Thus the axis of rotation appears to be moving relative to a fixed position on the Earth; hence the term "motion of the pole."

Let us establish a rectangular coordinate system centered at a point  $F$  fixed on the surface of the Earth with  $F$  near the point  $P$  around 1900, and take measurements of the rectangular coordinates of the point  $P$  during the period 1900.0 - 1906.0. It is observed that the point  $P$  moves in roughly circular motion in this coordinate system with two distinct periods, one period of approximately 12 months and one period of 14 months. We define the mean position of  $P$  during this period to be the point  $P_0$ , the mean pole of 1900.0 - 1906.0.

The average is taken over a six year period in order to average out both the 12 month period and the 14 month period simultaneously (since 6 times 12 months = 72 months and  $72/14 = 5$  periods approximately of the 14 month term). The radius of this observed circle varies between 15-35 feet.

In addition to the periodic motion of  $P$  about  $P_0$ , by taking six year means of  $P$  in the years after 1900 - 1906, called  $P_m$ , there is seen to be a secular motion of the mean position of the pole away from its original mean position  $P_0$  in the years 1900 - 1906 at the rate of

POLE

approximately 0<sup>0</sup>0032/year in the direction of the meridian 60° W, and a libration motion of a period of approximately 24 years with a coefficient of about 0<sup>0</sup>022. The short periodic motions over a period of six years average about 0<sup>0</sup>2 - 0<sup>0</sup>3.

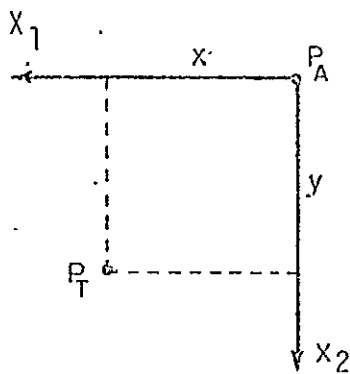
POLE

#### Effect on the Position of a Station

This motion of the pole means that the observing stations are moving with respect to our "Earth-fixed" coordinate system used in NONAME. The station positions must be corrected for this effect.

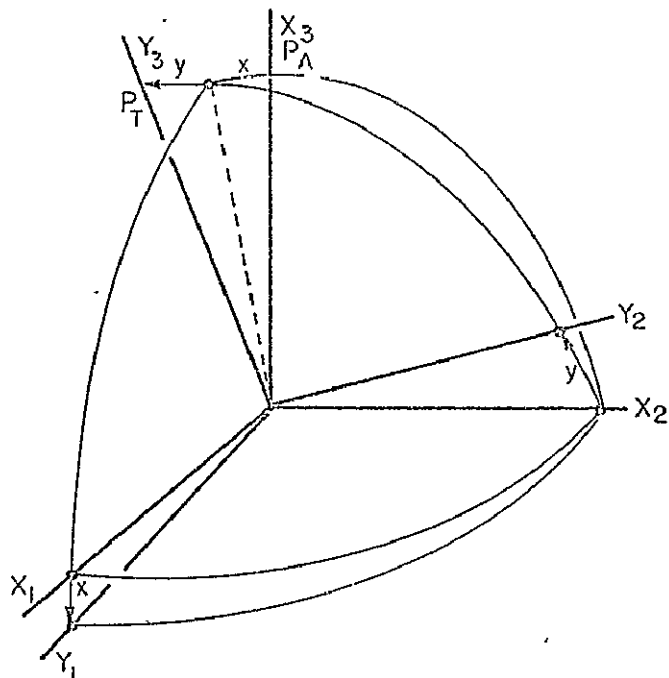
The position of the instantaneous or true pole is computed by linear interpolation in a table of observed values for the true pole relative to the mean pole of 1900 - 1905. The table increment is 10 days; the current range of data is from December 1, 1960 to August 1, 1970. The user should be aware of the fact that this table is expanded as new information becomes available. If the requested time is not in the range of the table, the value for the closest time is used.

The data in the table is in the form of the coordinates of the true pole relative to the mean pole measured in seconds of arc. This data was obtained from "Circular D" which is published by BII. The appropriate coordinate system and rotation are illustrated in Figures 1 and 2.



$P_A$  = Center of Coordinate System  
 $P_T$  = Adopted Mean Pole  
 $x_1$  = Direction of 1<sup>st</sup> Principal Axis (along meridian directed to Greenwich)  
 $x_2$  = Direction of 2<sup>nd</sup> Principal Axis (along 90° West meridian)  
 $P_T$  = Instantaneous Axis of Rotation  
 $x, y$  = Coordinates of  $P_T$  Relative to  $P_A$  Measured in seconds of arc

Figure 1: Coordinates of the Instantaneous Axis of Rotation



$x, y$  = Rectangular Coordinates of  $P_T$  Relative to  $P_A$   
 $x_1 x_2$  Plane = Mean Adopted Equator Defined by Direction of Adopted Pole  $P_A$   
 $y_1 y_2$  Plane = Instantaneous Equator Defined by Direction of Instantaneous Pole  $P_T$

Figure 2: Rotation of Coordinate System from Adopted Mean Pole System to Instantaneous Pole System

Consider the station vector  $\bar{X}$  in a system attached to the Earth of the mean pole and the same vector  $\bar{Y}$  in the "Earth-fixed" system of NONAME. The transformation between  $\bar{Y}$  and  $\bar{X}$  consists of a rotation of  $x$  about the  $X_2$  axis and a rotation of  $y$  about the  $X_1$  axis; that is

TRUEP

$$\bar{Y} = R_1(y) R_2(x) \bar{X} \quad (1)$$

$$= \begin{bmatrix} 1 & 0 & 0 \\ 0 & \cos y & \sin y \\ 0 & -\sin y & \cos y \end{bmatrix} \begin{bmatrix} \cos x & 0 & -\sin x \\ 0 & 1 & 0 \\ \sin x & 0 & \cos x \end{bmatrix} \bar{X}$$

Because  $x$  and  $y$  are small angles, their cosines are set to 1 and their sines equal to their values in radians. Consequently,

$$\bar{Y} = \begin{bmatrix} 1 & 0 & -x \\ xy & 1 & y \\ x & & 1 \end{bmatrix} \bar{X} \quad (2)$$

In the NONAME system, the position of the true pole is computed by subroutine POLE. The station vectors are referenced to the true pole by subroutine TRUEP.

POLE  
TRUEP

## SECTION 2.6

### MEASUREMENT MODELING AND RELATED DERIVATIVES

The observations in NONAME are geocentric in nature. The computed values for the observations are obtained by applying these geometric relationships to the computed values for the relative positions and velocities of the satellite and the observer at the desired time.

In addition to the geometric relationships, NONAME allows for a timing bias and for a constant bias to be associated with a measurement type from a given station. Both of these biases are optional.

The measurement model for NONAME is therefore

$$C_{t+\Delta t} = f_t(\bar{r}, \dot{\bar{r}}, \bar{r}_{ob}) + b + \dot{f}_t(\bar{r}, \dot{\bar{r}}, \bar{r}_{ob}) \cdot \Delta t \quad (1)$$

where

$C_{t+\Delta t}$  is the computed equivalent of the observation taken at time  $t+\Delta t$ ,

$\bar{r}$  is the Earth-fixed position vector of the satellite,

$\bar{r}_{ob}$  is the Earth-fixed position vector of the station,

$f_t(\bar{r}, \dot{\bar{r}}, \bar{r}_{ob})$  is the geometric relationship defined by the particular observation type at time  $t$ ,

$b$  is a constant bias on the measurement, and

$\Delta t$  is the timing bias associated with the measurement.

The functional dependence of  $f_t$  was explicitly stated for the general case. Many of the measurements are functions only of the position vectors and are hence not functions of the satellite velocity vector  $\bar{r}$ . We will hereafter refer to  $f_t$  without the explicit functional dependence for rotational convenience.

As was indicated earlier in Section 2.2.2, we require the partial derivatives of the computed values for the measurements with respect to the parameters being determined (see also Section 2.10.1). These parameters are:

- o the true of date position and velocity of the satellite at epoch. These correspond to the inertial position and velocity which are the initial conditions for the equations of motion,
- o force model parameters,
- o the Earth-fixed station positions,
- o measurement biases.

These parameters are implicitly divided into a set  $\bar{\alpha}$  which are not concerned with the dynamics of satellite motion, and a set  $\bar{\beta}$  which are.

The partial derivatives associated with the parameters  $\bar{\alpha}$ ; i.e., station positions and measurement biases are computed directly at the given observation times. The partial derivatives with respect to the parameters  $\bar{\beta}$ ; i.e., the epoch position and velocity and the force model parameters, must be determined according to a chain rule:

$$\frac{\partial C_{t+\Delta t}^1}{\partial \bar{\beta}} = \frac{\partial C_{t+\Delta t}}{\partial \bar{x}_t} \frac{\partial \bar{x}_t}{\partial \bar{\beta}} \quad (2)$$

where

$\bar{x}_t$  is the vector which describes the satellite position and velocity in true of date coordinates.

The partial derivatives  $\frac{\partial C_{t+\Delta t}}{\partial \bar{x}_t}$  are computed directly at the given observation times, but the partial derivatives  $\frac{\partial \bar{x}_t}{\partial \bar{\beta}}$  may not be so obtained. These latter relate the true of date position and velocity of the satellite at the given time to the parameters at epoch through the satellite dynamics.

The partial derivatives  $\frac{\partial \bar{x}_t}{\partial \bar{\beta}}$  are called the variational partials and are obtained by direct numerical integration of the variational equations. As will be shown in Section 2.8.2, these equations are analogous to the equations of motion.

Let us first consider the partial derivatives of the computed values associated with the parameters in  $\bar{\beta}$ . We have

$$\frac{\partial C_{t+\Delta t}}{\partial \bar{\beta}} = \frac{\partial f_t}{\partial \bar{x}_t} \frac{\partial \bar{x}_t}{\partial \bar{\beta}} \quad (3)$$

Note that we have dropped the partial derivative with respect to  $\bar{\beta}$  of the differential product  $\int_t \Delta t$ . This is because we use first order Taylor series approximation in our error model and hence higher order terms are assumed negligible. This linearization is also completely consistent with the linearization assumptions made in the solution to the estimation equations (Section 2.10.1).

The partial derivatives  $\frac{\partial f_t}{\partial \bar{x}_t}$  are computed by transforming the partial derivatives  $\frac{\partial f_t}{\partial \bar{r}}$  and  $\frac{\partial f_t}{\partial \bar{r}}$  from the Earth-fixed system to the true of date system (see Section 2.3.4). These last are the partial derivatives of the geometric relationships given later in this section (2.6.2).

In summary, the partial derivatives required for computing the  $\frac{\partial C_{t+\Delta t}}{\partial \beta}$ , the partial derivatives of the computed value for a given measurement, are the variational partials and the Earth-fixed geometric partial derivatives.

The partial derivatives of the computed values with respect to the station positions are simply related to the partial derivatives with respect to the satellite position at time  $t$ :

$$\frac{\partial C_{t+\Delta t}}{\partial \bar{r}_{ob}} = \frac{\partial f_t}{\partial \bar{r}_{ob}} = - \frac{\partial f_t}{\partial \bar{r}} \quad (4)$$

where  $\bar{r}$  is of course the satellite position vector in Earth-fixed coordinates. This simple relationship is a direct result of the symmetry in position coordinates. The function  $f$  is a geometric function of the relative position; i.e., the differences in position coordinates which will be the same in any coordinate system.

The partial derivatives with respect to the biases are obvious:

$$\frac{\partial C_{t+\Delta t}}{\partial b} = 1 \quad (5)$$

$$\frac{\partial C_{t+\Delta t}}{\partial (\Delta t)} = f_t \quad (6)$$

In the remainder of this section, we will be concerned with the calculation of the geometric function  $f_t$  and its derivatives. These derivatives have been shown above to be the partial derivatives with respect to satellite position and velocity at time  $t$  and the time rate of change of the function,  $f_t$ .

The subroutine breakdown for the calculation of these quantities in NONAME is as follows: The geometric relationships and the geometric partial derivatives are implemented in subroutine PREDCT. The time rates of change are coded in subroutine OBSDOT.

The data preprocessing also requires some use of these formulas for computing measurement equivalents. These are then also implemented in subroutine PROCES.

PREDCT

OBSDOT

PROCES

### 2.6.1 The Geometric Relationships

The current types of observation in NONAME are:

- o right ascension and declination
- o range
- o range rate
- o l and m direction cosines
- o X and Y angles
- o azimuth and elevation.
- o altimeter height and rate\*

The geometric relationship which corresponds to each of these observations is presented below: It should be noted that in addition to the Earth-fixed or inertial coordinate systems, some of these utilize topocentric coordinate systems. These last are presented in Section 2.5.2.

---

\* There is currently no input format set for these measurement types.

Range:

Consider the station-satellite vector:

GRHRAN

$$\bar{\rho} = \bar{r} - \bar{r}_{ob} \quad (1)$$

where

$\bar{r}$  is the satellite position vector ( $x, y, z$ ) in the geocentric Earth-fixed system, and

$\bar{r}_{ob}$  is the station vector in the same system.

The magnitude of this vector,  $\rho$ , is the (slant) range, which is one of the measurements.

Range rate:

The time rate of change of this vector  $\bar{\rho}$  is

GRHRAN

$$\dot{\bar{\rho}} = \dot{\bar{r}} \quad (2)$$

PREDCT

OBSDOT

as the velocity of the observer in the Earth-fixed system is zero. Let us consider that

$$\bar{\rho} = \rho \hat{u} \quad (3)$$

where

$\hat{u}$  is the unit vector in the direction of  $\bar{\rho}$ .

Thus we have

GRHRAN  
PREDCT  
OBSDOT

$$\dot{\rho} = \dot{\rho} \hat{u} + \dot{\rho} \hat{u} \quad (4)$$

The quantity  $\dot{\rho}$  in the above equation is the computed value for the range rate and is determined by

$$\dot{\rho} = \dot{u} + \dot{r} \quad (5)$$

Altimeter height:

The altimeter height and rate are unique in that the satellite is making the observation. While these are actually measurements from the satellite to the surface of the Earth, they are taken to be measurements of the spheroid height and the time rate of change of that quantity for obvious reasons. Using the formula for spheroid height previously determined in Section 2.5.1, we have:

PREDCT

$$H_{alt} = r - a_e - \frac{3}{2} a_e f^2 \left(\frac{z}{r}\right)^4 \quad (6)$$

$$+ (a_e f + \frac{3}{2} a_e f^2) \left(\frac{z}{r}\right)^2$$

where ,

PREDCT

$a_e$  is the Earth's mean equatorial radius,

$f$  is the Earth's flattening, and

$z$  is  $r_3$ , the z component of the Earth-fixed satellite vector

Altimeter rate:

The altimeter rate is determined by a chain rule:

PREDCT

$$\dot{H}_{alt} = \nabla H_{alt} \cdot \dot{\vec{r}} \quad (7)$$

The required partial derivatives are given in the section on geometric partials.

The topocentric right ascension  $\alpha$  and declination  $\delta$  are inertial coordinate system measurements as illustrated in Figure 1. NONAME computes these angles from the components of the Earth-fixed station-satellite vector and the Greenwich hour angle  $\Omega_g$ .

$$\alpha = \tan^{-1} \left( \frac{\rho_2}{\rho_1} \right) + \Omega_g \quad (8)$$

$$\delta = \sin^{-1} \left( \frac{\rho_3}{\rho} \right) \quad (9)$$

The remaining measurements are in the topocentric horizon coordinate system. These all require the  $\hat{N}$ ,  $\hat{Z}$ , and  $\hat{E}$  (north, zenith, and east baseline) unit vectors which describe the coordinate system.

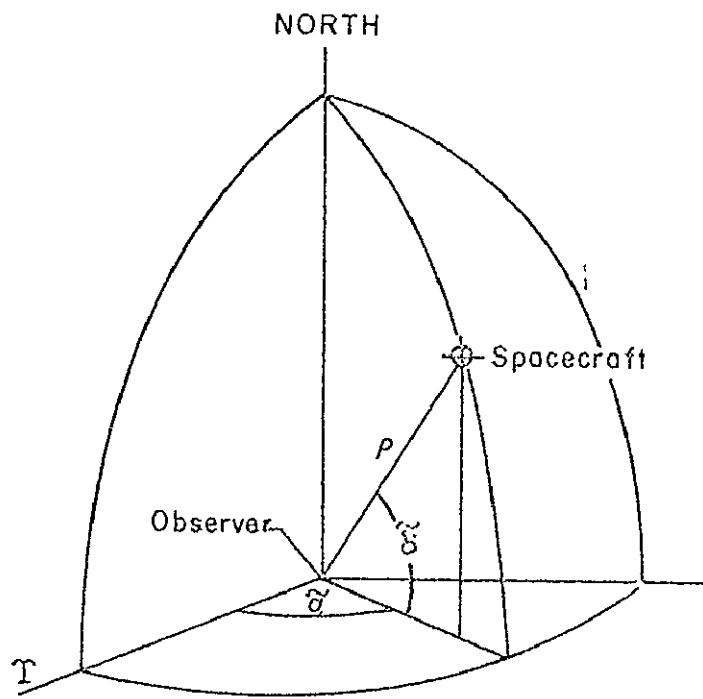


FIGURE 1. Topocentric right ascension & declination angles

Direction cosines:

There are three direction cosines associated with the station-satellite vector in the topocentric system. These are:

$$\ell = \hat{u} \cdot \hat{E} \quad (10)$$

$$m = \hat{u} \cdot \hat{N}$$

$$n = \hat{u} \cdot \hat{Z}$$

The  $\ell$  and  $m$  direction cosines are observation types for NONAME.

X and Y angles:

The X and Y angles are illustrated in Figure 2. They are computed by

$$x_a = \tan^{-1} \left( \frac{\ell}{n} \right) \quad (11)$$

$$y_a = \sin^{-1} (m) \quad (12)$$

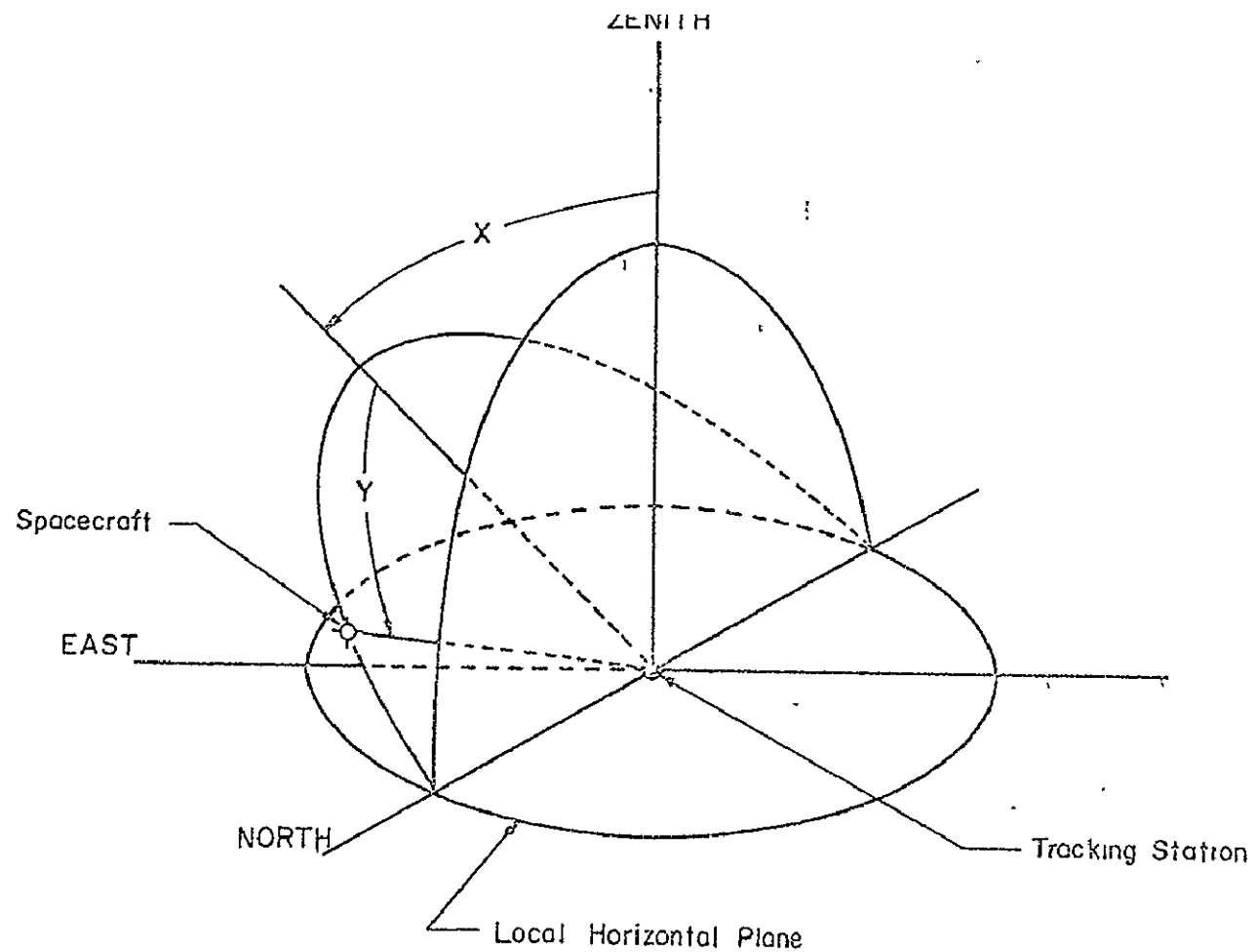


FIGURE 2. X and Y Angles

Figure 3 illustrates the measurements of azimuth and elevation. These angles are computed by:

PREDCT

$$A_z = \tan^{-1} \frac{\lambda}{m} \quad ; \quad (13)$$

$$E_\lambda = \sin^{-1} (n) \quad (14)$$

### 2.6.2 The Geometric Partial Derivatives

PREDCT

The partial derivatives for each of the calculated geometric equivalents with respect to the satellite positions and velocity are given here. All are in the geocentric, Earth-fixed system. (The  $r_i$  refer to the Earth-fixed components of  $\vec{r}$ .)

Range:

$$\frac{\partial \rho}{\partial r_i} = \frac{r_i}{\rho} \quad (1)$$

Range rate:

$$\frac{\partial \dot{\rho}}{\partial r_i} = \frac{1}{\rho} \left[ \dot{r}_i - \frac{\dot{\rho} r_i}{\rho} \right] \quad (2)$$

$$\frac{\partial \dot{\rho}}{\partial \dot{r}_i} = \frac{r_i}{\rho} \quad (3)$$

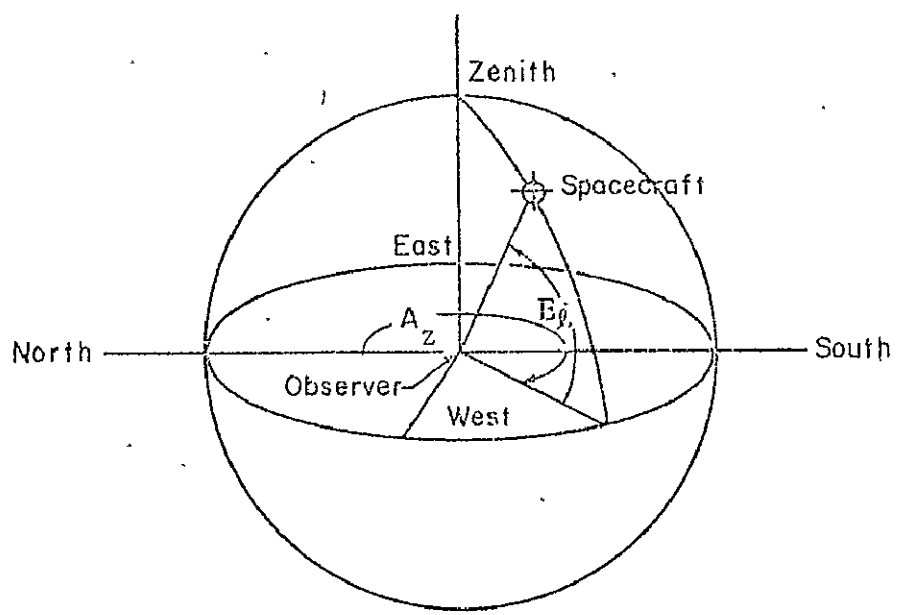


FIGURE 3. Azimuth and Elevation Angles

Altimeter range.

PREDCT

$$\frac{\partial H_{alt}}{\partial r_i} = \frac{r_i}{r} + \frac{1}{r} \left[ \left( 2 a_c f + 3 a_e f^2 \right) \left( \frac{z}{r} \right) - 6 a_e f^2 \left( \frac{z}{r} \right)^3 \right] \times$$

$$\left[ \frac{\partial z}{\partial r_i} - \frac{z x_j}{r^2} \right]$$

Altimeter Range Rate:

$$\frac{\partial H_{alt}}{\partial r_i} = \frac{\partial}{\partial r_i} \left( \nabla H_{alt} \right) \cdot \frac{\dot{r}}{r} \quad (5)$$

$$\frac{\partial^2 H_{alt}}{\partial r_i \partial r_j} = \frac{1}{r} \left[ \frac{\partial r_j}{\partial r_i} - \frac{r_i r_j}{r^2} \right] \quad (6)$$

$$+ \left[ \left( 2 a_c f + 3 a_e f^2 \right) \left( \frac{z}{r} \right) - 6 a_e f^2 \left( \frac{z}{r} \right)^3 \right] \times$$

$$\left[ \frac{1}{r^2} \left( \frac{-r_j}{r} \frac{\partial z}{\partial r_i} - \frac{r_i}{r} \frac{\partial z}{\partial r_j} + \frac{3 z r_i r_j}{r^3} \right. \right. \\ \left. \left. - \frac{z}{r} \frac{\partial r_i}{\partial r_j} \right) \right] +$$

$$\left[ \left( 2 a_c f + 3 a_e f^2 \right) - 18 a_e f^2 \left( \frac{z}{r} \right)^2 \right] X$$

$$\left[ \frac{1}{r} \frac{\partial z}{\partial r_i} - \frac{z r_i}{r^3} \right] \left[ \frac{1}{r} \frac{\partial z}{\partial r_j} - \frac{z r_j}{r^3} \right]$$

$$\frac{\partial H_{alt}}{\partial r_i} = \frac{\partial H_{alt}}{\partial r_i}$$

Right Ascension:

$$\frac{\partial \alpha}{\partial r_1} = \frac{-\rho_2}{\sqrt{\rho_1^2 + \rho_2^2}} \quad (7)$$

$$\frac{\partial \alpha}{\partial r_2} = \frac{\rho_1}{\sqrt{\rho_1^2 + \rho_2^2}} \quad (8)$$

$$\frac{\partial \delta}{\partial r_3} = 0 \quad (9)$$

Declination:

$$\frac{\partial \delta}{\partial r_1} = \frac{-\rho_1 \rho_3}{\rho^2 \sqrt{\rho_1^2 + \rho_2^2}} \quad (10)$$

$$\frac{\partial \delta}{\partial r_2} = \frac{-\rho_2 \rho_3}{\rho \sqrt{\rho_1^2 + \rho_2^2}} \quad (11) \quad \text{PREDCT}$$

$$\frac{\partial \delta}{\partial r_3} = \frac{\sqrt{\rho_1^2 + \rho_2^2}}{\rho^2} \quad (12)$$

Direction Cosines:

$$\frac{\partial \ell}{\partial r_i} = \frac{1}{\rho} \left[ E_i - \ell u_i \right] \quad (13)$$

$$\frac{\partial m}{\partial r_i} = \frac{1}{\rho} \left[ N_i - m u_i \right] \quad (14)$$

$$\frac{\partial n}{\partial r_i} = \frac{1}{\rho} \left[ Z_i - n u_i \right] \quad (15)$$

X and Y Angles:

PREDCT

$$\frac{\partial X_a}{\partial r_i} = \frac{nE_i - \ell Z_i}{\rho(1-m^2)} \quad (16)$$

$$\frac{\partial Y_a}{\partial r_i} = \frac{N_i - mu_i}{\rho\sqrt{1-m^2}} \quad (17)$$

Azimuth and Elevation:

$$\frac{\partial A_z}{\partial r_i} = \frac{mE_i - \ell N_i}{\rho\sqrt{1-n^2}} \quad (18)$$

$$\frac{\partial E_\ell}{\partial r_i} = \frac{Z_i - nu_i}{\rho(1-n^2)} \quad (19)$$

The derivatives of each measurement type with respect to time is presented below. All are in the Earth-fixed system.

Range:

$$\dot{\rho} = \hat{u} \cdot \dot{\bar{r}} \quad (1)$$

Range Rate:

The range rate derivative deserves special attention. Remembering that

$$\dot{\bar{r}} = \dot{\bar{r}} , \quad (2)$$

We write

$$\dot{\rho} = \hat{u} \cdot \dot{\bar{\rho}} \quad (3)$$

Thus

$$\ddot{\rho} = \hat{u} \cdot \dot{\bar{\rho}} + \hat{\bar{u}} \cdot \ddot{\bar{\rho}} \quad (4)$$

Because

OBS DOT

$$\dot{\bar{\rho}} = \frac{d}{dt} (\bar{\rho} \hat{u}) = \bar{\rho} \dot{\hat{u}} + \hat{u} \dot{\bar{\rho}} \quad (5)$$

we may substitute in Equation 4 above for  $\hat{u}$ :

$$\ddot{\rho} = \frac{1}{\rho} (\dot{\bar{\rho}} + \dot{\rho} - \dot{\bar{\rho}} \hat{u} + \hat{u} \ddot{\bar{\rho}}) + \hat{u} \cdot \ddot{\bar{\rho}} \quad (6)$$

or, as

$$\dot{\rho} = \hat{u} \cdot \dot{\bar{\rho}} \quad (7)$$

we may write

$$\ddot{\rho} = \frac{1}{\rho} (\dot{\bar{\rho}} + \dot{\rho} - \dot{\rho}^2 + \bar{\rho} \cdot \ddot{\bar{\rho}}) \quad (8)$$

In order to obtain  $\ddot{\bar{\rho}}$ , we use the limited gravity potential (see Section 2.8.3):

$$= \frac{GM}{r} \left( 1 - \frac{C_{20} a_e^2}{r^2} P_2^0 (\sin \phi) \right) \quad (9)$$

The gradient of this potential with respect to the Earth-fixed position coordinates of the satellite is the part of  $\vec{\rho}$  due to the geopotential: OBSDOT

$$\frac{\partial U}{\partial r_i} = -\frac{GM}{r^3} \left[ 1 - \frac{3 a_e^2 C_{20}}{2 r^2} \left( 5 \sin^2 \phi - 1 - 2 \frac{z}{r_i} \right) \right] r_i \quad (10)$$

We must add to this the effect of the rotation of the coordinate system. (The Earth-fixed coordinate system rotates with respect to the true of date coordinates with a rate  $\dot{\theta}_g$ , the time rate of change of the Greenwich hour angle.)

The components of  $\vec{\rho}$  are then

$$\rho_1 = \frac{\partial U}{\partial r_1} + [x \cos \theta_g + y \sin \theta_g] \dot{\theta}_g + r_2 \dot{\theta}_g \quad (11)$$

$$\rho_2 = \frac{\partial U}{\partial r_2} + [-x \sin \theta_g + y \cos \theta_g] \dot{\theta}_g - r_1 \dot{\theta}_g \quad (12)$$

$$\rho_3 = \frac{\partial U}{\partial r_3} = \frac{\partial U}{\partial z} \quad (13)$$

The bracketed quantities above correspond to the coordinate transformations coded in subroutines XEFIX and YEFIX. These XEFIX transforms are used on the true of date satellite velocity components x and y. The interested reader should refer to Section 2.3.4 for further information on transformations between Earth-fixed and true of date coordinates. OBSDOT YEFIX

It should be noted that all quantities in this formula, with the exception of those quantities bracketed, are Earth-fixed values. (The magnitude  $r$  is invariant with respect to the coordinate system transformations.)

ORSDO'

The remaining time derivatives are tabulated here:

$$\text{Right ascension: } \dot{\alpha} = \frac{u_1 \dot{r}_2 - u_2 \dot{r}_1}{\rho (1-u_3^2)} \quad (14)$$

$$\text{Declination: } \dot{\delta} = \frac{\dot{r}_3 - \rho u_3}{\rho \sqrt{1-u_3^2}} \quad (15)$$

$$\text{Direction Cosines: } \dot{\ell} = \frac{\dot{\rho} \cdot \hat{E} - \ell \dot{\rho}}{\rho} \quad (16)$$

$$\dot{m} = \frac{\dot{\rho} \cdot \hat{N} - m \dot{\rho}}{\rho} \quad (17)$$

X and Y angles:  $\dot{X}_a = \frac{\dot{\rho} \cdot (\hat{n} \cdot \hat{E} - \lambda \hat{Z})}{\rho (1 - m^2)}$  OBS DOT (18)

$\dot{Y}_a = \frac{\dot{\rho} \cdot \hat{N} - m \dot{\rho}}{\rho \sqrt{1 - m^2}}$  (19)

Azimuth:  $\dot{A}_z = \frac{\dot{\rho} \cdot (\hat{m} \hat{E} - \lambda \hat{N})}{\rho (1 - m^2)}$  (20)

Elevation:  $\dot{E}_\lambda = \frac{\dot{\rho} \cdot \hat{Z} - m \dot{\rho}}{\rho \sqrt{1 - m^2}}$  (21)

## SECTION 2.7

### DATA PREPROCESSING

The function of data preprocessing is to convert and correct the data. These corrections and conversions relate the data to the physical model and to the coordinate and time reference systems used in NONAME. The data corrections and conversions implemented in NONAME are to

- transform all observation times to Al time at the satellite
- refer right ascension and declination observations to the true equator and equinox of date.
- correct range measurements for transponder delay and gating effects
- correct SAO right ascension and declination observations for diurnal aberration
- correct for refraction
- convert TRANET Doppler observations into range rate measurements.

These conversions and corrections are applied to the data on the first iteration of each arc. Each of these preprocessing items is considered in greater detail in the subsections which follow.

### 2.7.1 Time Preprocessing

The time reference system used to specify the time of each observation is determined by a time identifier on the data record. This identifier also specifies whether the time recorded was the time at the satellite or at the observing station.

The preprocessing in NONAME transforms all observations to Al time in either GEOSRD or DODSRD. If the time recorded is the time at the station, it is converted to time at the satellite. This conversion is applied in subroutine PROCES using a correction equal to the propagation time between the spacecraft and the observing station. The station-satellite distance used for this correction is computed from the initial estimate of the trajectory.

DODSRD  
GEOSRD  
PROCES

There is special preprocessing for right ascension and declination measurements from the GEOS satellites when input in National Space Science Data Center format. If the observation is passive, the image recorded is an observation of light reflected from the satellite and the times are adjusted for propagation delay as above. If the observation is active, the image recorded is an observation of light transmitted from the optical beacon on the satellite. The beacons on the GEOS satellites are programmed to produce a sequence of seven flashes at four second intervals starting on an even minute. For the active observations, the times are set equal to the programmed flash time with a correction applied for known clock errors (Reference 1), plus half a millisecond, the time allowed for flash buildup.

GEOSRD

The corrections for the active observations are applied in GEOSRD, which calls SATCLC and SATCL2 to evaluate the corrections for GEOS 1 and GEOS 2, respectively. These routines compute the correction by simple linear interpolation in a table of known errors in the satellite on-board clock.

GEOSRD  
SATCLC  
SATCL2

### 2.7.2 Reference System Conversion to True of Date

DODSRD  
EQUATR  
GEOSRD

The camera observations, right ascension and declination, may be input referred to the mean equator and equinox of date, to the true equator and equinox of date, or to the mean equator and equinox of some standard epoch. The NONAME system transforms these observations to the true equator and equinox of date in subroutines GEOSRD and DODSRD. The necessary precession and nutation is performed by subroutine EQUATR.

### 2.7.3 Transponder Delay and Gating Effects

The range observations may be corrected for transponder delay or gating errors. If requested, the NONAME subroutine PROCES applies the corrections.

PROCES

The transponder delay correction is computed as a polynomial in the range rate:

$$\Delta\rho = a_0 + a_1 \rho + a_2 (\rho)^2 \quad (1)$$

where  $a_0$ ,  $a_1$ , and  $a_2$  depend on the characteristics of the particular satellite.

A gating error is due to the fact that actual range measurements are either time delays between transmitted and received radar pulses or the phase

shifts in the modulation of a received signal with respect to a coherent transmitted signal. Thus there is the possibility of incorrectly identifying the returned pulse or the number of integral phase shifts. The difference between the observed range and the computed range on the first iteration of the arc is used to determine the appropriate correction. The correction is such that there is less than half a gate, where the gate is the range equivalent of the pulse spacing or phase shift. The appropriate gate of course depends on the particular station.

PROCES

:

#### 2.7.4 Diurnal Aberration

Right ascension and declination may be corrected for diurnal aberration, which is an effect due to the rotation of the Earth. The corrections for these are given by

PROCES

$$\Delta\alpha = 0.0213 r_{ob} \cos \phi' \cos h_s \sec \delta \quad (1)$$

$$\Delta\delta = 0.320 r_{ob} \cos \phi' \sin h_s \sin \delta \quad (2)$$

where

$r_{ob}$  is the geocentric distance in units of Earth radius (assumed to be 1).

$\phi'$  is the geocentric latitude of the station, and

$h_s$  is the hour angle

PROCES

$\delta$  as shown in the formula is the observed declination.

This and related topics are discussed in great detail in the Explanatory Supplement.

This correction is applied in subroutine PROCES. It should be noted that this applies only to SAO network stations.

#### 2.7.5 Refraction Corrections

The NONAME system can apply corrections to all of the observational types significantly affected by refraction. The corrections requested are applied by subroutine PROCES.

PROCES

Right Ascension and Declination:

The right ascension and declination measurements for SAO stations may require correction for parallactic refraction:

$$\alpha = \alpha' - \Delta R \sec \delta' \sin P_a \quad (1)$$

$$\delta = \delta' - \Delta R \cos \delta' \sin P_a \quad (2)$$

v

where

PROCES

$\Delta R$  is the differential refraction;

$P_a$  is the parallactic angle; i.e., the angle at the object in the pole - object - zenith; and

$\alpha'$  and  $\delta'$  are the observed values of the right ascension and declination.

The differential refraction  $\Delta R$  is computed by (Reference 2)

$$\Delta R = 435\text{''}0 \frac{\tan Z_o}{\rho \cos Z_o} \left| 1 - \exp(-0.1385 \rho \cos Z_o) \right| \quad (3)$$

where

$Z_o$  is the observed zenith angle,

$\rho$  is the topoconic range in kilometers, and

$\Delta R$  is the differential refraction in minutes of arc

Range:

The refraction corrections  $\Delta\rho$  applied to range observations is computed as follows:

$$\Delta\rho = \frac{2.77n_s}{328.5(0.026+\sin E_\ell)} \quad (4)$$

where

$E_\ell$  is the elevation angle computed from the initial estimate of the trajectory

and

$n_s$  is the surface index of refraction; if this value is not specified, it is assumed to be 1.

Range Rate:

For range-rate, the correction  $\Delta\rho$  is derived from the range correction:

$$\Delta\rho = \frac{2.77n_s \cos E_\ell}{328.5(0.026+\sin E_\ell)^2} \dot{E}_\ell \quad (5)$$

where

PROCES

$E_\ell$  is the computed rate of change of elevation.

For observations of range or range rate from certain stations, there is a correction to account for the mean daily variation of the surface index of refraction. This correction, which is a correction to the product  $\left(\frac{2.77}{328.5} n_s\right)$ , is computed by subroutine REFION by linear interpolation in an hourly table.

REFION

Elevation:

For elevation observations the correction  $\Delta E_\ell$  is computed as follows:

PROCES

$$\Delta E_\ell = \frac{n_s 10^3}{16.44 + 930 \tan E_\ell} \quad (6)$$

Azimuth is not affected by refraction.

Direction Cosines:

The corrections  $\Delta \ell$  and  $\Delta m$  are derived from the elevation correction:

$$\Delta \ell = -\sin A_z \sin (E_\ell) \Delta E_\ell \quad (7)$$

$$\Delta m = -\cos A_z \sin (E_\ell) \Delta E_\ell \quad (8)$$

where  $A_z$  is the azimuth angle computed from the initial estimate of the trajectory.

PROCES

X and Y Angles:

For X and Y angles the corrections  $\Delta X$  and  $\Delta Y$  are computed as follows:

$$\Delta X_a = - \frac{\sin A_z \Delta E_\ell}{(\sin^2 E_\ell + \sin^2 A_z \cos^2 E_\ell)} \quad (9)$$

$$\Delta Y_a = - \frac{\cos A_z \sin E_\ell \Delta E_\ell}{\sqrt{1 - \cos^2 A_z \cos^2 E_\ell}} \quad (10)$$

Note that these are also derived from the elevation correction.

#### 2.7.6 Tranet Doppler Observations

TRANET Doppler observations are received as a series of measured frequencies with an associated base frequency for each station pass. Using the following relationship, the NONAME system converts these observations to range rate measurements in subroutine GEOSRD:

GEOSRD

$$\rho = \frac{c(F_B - F_M)}{F_M} \quad (1)$$

where

$F_M$  is the measured frequency,

$F_B$  is the base frequency,

and

$c$  is the velocity of light.

SECTION 2.8  
FORCE MODEL AND VARIATIONAL EQUATIONS

A fundamental part of the NONAME system requires computing positions and velocities of the spacecraft at each observation time. The dynamics of the situation are expressed by the equations of motion, which provide a relationship between the orbital elements at any given instant and the initial conditions of epoch. There is an additional requirement for variational partials, which are the partial derivatives of the instantaneous orbital elements with respect to the parameters at epoch. These partials are generated using the variational equations, which are analogous to the equations of motion.

2.8.1 Equations of Motion

In a geocentric inertial rectangular coordinate system, the equations of motion for a spacecraft are of the form

$$\ddot{\bar{r}} = -\frac{\mu \bar{r}}{r^3} + \bar{A} \quad (1)$$

where

$\bar{r}$  is the position vector of the satellite.

$\mu$  is  $GM$ , where  $G$  is the gravitational constant and  $M$  is the mass of the Earth.

$\bar{A}$  is the acceleration caused by the asphericity of the Earth, extra-terrestrial gravitational forces, atmospheric drag, and solar radiation.

This provides a system of second order equations which, given the epoch position and velocity components, may be integrated to obtain the position and velocity at any other time. This direct integration of these accelerations in Cartesian coordinates is known as Cowell's method and is the technique used in NONAME's orbit generator. This method was selected for its simplicity and its capacity for easily incorporating additional perturbative forces.

There is an alternative way of expressing the above equations of motion:

$$\ddot{\bar{r}} = \nabla U + \bar{A}_D + \bar{A}_R \quad (2)$$

where

$U$  is the potential field due to gravity,

$\bar{A}_D$  contains the accelerations due to drag, and

$\bar{A}_R$  contains the accelerations due to solar radiation pressure.

This is, of course, just a regrouping of terms coupled with a recognition of the existence of a potential field. This is the form used in NONAME.

The inertial coordinate system in which these equations of motion are integrated in NONAME is that system corresponding to the true of date system of  $o^h_o$  of the epoch day. The complete definitions for these coordinate systems (and the Earth-fixed system) are presented in Section 2.3.

The evaluation of the accelerations for  $\ddot{\vec{r}}$  is controlled by subroutine F. This evaluation is performed in the true of date system. Thus there is a requirement that the inertial position and velocity output from the integrator be transformed to the true of date system for the evaluation of the accelerations, and a requirement to transform the computed accelerations from the true of date system to the inertial system. These transformations are performed by subroutine REFCOR (which controls the precession and nutation routines, PRECES and NUTATE) and is controlled by subroutine F.

F

REFCOR

### 2.8.2 The Variational Equations

The variational equations have the same relationship to the variational partials as the satellite position vector does to the equations of motion. The variational partials are defined as the  $\frac{\partial \vec{x}}{\partial \beta}$  where  $\vec{x}_t$  spans the true of date position and velocity of the satellite at a given time; i.e.,

VEVAL

$$\bar{x}_t = \{x, y, z, \dot{x}, \dot{y}, \dot{z}\} ;$$

VEVAL

and  $\bar{\beta}$  spans the epoch parameters; i.e.,

$x_0, y_0, z_0$  the satellite position vector at epoch

$\dot{x}_0, \dot{y}_0, \dot{z}_0$  the satellite velocity vector at epoch

$C_D$  the satellite drag factor

$C_R$  the satellite emissivity factor

$C_{nm}, S_{nm}$  gravitational harmonic coefficients for each  $n, m$  pair being determined.

Let us first realize that the variational partials may be partitioned according to the satellite position and velocity vectors at the given time. Thus the required partials are

$$\frac{\partial \bar{r}}{\partial \bar{\beta}}, \frac{\partial \dot{\bar{r}}}{\partial \bar{\beta}} \quad (1)$$

where

VEVAL

$\bar{r}$  is the satellite position vector  $(x, y, z)$  in the true of date system, and

$\dot{\bar{r}}$  is the satellite velocity vector  $(\dot{x}, \dot{y}, \dot{z})$  in the same system.

The first of these,  $\frac{\partial \bar{r}}{\partial \beta}$ , can be obtained by the double integration of

$$\frac{d^2}{dt^2} \left( \frac{\partial \bar{r}}{\partial \beta} \right) \quad (2)$$

or rather, since the order of differentiation may be exchanged,

$$\frac{\partial \ddot{\bar{r}}}{\partial \beta} \quad (3)$$

Note that the second set of partials,  $\frac{\partial \dot{\bar{r}}}{\partial \beta}$ , may be obtained by a first order integration of  $\frac{\partial \ddot{\bar{r}}}{\partial \beta}$ . Hence we recognize that the quantity to be integrated is  $\frac{\partial \dot{\bar{r}}}{\partial \beta}$ . Using the second form given for the equations of motion in the previous subsection, the variational equations are given by

$$\frac{\partial \ddot{\mathbf{r}}}{\partial \beta} = \frac{\partial}{\partial \beta} (\nabla U + \bar{A}_R + \bar{A}_D) \quad \text{VEVAL (4)}$$

where

$U$  is the potential field due to gravitational effects

$\bar{A}_R$  is the acceleration due to radiation pressure

$\bar{A}_D$  is the acceleration due to drag

The similarity to the equations of motion is now obvious.

At this point we must consider a few items:

VEVAL

- The potential field is a function only of position. Thus we have

$$\frac{\partial}{\partial \bar{\beta}} \left( \frac{\partial U}{\partial r_i} \right) = \sum_{m=1}^3 \left( \frac{\partial^2 U}{\partial r_i \partial r_m} \right) \frac{\partial r_m}{\partial \bar{\beta}} \quad (5)$$

- The partials of solar radiation pressure with respect to the geopotential coefficients, the drag coefficient, and the satellite velocity are zero, and the partials, with respect to satellite position, are negligible.
- Drag is a function of position, velocity, and the drag coefficient. The partials, with respect to the geopotential coefficients and satellite emissivity, are zero, but we have

$$\frac{\partial \bar{A}_D}{\partial \bar{\beta}} = \frac{\partial A_D}{\partial \bar{x}} \frac{\partial \bar{x}_t}{\partial \bar{\beta}} + \frac{\partial \bar{A}_D}{\partial C_D} \quad (6)$$

Let us write our variational equations in matrix notation. We define

VEVAL

$n$  to be the number of epoch parameters in  $\bar{\beta}$

$F$  is a  $3 \times n$  matrix whose  $j^{\text{th}}$  column vectors are  $\frac{\partial \bar{r}}{\partial \beta_j}$

$U_{2C}$  is a  $3 \times 6$  matrix whose last 3 columns are zero and whose first 3 columns are such that the  $i, j^{\text{th}}$  element is given by

$$\frac{\partial^2 U}{\partial r_i \partial r_j}$$

$D_r$  is a  $3 \times 6$  matrix whose  $j^{\text{th}}$  column is defined by  $\frac{\partial \bar{A}_D}{\partial x_t}_j$

$X_m$  is a  $6 \times n$  matrix whose  $i^{\text{th}}$  row is given by  $\frac{\partial \bar{x}_t}{\partial \beta_j}$ . Note that  $X_m$  contains the variational partials.

$f$  is a  $3 \times n$  matrix whose first six columns are zero and whose last  $n-6$  columns are such that the  $i, j^{\text{th}}$  element is given by

$\frac{\partial}{\partial \beta_j} (\nabla U + \bar{A}_D + \bar{A}_R)$ . Note that the first six columns correspond to the first six elements of  $\bar{\beta}$  which are the epoch position and velocity. (This matrix contains the direct partials of  $\bar{x}_t$  with respect to  $\bar{\beta}$ .)

We may now write

VEVAL

$$F = [U_{2C} + D_r] X_m + f \quad (7)$$

This is a matrix form of the variational equations.

Note that  $U_{2C}$ ,  $D_r$ , and  $f$  are evaluated at the current time, whereas  $X_m$  is the output of the integration. Initially, the first six columns of  $X_m$  plus the six rows form an identity matrix; the rest of the matrix is zero (for  $i=j$ ,  $X_{m,i,j} = 1$ ; for  $i \neq j$ ,  $X_{m,i,j} = 0$ ).

Because each force enters into the variational equations in a manner which depends directly on its model, the specific contribution of each force is discussed in the section with the force model. We shall, however, note a few clerical details here.

The task of computing these variational equations in the NONAME system is largely accomplished by subroutine VEVAL. The matrix dimensions given were for notational convenience; empty rows and columns are not programmed.

The above equation is also applied in subroutine PREDCT to "chain the partials back to epoch," that is, to relate the partials at the time of each set of measurements back to epoch.

PREDCT

The matrix for  $\frac{\partial \bar{x}_t}{\partial \beta}$ ,  $\bar{x}_m$  above, is initialized in ORBIT subroutine ORBIT.

The contributions of subroutines DENSTY, DRAG, . DENSTY  
EGRAV, F, and RESPAR will be discussed as part of the DRAG  
following subsections. The matrices  $U_{2c}$  and f will F  
be referred to in each subsection as though the par- RESPAR  
ticular force being discussed had the only contribution.

### 2.8.3 The Earth's Potential

The Earth's potential is most conveniently expressed in a spherical coordinate system as is shown in Figure 1. By inspection:

- $\phi'$ , the geocentric latitude, is the angle measured from  $\overline{OA}$ , the projection of  $\overline{OP}$  in the X-Y plane, to the vector  $\overline{OP}$ .
- $\lambda$ , the east longitude, is the angle measured from the positive direction of the X axis to  $\overline{OA}$ .
- $r$  is the magnitude of the vector  $\overline{OP}$ .

Let us consider the point P to be the satellite position. Thus,  $\overline{OP}$  is the geocentric Earth-fixed satellite vector corresponding to  $\overline{r}$ , the true of date satellite vector, whose components are  $(x, y, z)$ . The relationship between the spherical coordinates (Earth-fixed) and the satellite position coordinates (true of date) is then given by

$$r = \sqrt{x^2 + y^2 + z^2} \quad (1)$$

$$\phi' = \sin^{-1} \left( \frac{z}{r} \right) \quad (2)$$

$$\lambda = \tan^{-1} \left( \frac{y}{x} \right) - \theta_g \quad (3)$$

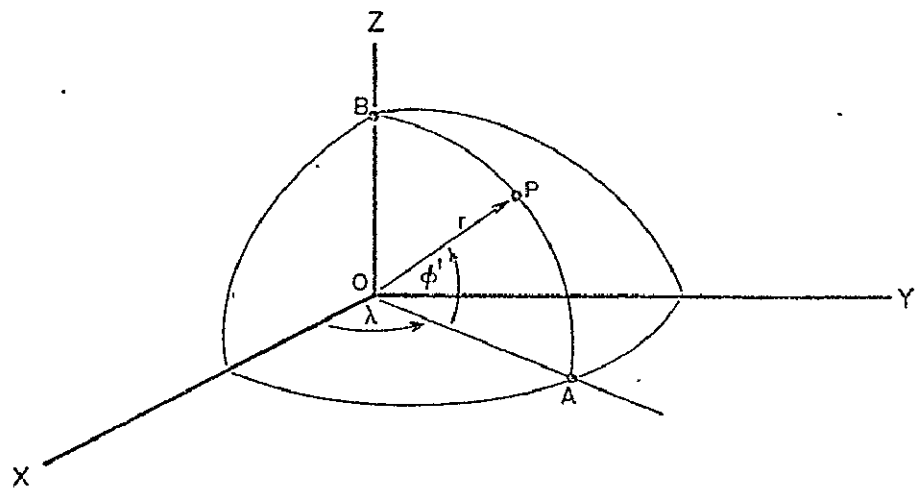


Figure 1: Spherical Coordinates

where  $\theta_g$  is the rotation angle between the true of date system and the Earth-fixed system (see Section 2.3.4).

ENGRAV

The Earth's gravity field is represented by the normal potential of an ellipsoid of revolution and small irregular variations, expressed by a sum of spherical harmonics. This formulation, used in the NONAME system, is

$$U = \frac{GM}{r} \left\{ 1 + \sum_{n=2}^{n_{\max}} \sum_{m=0}^n \left( \frac{a_e}{r} \right)^n P_n^m \left( \sin \phi \right) \left[ C_{nm} \cos m\lambda + S_{nm} \sin m\lambda \right] \right\} \quad (4)$$

where

$G$  is the universal gravitational constant,

$M$  is the mass of the earth,

$r$  is the geocentric satellite distance,

$n_{\max}$  is the upper limit for the summation (highest degree),

$a_e$  is the Earth's mean equatorial radius,

$\phi'$  is the satellite geocentric latitude,

EGRAV

$\lambda$  is the satellite east longitude,

$P_n^m(\sin \phi)$  indicate the associated six Legendre functions, and

$C_{nm}$  and  $S_{nm}$  are the denormalized gravitational coefficients.

The relationships between the normalized coefficients  $(\bar{C}_{nm}, \bar{S}_{nm})$  and the denormalized coefficients are as follows:

DENORM

$$C_{nm} = \left[ \frac{(n-m)! (2n+1) (2-\delta_{om})}{(n+m)!} \right]^{1/2} \bar{C}_{nm} \quad (5)$$

where

$\delta_{om}$  is the Kronecker delta,

$\delta_{om}=1$  for  $m=0$  and  $\delta_{om}=0$  for  $m \neq 0$ .

A similar expression is valid for the relationship between  $\bar{S}_{nm}$  and  $S_{nm}$ . This conversion factor is computed by the NONAME system function DENORM.

The gravitational accelerations in true of date coordinates  $(\ddot{x}, \ddot{y}, \ddot{z})$  are computed from the geopotential,  $U(r, \phi', \lambda)$ , by the chain rule; e.g.,

$$\ddot{x} = \frac{\partial U}{\partial r} \frac{\partial r}{\partial x} + \frac{\partial U}{\partial \phi'} \frac{\partial \phi'}{\partial x} + \frac{\partial U}{\partial \lambda} \frac{\partial \lambda}{\partial x} \quad (6)$$

The accelerations  $\ddot{y}$  and  $\ddot{z}$  are determined likewise. The partial derivatives of  $U$  with respect to  $r$ ,  $\phi'$ , and  $\lambda$  are given by

$$\frac{\partial U}{\partial r} = \frac{GM}{r^2} \left[ 1 + \sum_{n=2}^{n_{\max}} \left( \frac{a_e}{r} \right)^n \sum_{m=0}^n (C_{nm} \cos m\lambda + S_{nm} \sin m\lambda) (n+1) P_n^m (\sin \phi') \right] \quad (7)$$

$$\frac{\partial U}{\partial \lambda} = \frac{GM}{r} \sum_{n=2}^{n_{\max}} \left( \frac{a_e}{r} \right)^n \sum_{m=0}^n (S_{nm} \cos m\lambda - C_{nm} \sin m\lambda) \quad (8)$$

$$m P_n^m (\sin \phi')$$

$$\frac{\partial U}{\partial \phi'} = \frac{GM}{r} \sum_{n=2}^{n_{\max}} \left( \frac{a_e}{r} \right)^n \sum_{m=0}^n (C_{nm} \cos m\lambda + S_{nm} \sin m\lambda) \quad (9)$$

$$\left[ P_n^{m+1} (\sin \phi') - m \tan \phi' P_n^m (\sin \phi') \right]$$

The partial derivatives of  $r$ ,  $\phi'$ , and  $\lambda$  with respect to the true of date satellite position components are

$$\frac{\partial r}{\partial r_i} = \frac{r_i}{r} \quad (10)$$

$$\frac{\partial \phi'}{\partial r_i} = \frac{1}{\sqrt{x^2+y^2}} \left[ -\frac{zr_i}{r^2} + \frac{\partial z}{\partial r_i} \right] \quad (11)$$

$$\frac{\partial \lambda}{\partial r_i} = \frac{1}{\sqrt{x^2+y^2}} \left[ \frac{\partial y}{\partial r_i} - \frac{y}{x} \frac{\partial x}{\partial r_i} \right] \quad (12)$$

The Legendre functions are computed via recursion formulae:      EGRAV

Zonals:  $m=0$

$$P_n^0(\sin \phi) = \frac{1}{n} \left[ (2n-1) \sin \phi P_{n-1}^0(\sin \phi) - (n-1) P_{n-2}^0(\sin \phi) \right] \quad (13)$$

$$P_1^0(\sin \phi) = \sin \phi \quad (14)$$

Tesserals:  $m \neq 0$  and  $m \leq n$

$$P_n^m(\sin \phi) = P_{n-2}^m(\sin \phi) + (2n-1) \cos \phi P_{n-1}^{m-1}(\sin \phi) \quad (15)$$

$$P_1^1(\sin \phi) = \cos \phi \quad (16)$$

Sectorals:  $m=n$

$$P_n^n = (2n-1) \cos \phi P_{n-1}^{n-1}(\sin \phi) \quad (17)$$

The derivative relationship is given by

EGRAV

$$\frac{d}{d\phi'} \left( P_n^m (\sin \phi') \right) = P_n^{m+1} (\sin \phi') - m \tan \phi' P_n^m (\sin \phi') \quad (18)$$

It should also be noted that multiple angle formulas are used for evaluating the sine and cosine of  $m\lambda$ .

EGRAV

VEVAL

These accelerations on the spacecraft are computed in subroutine EGRAV. Arrays containing certain intermediate data are passed to subroutine VEVAL for use in the computations for the variational equations. These contain the values for:

$$\frac{GM}{r} \left( \frac{a}{c} \right)^n \quad (19)$$

$$P_n^m (\sin \phi')$$

$$\sin m\lambda$$

$$\cos m\lambda$$

$$m \tan \phi'$$

for each  $m$  and/or  $n$ .

The following discussion relates primarily to the mathematical formulations utilized in subroutine VEVAL.

VEVAL

The variational equations require the computation of the matrix  $U_{2c}$ , whose elements are given by

$$\left( U_{2c} \right)_{i,j} = \frac{\partial^2 U}{\partial r_i \partial r_j} \quad (20)$$

where

$r_i = \{x, y, z\}$ , the true of date satellite position.

$U$  is the geopotential.

Because the Earth's field is in terms of  $r$ ,  $\sin \phi'$ , and  $\lambda$ , we write

$$U_{2c} = C_1^T U_2 C_1 + \sum_{k=1}^3 \frac{\partial U}{\partial e_k} C_{2k} \quad (21)$$

where

$e_k$  ranges over the elements  $r$ ,  $\sin \phi'$ , and  $\lambda$

$U_2$  is the matrix whose  $i, j^{\text{th}}$  element is given by  $\frac{\partial^2 U}{\partial e_i \partial e_j}$

$C_1$  is the matrix whose  $i, j^{\text{th}}$  element is given by  $\frac{\partial c_i}{\partial r_j}$  .

and

$C_{2k}$  is a set of three matrices whose  $i, j^{\text{th}}$  elements are given by  $\frac{\partial^2 c_k}{\partial r_i \partial r_j}$

We compute the second partial derivatives of the potential  $U$  with respect to  $r$ ,  $\phi'$ , and  $\lambda$ :

$$\frac{\partial^2 U}{\partial r^2} = \frac{2GM}{r^3} + \frac{GM}{r^3} \sum_{n=2}^{\text{nmax}} (n+1) (n+2) \left(\frac{a_e}{r}\right)^n \sum_{m=0}^n (C_{nm} \cos m\lambda + S_{nm} \sin m\lambda) P_m^n (\sin \phi') \quad (22)$$

$$\begin{aligned} \frac{\partial^2 U}{\partial r \partial \phi'} &= -\frac{GM}{r^2} \sum_{n=2}^{\text{nmax}} (n+1) \left(\frac{a_e}{r}\right)^n \sum_{m=0}^n (C_{nm} \cos m\lambda + S_{nm} \sin m\lambda) \frac{\partial}{\partial \phi'} (P_m^n (\sin \phi')) \\ &+ S_{nm} \sin m\lambda \end{aligned} \quad (23)$$

$$\begin{aligned} \frac{\partial^2 U}{\partial r \partial \lambda} &= \frac{GM}{r^2} \sum_{n=2}^{\text{nmax}} (n+1) \left(\frac{a_e}{r}\right)^n \sum_{m=0}^n m (-C_{nm} \sin m\lambda + S_{nm} \cos m\lambda) P_m^n (\sin \phi') \\ &+ (-C_{nm} \sin m\lambda + S_{nm} \cos m\lambda) \end{aligned} \quad (24)$$

$$\frac{\partial^2 U}{\partial \phi^2} = \frac{GM}{r} \sum_{n=2}^{n_{\max}} \left(\frac{a_e}{r}\right)^n \sum_{m=0}^n (C_{nm} \cos m\lambda + S_{nm} \sin m\lambda) \quad (25)$$

$$\frac{\partial^2}{\partial \phi^2} \left( P_n^m (\sin \phi) \right)$$

$$\frac{\partial^2 U}{\partial \phi \partial \lambda} = \frac{GM}{r} \sum_{n=2}^{n_{\max}} \left(\frac{a_e}{r}\right)^n \sum_{m=0}^n m (-C_{nm} \sin m\lambda \quad (26)$$

$$+ S_{nm} \cos m\lambda) \frac{\partial}{\partial \phi} \left( P_n^m (\sin \phi) \right)$$

$$\frac{\partial^2 U}{\partial \lambda^2} = - \frac{GM}{r} \sum_{n=2}^{n_{\max}} \left(\frac{a_e}{r}\right)^n \sum_{m=0}^n m^2 (C_{nm} \cos m\lambda \quad (27)$$

$$+ S_{nm} \sin m\lambda) P_n^m (\sin \phi)$$

where

$$\frac{\partial}{\partial \phi} \left( P_n^m (\sin \phi) \right) = P_n^{m+1} (\sin \phi) - m \tan \phi P_n^m (\sin \phi) \quad (28)$$

$$\begin{aligned}
 \frac{\partial^2}{\partial \phi'^2} \left( P_n^m (\sin \phi') \right) &= P_n^{m+2} (\sin \phi') - (m+1) \tan \phi' P_n^{m+1} (\sin \phi') \\
 &- m \tan \phi' \left[ P_n^{m+1} (\sin \phi') - m \tan \phi' P_n^m (\sin \phi') \right] \\
 &- m \sec^2 \phi' P_n^m (\sin \phi') \tag{29}
 \end{aligned}$$

The elements of  $U_2$  have almost been computed. What remains is to transform from  $(r, \phi', \lambda)$  to  $(r, \sin \phi', \lambda)$ . This affects only the partials involving  $\phi'$ :

$$\frac{\partial U}{\partial \sin \phi'} = \frac{\partial U}{\partial \phi'} \frac{\partial \phi'}{\partial \sin \phi'} \tag{30}$$

$$\frac{\partial^2 U}{\partial \sin \phi'^2} = \frac{\partial \phi'}{\partial \sin \phi'} \left( \frac{\partial^2 U}{\partial \phi'^2} \right) \frac{\partial \phi'}{\partial \sin \phi'} + \frac{\partial U}{\partial \phi'} \frac{\partial^2 \phi'}{\partial \sin \phi'^2} \tag{31}$$

where

$$\frac{\partial \phi'}{\partial \sin \phi'} = \sec \phi' \tag{32}$$

$$\frac{\partial^2 \phi'}{\partial \sin \phi'^2} = \sin \phi' \sec^3 \phi' \tag{33}$$

For the  $C_1$  and  $C_{2k}$  matrices, the partials of  $r$ ,  $\sin \phi'$ , and  $\lambda$  are obtained from the usual formulas:

VEVAL

$$r = \sqrt{x^2 + y^2 + z^2} \quad (34)$$

$$\sin \phi' = \frac{z}{r} \quad (35)$$

$$\lambda = \tan^{-1} \left( \frac{y}{x} \right) - \theta_g \quad (36)$$

We have for  $C_1$ :

$$\frac{\partial r}{\partial r_i} = \frac{r_i}{r} \quad (37)$$

$$\frac{\partial \sin \phi'}{\partial r_i} = \frac{-z r_i}{r^3} + \frac{1}{r} \frac{\partial z}{\partial r_i} \quad (38)$$

$$\frac{\partial \lambda}{\partial r_i} = \frac{1}{x^2 + y^2} \left[ x \frac{\partial y}{\partial r_i} - y \frac{\partial x}{\partial r_i} \right] \quad (38)$$

The  $C_{2k}$  are symmetric. The necessary elements are given by

VIEWER

$$\frac{\partial^2 r}{\partial r_i \partial r_j} = \frac{r_i r_j}{r^3} + \frac{1}{r} \frac{\partial r_i}{\partial r_j} \quad (39)$$

$$\frac{\partial^2 \sin \phi'}{\partial r_i \partial r_j} = \frac{3z r_i r_j}{r^5} - \frac{1}{r^3} \left[ r_j \frac{\partial z}{\partial r_i} + r_i \frac{\partial z}{\partial r_j} + z \frac{\partial r_i}{\partial r_j} \right] \quad (40)$$

$$\frac{\partial^2 \lambda}{\partial r_i \partial r_j} = \frac{-2r_j}{(x^2+y^2)^2} \left[ x \frac{\partial y}{\partial r_i} - y \frac{\partial x}{\partial r_i} \right] \quad (41)$$

$$+ \frac{1}{x^2+y^2} \left[ \frac{\partial x}{\partial r_j} \frac{\partial y}{\partial r_j} - \frac{\partial y}{\partial r_j} \frac{\partial x}{\partial r_j} \right]$$

If gravitational constants,  $C_{nm}$  or  $S_{nm}$  are being estimated, we require their partials in the f matrix for the variational equations computations. These partials are

RESPAR

$$\frac{\partial}{\partial C_{nm}} \left( - \frac{\partial U}{\partial r} \right) = (n+1) \frac{GM}{r^2} \left( \frac{a_e}{r} \right)^n \cos (m\lambda) P_n^m (\sin \phi) \quad (42)$$

$$\frac{\partial}{\partial C_{nm}} \left( - \frac{\partial U}{\partial \lambda} \right) = m \frac{GM}{r} \left( \frac{a_e}{r} \right)^n \sin (m\lambda) P_n^m (\sin \phi) \quad (43)$$

$$\begin{aligned}
 \frac{\partial}{\partial C_{nm}} \left( -\frac{\partial U}{\partial \phi'} \right) = & - \frac{GM}{r} \left( \frac{a_e}{r} \right)^n \cos(m\lambda) \left[ P_n^{m+1} (\sin \phi') \right. \\
 & \left. - m \tan \phi' P_n^m (\sin \phi') \right] \quad (44)
 \end{aligned}$$

The partials for  $S_{nm}$  are identical with  $\cos(m\lambda)$  replaced by  $\sin(m\lambda)$  and with  $\sin(m\lambda)$  replaced by  $-\cos(m\lambda)$ .

These partials are converted to inertial to true of date coordinates using the chain rule; e.g.,

$$\begin{aligned}
 \frac{\partial}{\partial C_{nm}} \left( -\frac{\partial U}{\partial x} \right) = & \frac{\partial}{\partial C_{nm}} \left( \frac{-\partial U}{\partial r} \right) \frac{\partial r}{\partial x} + \frac{\partial}{\partial C_{nm}} \left( \frac{-\partial U}{\partial \lambda} \right) \frac{\partial \lambda}{\partial x} \quad (45) \\
 & + \frac{\partial}{\partial C_{nm}} \left( \frac{-\partial U}{\partial \phi'} \right) \frac{\partial \phi'}{\partial x}
 \end{aligned}$$

This particular set of computations is performed by subroutine RESPAR. The items which EGRAV computes for VEVAL are also available to RESPAR and are therefore utilized.

The perturbations caused by a third body on a satellite orbit are treated by defining a function,  $R_d$ , which is the third body disturbing potential. This potential takes on the following form:

$$R_d = \frac{GMm_d}{r_d} \left[ \left( 1 - \frac{2r}{r_d} s + \frac{r^2}{r_d^2} \right)^{-1/2} - \frac{r}{r_d} s \right] \quad (1)$$

where

$m_d$  is the mass of the disturbing body.

$\bar{r}_d$  is the geocentric true of date position vector to the disturbing body.

$s$  is equal to the cosine of the enclosed angle between  $\bar{r}$  and  $\bar{r}_d$ .

$\bar{r}$  is the geocentric true of date position vector of the satellite.

$G$  is the universal gravitational constant, and

$M$  is the mass of the Earth.

The third body perturbations considered in NONAME are for the Sun and the Moon. Both are computed in subroutine SUNGRV by .

$$\bar{a}_d = -GMm_d \left[ \frac{\bar{d}}{D_d} + \frac{1}{r_d} \left( \frac{\bar{r}_d}{r_d} \right) \right] \quad (2) \quad \text{SUNGRV}$$

where

$$\bar{d} = \bar{r} - \bar{r}_d$$

$$D_d = \left[ r_d^2 - 2r_r r_d s + r^2 \right]^{3/2}$$

These latter quantities,  $\bar{d}$  and  $D$  as well as  $D^{2/3}$  for the Moon are passed to subroutine VEVAL for the variational equation calculations. VEVAL computes the matrix  $U_{2C}$  whose  $i, j^{\text{th}}$  elements is given by

$$\frac{\partial^2 R_d}{\partial r_i \partial r_j} = - \frac{GMm_d}{D_d} \left[ \frac{\partial r_i}{\partial r_j} + \frac{3d_i d_j}{D_d^{2/3}} \right] \quad (3)$$

This matrix is a fundamental part of the variational equations.

#### 2.8.5 Solar Radiation Pressure

The force due to solar radiation can have a significant effect on the orbits of satellites with a large area to mass ratio. The accelerations due to solar radiation pressure are formulated in the

NONAME system as

F

$$\bar{A}_R = -v C_R \frac{A_s}{m_s} p_s \hat{r}_s \quad (1)$$

where

$v$  is the eclipse factor, such that

$v=0$  when the satellite is in the Earth's shadow

$v=1$  when the satellite is illuminated by the Sun

$C_R$  is a factor depending on the reflective characteristics of the satellite,

$A_s$  is the cross sectional area of the satellite;

$m_s$  is the mass of the satellite,

$p_s$  is the solar radiation pressure in the vicinity of the Earth, and

$\hat{r}_s$  is the (geocentric) true of date unit vector pointing to the Sun.

The unit vector  $\hat{r}_s$  is determined as part of the luni-solar ephemeris computations.

The eclipse factor,  $\nu$ , is determined as follows: F  
Compute

$$D = \bar{r} \cdot \hat{r}_s \quad (2)$$

where  $\bar{r}$  is the true of date position vector of the satellite. If  $D$  is positive, the satellite is always in sunlight. If  $D$  is negative, compute the vector  $\bar{p}_R$ .

$$\bar{p}_R = \bar{r} - D \hat{r}_s. \quad (3)$$

This vector is perpendicular to  $\hat{r}_s$ . If its magnitude is less than an Earth radius, or rather if

$$\bar{p}_R \cdot \bar{p}_R < a_e^2, \quad (4)$$

the satellite is in shadow.

The satellite is assumed to be specularly reflecting with reflectivity  $\rho_s$ ; thus

$$C_R = 1 + \rho_s \quad (5)$$

When a radiation pressure coefficient is being determined; i.e.,  $C_R$ , the partials for the  $f$  matrix

in the variational equations computation must be  
computed. The  $i^{\text{th}}$  element of this column matrix is  
given by

$$f_i = -v \frac{A_s}{m_s} P_s r_{s_i} \quad (6)$$

These computations for the effects of solar  
radiation pressure are done in subroutine F.

#### 2.8.6 Atmospheric Drag

A satellite moving through an atmosphere ex-  
periences a drag force. The acceleration due to  
this force is given by

$$\bar{A}_D = -\frac{1}{2} C_D \frac{A_s}{m_s} \rho_D v_r \bar{v}_r \quad (1)$$

where

$C_D$  is the satellite drag coefficient

$A_s$  is the cross-sectional area of the satellite

F  
VEVAL

$m_s$  is the mass of the satellite,

DRAG

$\rho_D$  is the density of the atmosphere at the satellite position, and

$\bar{v}_r$  is the velocity vector of the satellite relative to the atmosphere;

Both  $A_s$  and  $C_D$  are treated as constants in NONAME. Although  $A_s$  depends somewhat on satellite attitude, the use of a mean cross-sectional area does not lead to significant errors for geodetically useful satellites. The factor  $C_D$  varies slightly with satellite shape and atmospheric composition. However, for any geodetically useful satellite, it may be treated as a satellite dependent constant.

The relative velocity vector,  $\bar{v}_r$ , is computed assuming that the atmosphere rotates with the Earth. The true of date components of this vector are then

$$\dot{x}_r = \dot{x} - \dot{\theta}_g y \quad (2)$$

$$\dot{y}_r = \dot{y} - \dot{\theta}_g x \quad (3)$$

$$\dot{z}_r = \dot{z} \quad (4)$$

as is indicated from Section 2.3.4, the subsection on transformations between Earth-fixed and true of date systems. The quantities  $\dot{x}$ ,  $\dot{y}$ , and  $\dot{z}$  are of course the components of  $\dot{r}$ , the satellite velocity vector in true of date coordinates.

The drag accelerations are computed in the NONAME system by subroutine DRAG, with the atmospheric density  $\rho_D$  being evaluated by subroutine DENSTY. In addition, subroutine DRAG computes the direct partials for the  $f$  matrix of the variational equations when the drag coefficient  $C_D$  is being determined. These partials are given by

$$f = -\frac{1}{2} \frac{A_s}{m_s} \rho_D \dot{v}_r \ddot{v}_r \quad (5)$$

When drag is present in an orbit determination run, the  $D_r$  matrix in the variational equations must also be computed. This matrix, which contains the partial derivatives of the drag acceleration with respect to the Cartesian orbital elements, is constructed in subroutine VEVAL. We have

$$D_r = -\frac{1}{2} C_D \frac{A_s}{m_s} \left[ \rho_D v_r \frac{\partial \ddot{v}_r}{\partial \bar{x}_t} + \rho_D \frac{\partial v_r}{\partial \bar{x}_t} \ddot{v}_r + \frac{\partial \rho_D}{\partial \bar{x}_t} v_r \ddot{v}_r \right] \quad (6)$$

where

$\bar{x}_t$  is  $(x, y, z, \dot{x}, \dot{y}, \dot{z})$ ; i.e.,  $\bar{x}_t$  spans  $\bar{r}$  and  $\dot{r}$ .

DRAG  
DENSTY

VEVAL

$$\frac{\partial \bar{v}_r}{\partial \bar{x}_t} = \begin{bmatrix} 0 & -\dot{\theta}_g & 0 \\ \dot{\theta}_g & 0 & 0 \\ 0 & 0 & 0 \\ 1 & 0 & 0 \\ 0 & 1 & 0 \\ 0 & 0 & 1 \end{bmatrix} \quad (7)$$

$$\frac{\partial v_r}{\partial \bar{x}_t} \bar{v}_r = \frac{1}{v_r} \begin{bmatrix} \dot{y}_r \dot{\theta}_g \dot{x}_r & -\dot{y}_r \dot{\theta}_g \dot{y}_r & -\dot{y}_r \dot{\theta}_g \dot{z}_r \\ \dot{x}_r \dot{\theta}_g \dot{x}_r & \dot{x}_r \dot{\theta}_g \dot{y}_r & \dot{x}_r \dot{\theta}_g \dot{z}_r \\ 0 & 0 & 0 \\ \dot{x}_r \dot{x}_r & \dot{x}_r \dot{y}_r & \dot{x}_r \dot{z}_r \\ \dot{y}_r \dot{x}_r & \dot{y}_r \dot{y}_r & \dot{y}_r \dot{z}_r \\ \dot{z}_r \dot{x}_r & \dot{z}_r \dot{y}_r & \dot{z}_r \dot{z}_r \end{bmatrix} \quad (8)$$

and

$\frac{\partial \rho_D}{\partial \bar{x}_t}$  is the matrix containing the partial derivatives of the atmospheric density with respect to  $\bar{x}_t$  and is partially computed in subroutine DENSTY (see section 2.8.7.4 on atmospheric density partial derivatives). Because the density is not a function of the satellite velocity, the required partials are  $\frac{\partial \rho_D}{\partial \bar{r}}$ .

### 2.8.7 Atmospheric Density

The atmospheric density is the factor which is least well known in the computation of drag; however, it is essential to the computation of realistic perturbations due to drag. The NONAME solution is to use the Jacchia-Nicolet model, which is perhaps the most descriptive model presently available. This model gives densities between 120 km and 1000 km with an extrapolation formula for higher altitudes.

DENSTY

The NONAME model, as implemented in subroutine DENSTY, is based on Jacchia's 1965 report, "Static Diffusion Models of the Upper Atmosphere with Empirical Temperature Profiles" (Reference 2). The formulae for computing the exospheric temperature have in some cases been modified according to Jacchia's later papers. The density computation from the exospheric temperature is based on density data provided in that report, reproduced herein as Table 1, which presents density distribution versus altitude and exospheric temperature.

The discussion which follows will cover basically the assumptions behind the model and the formulae actually used in subroutine DENSTY. It will also cover the procedure for computing the density which was developed by WOLF.

The reader who is interested in the development of these empirical formulas and the reasoning behind them should consult the above mentioned report and Jacchia's later papers. For the convenience of this

Table 1 (Jacchia, Reference 2)

Densities as a function of height and exospheric temperature.

Decimal logarithms, g/cm<sup>3</sup>

	2100	2050	2000	1950	1900	1850	1800	1750	1700	1650	1600	1550	1500	1450	1400
3	-10.609	-10.609	-10.609	-10.609	-10.609	-10.609	-10.609	-10.609	-10.609	-10.609	-10.609	-10.609	-10.609	-10.609	-10.609
120	-10.609	-10.609	-10.609	-10.609	-10.609	-10.609	-10.609	-10.609	-10.609	-10.609	-10.609	-10.609	-10.609	-10.609	-10.609
130	-11.118	-11.118	-11.118	-11.118	-11.118	-11.118	-11.118	-11.118	-11.118	-11.118	-11.118	-11.118	-11.118	-11.118	-11.118
140	-11.447	-11.447	-11.447	-11.447	-11.447	-11.447	-11.447	-11.447	-11.447	-11.447	-11.447	-11.447	-11.447	-11.447	-11.447
150	-11.575	-11.575	-11.575	-11.575	-11.575	-11.575	-11.575	-11.575	-11.575	-11.575	-11.575	-11.575	-11.575	-11.575	-11.575
160	-11.881	-11.881	-11.881	-11.881	-11.881	-11.881	-11.881	-11.881	-11.881	-11.881	-11.881	-11.881	-11.881	-11.881	-11.881
170	-12.32	-12.32	-12.32	-12.32	-12.32	-12.32	-12.32	-12.32	-12.32	-12.32	-12.32	-12.32	-12.32	-12.32	-12.32
180	-12.123	-12.123	-12.123	-12.123	-12.123	-12.123	-12.123	-12.123	-12.123	-12.123	-12.123	-12.123	-12.123	-12.123	-12.123
190	-12.304	-12.304	-12.304	-12.304	-12.304	-12.304	-12.304	-12.304	-12.304	-12.304	-12.304	-12.304	-12.304	-12.304	-12.304
200	-12.415	-12.415	-12.415	-12.415	-12.415	-12.415	-12.415	-12.415	-12.415	-12.415	-12.415	-12.415	-12.415	-12.415	-12.415
210	-12.515	-12.515	-12.515	-12.515	-12.515	-12.515	-12.515	-12.515	-12.515	-12.515	-12.515	-12.515	-12.515	-12.515	-12.515
220	-12.609	-12.609	-12.609	-12.609	-12.609	-12.609	-12.609	-12.609	-12.609	-12.609	-12.609	-12.609	-12.609	-12.609	-12.609
230	-12.694	-12.694	-12.694	-12.694	-12.694	-12.694	-12.694	-12.694	-12.694	-12.694	-12.694	-12.694	-12.694	-12.694	-12.694
240	-12.715	-12.715	-12.715	-12.715	-12.715	-12.715	-12.715	-12.715	-12.715	-12.715	-12.715	-12.715	-12.715	-12.715	-12.715
250	-12.852	-12.852	-12.852	-12.852	-12.852	-12.852	-12.852	-12.852	-12.852	-12.852	-12.852	-12.852	-12.852	-12.852	-12.852
260	-12.923	-12.923	-12.923	-12.923	-12.923	-12.923	-12.923	-12.923	-12.923	-12.923	-12.923	-12.923	-12.923	-12.923	-12.923
270	-12.994	-12.994	-12.994	-12.994	-12.994	-12.994	-12.994	-12.994	-12.994	-12.994	-12.994	-12.994	-12.994	-12.994	-12.994
280	-13.041	-13.055	-13.055	-13.055	-13.055	-13.055	-13.055	-13.055	-13.055	-13.055	-13.055	-13.055	-13.055	-13.055	-13.055
290	-13.125	-13.125	-13.125	-13.125	-13.125	-13.125	-13.125	-13.125	-13.125	-13.125	-13.125	-13.125	-13.125	-13.125	-13.125
300	-13.196	-13.196	-13.196	-13.196	-13.196	-13.196	-13.196	-13.196	-13.196	-13.196	-13.196	-13.196	-13.196	-13.196	-13.196
310	-13.246	-13.252	-13.259	-13.265	-13.271	-13.278	-13.285	-13.293	-13.303	-13.313	-13.325	-13.339	-13.355	-13.374	-13.395
320	-13.304	-13.311	-13.316	-13.325	-13.332	-13.340	-13.348	-13.357	-13.368	-13.379	-13.393	-13.408	-13.425	-13.445	-13.469
330	-13.361	-13.361	-13.376	-13.384	-13.392	-13.401	-13.410	-13.420	-13.431	-13.444	-13.459	-13.475	-13.494	-13.516	-13.541
340	-13.415	-13.424	-13.433	-13.441	-13.450	-13.460	-13.470	-13.481	-13.494	-13.508	-13.523	-13.541	-13.562	-13.585	-13.612
350	-13.467	-13.478	-13.482	-13.497	-13.507	-13.517	-13.524	-13.541	-13.554	-13.570	-13.587	-13.606	-13.628	-13.653	-13.682
360	-13.522	-13.532	-13.542	-13.552	-13.563	-13.574	-13.585	-13.599	-13.614	-13.631	-13.649	-13.670	-13.693	-13.720	-13.750
370	-13.573	-13.584	-13.595	-13.606	-13.617	-13.629	-13.643	-13.657	-13.673	-13.690	-13.710	-13.732	-13.757	-13.785	-13.817
380	-13.623	-13.635	-13.646	-13.658	-13.671	-13.684	-13.698	-13.713	-13.730	-13.749	-13.770	-13.794	-13.820	-13.849	-13.883
390	-13.673	-13.685	-13.697	-13.710	-13.723	-13.737	-13.752	-13.769	-13.787	-13.807	-13.829	-13.854	-13.882	-13.913	-13.947
400	-13.721	-13.734	-13.747	-13.761	-13.775	-13.790	-13.805	-13.823	-13.843	-13.864	-13.887	-13.913	-13.942	-13.975	-14.011
410	-13.764	-13.782	-13.795	-13.811	-13.826	-13.842	-13.859	-13.877	-13.897	-13.920	-13.944	-13.972	-14.002	-14.035	-14.074
420	-13.815	-13.830	-13.844	-13.860	-13.875	-13.892	-13.910	-13.930	-13.951	-13.975	-14.000	-14.029	-14.061	-14.096	-14.135
430	-13.861	-13.876	-13.892	-13.908	-13.925	-13.942	-13.961	-13.982	-14.004	-14.029	-14.056	-14.086	-14.119	-14.159	-14.196
440	-13.917	-13.932	-13.939	-13.955	-13.973	-13.992	-14.012	-14.033	-14.057	-14.082	-14.110	-14.141	-14.176	-14.214	-14.256
450	-13.951	-13.965	-13.985	-14.002	-14.021	-14.040	-14.061	-14.084	-14.108	-14.135	-14.164	-14.196	-14.232	-14.271	-14.315
460	-13.993	-14.012	-14.030	-14.049	-14.068	-14.088	-14.110	-14.133	-14.159	-14.187	-14.217	-14.251	-14.288	-14.325	-14.373
470	-14.032	-14.056	-14.076	-14.094	-14.114	-14.135	-14.158	-14.183	-14.209	-14.238	-14.270	-14.304	-14.342	-14.394	-14.431
480	-14.111	-14.130	-14.139	-14.160	-14.182	-14.205	-14.231	-14.259	-14.299	-14.321	-14.357	-14.397	-14.442	-14.488	
490	-14.123	-14.143	-14.163	-14.183	-14.205	-14.228	-14.253	-14.279	-14.308	-14.339	-14.372	-14.404	-14.450	-14.495	-14.544
500	-14.172	-14.185	-14.206	-14.227	-14.250	-14.274	-14.299	-14.326	-14.356	-14.388	-14.423	-14.461	-14.503	-14.549	-14.599
510	-14.227	-14.248	-14.271	-14.294	-14.319	-14.345	-14.373	-14.404	-14.437	-14.473	-14.512	-14.555	-14.602	-14.654	
520	-14.247	-14.268	-14.276	-14.313	-14.317	-14.363	-14.390	-14.419	-14.451	-14.485	-14.522	-14.562	-14.607	-14.655	-14.709
530	-14.287	-14.309	-14.312	-14.356	-14.381	-14.407	-14.435	-14.465	-14.497	-14.533	-14.571	-14.612	-14.652	-14.703	-14.752
540	-14.324	-14.341	-14.373	-14.327	-14.423	-14.450	-14.479	-14.510	-14.544	-14.580	-14.619	-14.662	-14.709	-14.760	-14.816
550	-14.364	-14.414	-14.419	-14.465	-14.473	-14.523	-14.555	-14.587	-14.627	-14.671	-14.711	-14.759	-14.811	-14.859	

Table 1 (continued)

	1350	1300	1250	1200	1150	1100	1050	1000	950	900	850	800	750	700	650
120	-10.609	-10.609	-10.609	-10.609	-10.609	-10.609	-10.609	-10.609	-10.609	-10.609	-10.609	-10.609	-10.609	-10.609	-10.609
130	-11.111	-11.109	-11.108	-11.103	-11.100	-11.095	-11.091	-11.088	-11.081	-11.075	-11.068	-11.061	-11.054	-11.046	-11.038
140	-11.432	-11.429	-11.427	-11.424	-11.421	-11.418	-11.415	-11.411	-11.407	-11.403	-11.399	-11.395	-11.390	-11.386	-11.382
150	-11.671	-11.669	-11.668	-11.665	-11.665	-11.664	-11.663	-11.662	-11.663	-11.664	-11.665	-11.668	-11.671	-11.675	
160	-11.864	-11.863	-11.863	-11.864	-11.865	-11.863	-11.862	-11.862	-11.863	-11.868	-11.868	-11.908	-11.920	-11.934	
170	-12.079	-12.074	-12.073	-12.073	-12.075	-12.074	-12.074	-12.075	-12.075	-12.088	-12.104	-12.123	-12.145	-12.169	
180	-12.172	-12.171	-12.172	-12.170	-12.168	-12.176	-12.206	-12.218	-12.232	-12.269	-12.242	-12.320	-12.351	-12.336	
190	-12.302	-12.305	-12.311	-12.318	-12.327	-12.339	-12.352	-12.368	-12.387	-12.410	-12.436	-12.467	-12.502	-12.542	-12.588
200	-12.422	-12.427	-12.435	-12.444	-12.456	-12.470	-12.489	-12.503	-12.532	-12.561	-12.593	-12.631	-12.674	-12.722	-12.778
210	-12.533	-12.541	-12.552	-12.562	-12.577	-12.595	-12.616	-12.641	-12.669	-12.703	-12.741	-12.766	-12.836	-12.893	-12.957
220	-12.638	-12.647	-12.655	-12.674	-12.692	-12.713	-12.738	-12.765	-12.800	-12.839	-12.883	-12.933	-12.990	-13.055	-13.128
230	-12.737	-12.749	-12.753	-12.781	-12.801	-12.826	-12.854	-12.887	-12.925	-12.968	-13.018	-13.074	-13.138	-13.210	-13.291
240	-12.833	-12.846	-12.853	-12.883	-12.907	-12.934	-12.969	-13.003	-13.045	-13.093	-13.148	-13.210	-13.280	-13.358	-13.447
250	-12.942	-12.943	-12.951	-12.962	-13.006	-13.039	-13.074	-13.115	-13.161	-13.214	-13.274	-13.341	-13.416	-13.501	-13.595
260	-13.013	-13.031	-13.052	-13.073	-13.107	-13.141	-13.179	-13.224	-13.274	-13.331	-13.395	-13.467	-13.548	-13.637	-13.741
270	-13.093	-13.114	-13.143	-13.171	-13.202	-13.239	-13.281	-13.329	-13.383	-13.444	-13.512	-13.599	-13.675	-13.772	-13.880
280	-13.192	-13.203	-13.231	-13.261	-13.296	-13.335	-13.380	-13.431	-13.489	-13.553	-13.626	-13.707	-13.799	-13.901	-14.015
290	-13.263	-13.288	-13.316	-13.342	-13.385	-13.429	-13.477	-13.531	-13.592	-13.660	-13.737	-13.822	-13.918	-14.026	-14.147
300	-13.343	-13.369	-13.402	-13.335	-13.475	-13.520	-13.571	-13.628	-13.692	-13.764	-13.845	-13.935	-14.035	-14.148	-14.275
310	-13.420	-13.449	-13.481	-13.513	-13.561	-13.609	-13.662	-13.723	-13.790	-13.866	-13.950	-14.044	-14.149	-14.267	-14.401
320	-13.499	-13.526	-13.561	-13.601	-13.645	-13.696	-13.752	-13.815	-13.886	-13.965	-14.052	-14.151	-14.261	-14.334	-14.524
330	-13.572	-13.603	-13.639	-13.681	-13.728	-13.781	-13.840	-13.906	-13.979	-14.061	-14.153	-14.255	-14.370	-14.439	-14.645
340	-13.643	-13.677	-13.711	-13.760	-13.803	-13.864	-13.926	-13.994	-14.071	-14.156	-14.251	-14.358	-14.477	-14.611	-14.763
350	-13.714	-13.750	-13.771	-13.837	-13.888	-13.946	-14.015	-14.081	-14.161	-14.249	-14.348	-14.458	-14.582	-14.722	-14.880
360	-13.784	-13.822	-13.865	-13.913	-13.966	-14.026	-14.093	-14.167	-14.249	-14.341	-14.443	-14.557	-14.686	-14.831	-14.995
370	-13.852	-13.892	-13.937	-13.987	-14.043	-14.105	-14.174	-14.250	-14.336	-14.431	-14.536	-14.655	-14.788	-14.939	-15.109
380	-13.922	-13.962	-14.003	-14.060	-14.118	-14.182	-14.253	-14.333	-14.421	-14.519	-14.629	-14.751	-14.889	-15.045	-15.221
390	-13.986	-14.030	-14.078	-14.132	-14.192	-14.258	-14.332	-14.414	-14.505	-14.606	-14.719	-14.846	-14.988	-15.149	-15.332
400	-14.051	-14.096	-14.147	-14.202	-14.264	-14.333	-14.409	-14.494	-14.587	-14.692	-14.809	-14.940	-15.087	-15.253	-15.441
410	-14.110	-14.162	-14.214	-14.272	-14.336	-14.407	-14.485	-14.572	-14.669	-14.777	-14.897	-15.032	-15.184	-15.355	-15.548
420	-14.179	-14.227	-14.281	-14.340	-14.406	-14.479	-14.550	-14.650	-14.750	-14.861	-14.985	-15.124	-15.280	-15.455	-15.654
430	-14.241	-14.291	-14.347	-14.408	-14.475	-14.551	-14.634	-14.727	-14.829	-14.943	-15.071	-15.214	-15.375	-15.555	-15.758
440	-14.303	-14.354	-14.411	-14.474	-14.544	-14.622	-14.707	-14.802	-14.908	-15.025	-15.156	-15.303	-15.468	-15.653	-15.860
450	-14.363	-14.416	-14.475	-14.540	-14.612	-14.692	-14.780	-14.877	-14.986	-15.105	-15.241	-15.392	-15.561	-15.750	-15.959
460	-14.423	-14.478	-14.538	-14.605	-14.679	-14.761	-14.851	-14.951	-15.062	-15.186	-15.325	-15.479	-15.652	-15.844	-16.056
470	-14.462	-14.538	-14.601	-14.660	-14.745	-14.824	-14.922	-15.025	-15.139	-15.266	-15.407	-15.565	-15.742	-15.937	-16.150
480	-14.540	-14.598	-14.662	-14.743	-14.811	-14.897	-14.992	-15.297	-15.214	-15.344	-15.489	-15.650	-15.830	-15.928	-16.242
490	-14.594	-14.657	-14.723	-14.795	-14.875	-14.963	-15.061	-15.169	-15.289	-15.422	-15.570	-15.734	-15.917	-16.117	-16.330
500	-14.645	-14.715	-14.781	-14.857	-14.939	-15.030	-15.129	-15.240	-15.367	-15.499	-15.650	-15.817	-16.002	-16.203	-16.414
510	-14.711	-14.774	-14.843	-14.917	-15.003	-15.095	-15.197	-15.310	-15.436	-15.574	-15.728	-15.899	-16.086	-16.287	-16.495
520	-14.751	-14.812	-14.880	-15.066	-15.160	-15.265	-15.390	-15.508	-15.650	-15.806	-15.979	-16.167	-16.365	-16.572	
530	-14.822	-14.881	-14.960	-15.040	-15.128	-15.225	-15.331	-15.446	-15.582	-15.724	-15.883	-16.057	-16.247	-16.447	-16.645
540	-14.877	-14.934	-14.914	-15.106	-15.189	-15.289	-15.397	-15.518	-15.650	-15.797	-15.958	-16.134	-16.324	-16.522	-16.714
550	-14.931	-15.000	-15.074	-15.151	-15.251	-15.351	-15.463	-15.595	-15.720	-15.869	-16.032	-16.210	-16.399	-16.594	-16.778

Table 1 (continued)

$\sqrt{t}$	2100	2050	2000	1950	1900	1850	1800	1750	1700	1650	1600	1550	1500	1450	1400
560	-14.475	-14.420	-14.454	-14.480	-14.507	-14.540	-14.560	-14.523	-14.635	-14.673	-14.714	-14.757	-14.808	-14.862	-14.921
570	-14.441	-14.458	-14.493	-14.520	-14.567	-14.593	-14.647	-14.570	-14.710	-14.751	-14.807	-14.857	-14.912	-14.972	
580	-14.451	-14.505	-14.533	-14.560	-14.584	-14.621	-14.652	-14.587	-14.724	-14.764	-14.811	-14.865	-14.905	-14.955	-15.024
590	-14.512	-14.545	-14.577	-14.610	-14.641	-14.674	-14.700	-14.730	-14.768	-14.809	-14.833	-14.862	-14.954	-15.017	-15.075
600	-14.554	-14.593	-14.610	-14.634	-14.670	-14.702	-14.736	-14.772	-14.811	-14.853	-14.893	-14.942	-15.002	-15.061	-15.125
610	-14.593	-14.620	-14.649	-14.676	-14.707	-14.737	-14.774	-14.814	-14.854	-14.893	-14.934	-14.975	-15.030	-15.110	-15.175
620	-14.613	-14.657	-14.690	-14.711	-14.740	-14.772	-14.802	-14.836	-14.887	-14.941	-14.983	-15.041	-15.097	-15.158	-15.225
630	-14.666	-14.697	-14.724	-14.755	-14.780	-14.822	-14.852	-14.884	-14.940	-14.985	-15.033	-15.086	-15.144	-15.206	-15.274
640	-14.701	-14.731	-14.761	-14.793	-14.824	-14.862	-14.897	-14.930	-14.982	-15.028	-15.073	-15.131	-15.192	-15.254	-15.323
650	-14.757	-14.787	-14.799	-14.831	-14.865	-14.901	-14.933	-14.980	-15.024	-15.071	-15.121	-15.175	-15.236	-15.301	-15.371
660	-14.772	-14.803	-14.835	-14.862	-14.903	-14.940	-14.970	-15.020	-15.065	-15.113	-15.165	-15.221	-15.282	-15.346	-15.419
670	-14.807	-14.839	-14.871	-14.905	-14.941	-14.976	-15.010	-15.061	-15.106	-15.155	-15.208	-15.265	-15.327	-15.394	-15.467
680	-14.842	-14.874	-14.907	-14.942	-14.978	-15.016	-15.057	-15.101	-15.147	-15.197	-15.251	-15.309	-15.372	-15.440	-15.515
690	-14.877	-14.908	-14.943	-14.978	-15.015	-15.056	-15.095	-15.140	-15.187	-15.238	-15.287	-15.352	-15.417	-15.486	-15.562
700	-14.911	-14.944	-14.978	-15.014	-15.052	-15.092	-15.134	-15.179	-15.228	-15.273	-15.335	-15.395	-15.461	-15.531	-15.602
710	-14.945	-14.978	-15.014	-15.050	-15.089	-15.120	-15.173	-15.218	-15.268	-15.320	-15.377	-15.438	-15.505	-15.577	-15.644
720	-14.778	-15.013	-15.049	-15.085	-15.125	-15.167	-15.210	-15.257	-15.307	-15.351	-15.410	-15.481	-15.548	-15.621	-15.700
730	-15.017	-15.047	-15.083	-15.121	-15.161	-15.203	-15.246	-15.295	-15.347	-15.401	-15.462	-15.523	-15.592	-15.668	-15.746
740	-15.045	-15.081	-15.119	-15.156	-15.197	-15.240	-15.285	-15.334	-15.393	-15.451	-15.501	-15.565	-15.635	-15.710	-15.791
750	-15.078	-15.114	-15.152	-15.191	-15.233	-15.270	-15.323	-15.372	-15.425	-15.481	-15.542	-15.607	-15.677	-15.753	-15.835
760	-15.111	-15.148	-15.185	-15.226	-15.268	-15.313	-15.350	-15.410	-15.463	-15.520	-15.582	-15.648	-15.720	-15.797	-15.880
770	-15.143	-15.181	-15.220	-15.260	-15.303	-15.348	-15.395	-15.447	-15.502	-15.560	-15.622	-15.687	-15.762	-15.840	-15.924
780	-15.176	-15.214	-15.253	-15.295	-15.338	-15.384	-15.433	-15.484	-15.540	-15.599	-15.662	-15.730	-15.803	-15.887	-15.967
790	-15.225	-15.246	-15.287	-15.329	-15.373	-15.410	-15.459	-15.501	-15.557	-15.617	-15.684	-15.750	-15.824	-15.900	-15.983
800	-15.240	-15.279	-15.320	-15.362	-15.407	-15.455	-15.505	-15.558	-15.615	-15.676	-15.741	-15.811	-15.881	-15.966	-16.033
810	-15.271	-15.311	-15.353	-15.395	-15.442	-15.490	-15.540	-15.595	-15.652	-15.714	-15.780	-15.850	-15.926	-16.008	-16.095
820	-15.303	-15.343	-15.385	-15.422	-15.471	-15.524	-15.572	-15.631	-15.689	-15.751	-15.812	-15.880	-15.958	-16.049	-16.137
830	-15.334	-15.375	-15.414	-15.462	-15.504	-15.550	-15.601	-15.667	-15.726	-15.789	-15.857	-15.922	-16.006	-16.090	-16.178
840	-15.375	-15.407	-15.450	-15.495	-15.543	-15.593	-15.647	-15.702	-15.762	-15.826	-15.895	-15.964	-16.046	-16.126	-16.219
850	-15.345	-15.422	-15.479	-15.577	-15.627	-15.677	-15.727	-15.779	-15.833	-15.902	-16.006	-16.085	-16.169	-16.259	
860	-15.477	-15.514	-15.531	-15.607	-15.661	-15.715	-15.773	-15.834	-15.900	-15.972	-16.044	-16.124	-16.209	-16.293	
870	-15.437	-15.501	-15.544	-15.603	-15.642	-15.695	-15.750	-15.808	-15.870	-15.934	-16.007	-16.082	-16.152	-16.247	-16.327
880	-15.447	-15.512	-15.577	-15.625	-15.679	-15.734	-15.794	-15.853	-15.905	-15.972	-16.043	-16.119	-16.200	-16.286	-16.377
890	-15.514	-15.562	-15.602	-15.657	-15.708	-15.761	-15.817	-15.877	-15.941	-16.008	-16.080	-16.156	-16.237	-16.324	-16.415
900	-15.548	-15.573	-15.640	-15.697	-15.740	-15.794	-15.851	-15.911	-15.975	-16.043	-16.116	-16.193	-16.274	-16.361	-16.452
910	-15.577	-15.623	-15.670	-15.727	-15.787	-15.837	-15.894	-15.951	-16.019	-16.079	-16.151	-16.229	-16.311	-16.393	-16.482
920	-15.627	-15.653	-15.711	-15.751	-15.804	-15.859	-15.917	-15.979	-16.044	-16.113	-16.187	-16.265	-16.347	-16.434	-16.526
930	-15.636	-15.683	-15.732	-15.782	-15.835	-15.891	-15.949	-16.012	-16.078	-16.149	-16.222	-16.300	-16.383	-16.470	-16.561
940	-15.664	-15.713	-15.762	-15.813	-15.867	-15.923	-15.977	-16.044	-16.112	-16.182	-16.255	-16.335	-16.413	-16.505	-16.597
950	-15.694	-15.742	-15.782	-15.844	-15.882	-15.935	-16.015	-16.079	-16.145	-16.216	-16.281	-16.370	-16.453	-16.540	-16.631
960	-15.724	-15.772	-15.822	-15.874	-15.920	-15.987	-16.047	-16.111	-16.178	-16.242	-16.314	-16.404	-16.487	-16.574	-16.665
970	-15.752	-15.801	-15.852	-15.909	-15.960	-16.015	-16.072	-16.143	-16.211	-16.272	-16.358	-16.437	-16.521	-16.608	-16.698
980	-15.781	-15.831	-15.881	-15.935	-15.990	-16.047	-16.110	-16.175	-16.243	-16.315	-16.397	-16.470	-16.554	-16.631	-16.730
990	-15.811	-15.861	-15.911	-15.964	-16.021	-16.080	-16.142	-16.207	-16.275	-16.345	-16.424	-16.503	-16.586	-16.673	-16.762
1000	-15.847	-15.911	-15.964	-16.014	-16.061	-16.110	-16.173	-16.244	-16.307	-16.374	-16.442	-16.519	-16.597	-16.683	-16.773

Table 1 (continued)

	1350	130.	1250	1200	1150	1100	1050	1000	950	900	850	800	750	700	650	
560	-14.285	-14.255	-14.133	-14.019	-14.911	-14.714	-14.527	-14.332	-14.792	-14.940	-14.105	-14.283	-14.472	-14.662	-14.839	
570	-15.038	-15.112	-14.184	-14.076	-14.171	-14.476	-14.593	-14.718	-14.854	-14.311	-14.177	-14.355	-14.541	-14.728	-14.895	
580	-15.091	-14.164	-14.241	-14.334	-14.431	-14.518	-14.556	-14.714	-14.476	-14.340	-14.247	-14.424	-14.609	-14.792	-14.948	
590	-15.143	-14.212	-14.301	-14.391	-14.490	-14.570	-14.718	-14.544	-14.682	-14.147	-14.315	-14.492	-14.673	-14.847	-14.997	
600	-15.195	-14.272	-14.358	-14.447	-14.545	-14.632	-14.737	-14.911	-14.757	-14.214	-14.381	-14.567	-14.734	-14.902	-14.992	
610	-15.245	-15.321	-14.411	-14.500	-14.595	-14.719	-14.841	-14.975	-14.122	-14.279	-14.446	-14.620	-14.793	-14.955	-14.965	
620	-15.294	-15.377	-14.491	-14.589	-14.684	-14.775	-14.882	-14.938	-14.171	-14.242	-14.509	-14.480	-14.849	-14.972	-14.995	
630	-15.345	-15.429	-14.511	-14.615	-14.700	-14.836	-14.923	-14.993	-14.247	-14.405	-14.573	-14.111	-14.900	-14.704	-14.167	
640	-15.396	-15.485	-14.571	-14.667	-14.777	-14.894	-14.971	-14.159	-14.303	-14.465	-14.629	-14.793	-14.991	-14.791	-14.157	
650	-15.445	-14.531	-14.624	-14.723	-14.832	-14.951	-14.080	-14.012	-14.367	-14.524	-14.685	-14.846	-14.996	-14.131	-14.233	
660	-15.495	-14.583	-14.676	-14.777	-14.887	-14.907	-14.137	-14.277	-14.425	-14.581	-14.740	-14.896	-14.043	-14.169	-14.251	
670	-15.547	-14.633	-14.728	-14.830	-14.942	-14.063	-14.194	-14.334	-14.492	-14.636	-14.742	-14.944	-14.085	-14.205	-14.291	
680	-15.595	-14.683	-14.779	-14.883	-14.996	-14.118	-14.249	-14.389	-14.537	-14.689	-14.842	-14.997	-14.129	-14.236	-14.319	
690	-15.644	-14.731	-14.817	-14.925	-14.045	-14.172	-14.304	-14.464	-14.591	-14.741	-14.870	-14.030	-14.162	-14.271	-14.346	
700	-15.691	-14.781	-14.861	-14.961	-14.011	-14.225	-14.357	-14.497	-14.643	-14.791	-14.938	-14.074	-14.192	-14.301	-14.372	
710	-15.739	-14.831	-14.911	-14.037	-14.193	-14.278	-14.410	-14.549	-14.693	-14.832	-14.980	-14.113	-14.232	-14.331	-14.397	
720	-15.788	-14.881	-14.971	-14.057	-14.204	-14.329	-14.461	-14.603	-14.732	-14.884	-14.022	-14.150	-14.266	-14.359	-14.420	
730	-15.833	-14.926	-14.026	-14.137	-14.254	-14.370	-14.512	-14.643	-14.799	-14.925	-14.062	-14.187	-14.295	-14.387	-14.441	
740	-15.874	-14.974	-14.075	-14.186	-14.304	-14.429	-14.561	-14.697	-14.831	-14.973	-14.000	-14.219	-14.325	-14.412	-14.493	
750	-15.924	-14.020	-14.123	-14.234	-14.352	-14.478	-14.598	-14.743	-14.875	-14.010	-14.136	-14.251	-14.353	-14.419	-14.491	
760	-15.370	-14.368	-14.172	-14.282	-14.400	-14.525	-14.655	-14.787	-14.920	-14.049	-14.170	-14.281	-14.380	-14.482	-14.513	
770	-16.015	-16.112	-16.217	-16.323	-16.447	-16.571	-16.700	-16.821	-16.956	-16.086	-17.203	-17.310	-17.406	-17.491	-17.535	
780	-16.059	-16.157	-16.262	-16.374	-16.493	-16.617	-16.744	-16.873	-16.993	-17.121	-17.234	-17.338	-17.432	-17.510	-17.555	
790	-16.103	-16.202	-16.307	-16.420	-16.538	-16.651	-16.787	-16.913	-17.037	-17.154	-17.264	-17.367	-17.457	-17.533	-17.577	
800	-16.146	-16.244	-16.352	-16.464	-16.592	-16.734	-16.858	-16.982	-17.072	-17.187	-17.293	-17.392	-17.481	-17.555	-17.598	
810	-16.189	-16.287	-14.377	-14.507	-14.625	-14.745	-14.868	-14.999	-17.105	-17.217	-17.321	-17.417	-17.504	-17.577	-17.613	
820	-16.231	-16.332	-14.435	-14.550	-14.567	-14.735	-14.796	-14.826	-14.925	-17.025	-17.139	-17.247	-17.348	-17.441	-17.527	-17.618
830	-16.273	-16.374	-14.485	-14.592	-14.707	-14.826	-14.944	-14.998	-17.170	-17.275	-17.373	-17.465	-17.549	-17.620	-17.657	
840	-16.314	-16.417	-14.522	-14.633	-14.747	-14.854	-14.979	-14.992	-17.201	-17.302	-17.398	-17.488	-17.571	-17.641	-17.675	
850	-16.355	-16.450	-14.562	-14.673	-14.786	-14.901	-14.914	-17.124	-17.204	-17.323	-17.422	-17.511	-17.593	-17.662	-17.725	
860	-16.395	-16.494	-14.612	-14.711	-14.824	-14.934	-14.947	-17.155	-17.257	-17.354	-17.446	-17.533	-17.614	-17.682	-17.714	
870	-16.434	-16.535	-14.641	-14.740	-14.852	-14.971	-14.983	-17.184	-17.294	-17.378	-17.462	-17.555	-17.635	-17.703	-17.722	
880	-16.473	-16.574	-14.670	-14.785	-14.876	-14.994	-17.094	-17.111	-17.213	-17.310	-17.402	-17.490	-17.576	-17.656	-17.723	-17.751
890	-16.511	-16.612	-14.716	-14.822	-14.930	-14.037	-17.140	-17.240	-17.335	-17.425	-17.512	-17.597	-17.677	-17.742	-17.759	
900	-16.549	-16.752	-14.659	-14.763	-14.068	-14.169	-17.266	-17.354	-17.447	-17.533	-17.617	-17.697	-17.762	-17.786	-17.806	
910	-16.589	-14.644	-14.767	-14.822	-14.975	-14.098	-14.197	-14.291	-14.382	-14.460	-14.554	-14.638	-14.717	-14.781	-14.804	
920	-16.621	-16.720	-14.725	-14.727	-14.127	-14.223	-14.316	-14.404	-14.490	-14.574	-14.658	-14.737	-14.800	-14.821	-14.821	
930	-16.657	-16.755	-14.756	-14.957	-14.957	-14.165	-14.249	-14.340	-14.425	-14.511	-14.594	-14.677	-14.756	-14.819	-14.823	
940	-16.691	-16.794	-14.849	-14.849	-14.095	-14.192	-14.274	-14.362	-14.443	-14.531	-14.614	-14.697	-14.776	-14.838	-14.854	
950	-16.723	-16.822	-14.821	-14.918	-14.114	-14.208	-14.298	-14.389	-14.484	-14.551	-14.634	-14.716	-14.795	-14.855	-14.871	
960	-16.754	-16.854	-14.951	-14.047	-14.142	-14.233	-14.321	-14.406	-14.493	-14.570	-14.653	-14.735	-14.814	-14.875	-14.887	
970	-16.771	-16.856	-14.941	-14.076	-14.159	-14.258	-14.344	-14.427	-14.502	-14.580	-14.672	-14.754	-14.833	-14.933	-14.933	
980	-16.813	-16.916	-14.047	-14.102	-14.194	-14.281	-14.362	-14.447	-14.522	-14.608	-14.690	-14.773	-14.852	-14.911	-14.919	
990	-16.854	-14.644	-14.017	-14.130	-14.216	-14.304	-14.387	-14.463	-14.547	-14.627	-14.709	-14.792	-14.870	-14.929	-14.935	
1000	-14.494	-14.575	-14.056	-14.145	-14.242	-14.326	-14.407	-14.487	-14.565	-14.645	-14.727	-14.810	-14.889	-14.941	-14.952	

interested reader, the references\* for this section form a reasonably comprehensive bibliography.

DENSITY

#### 2.8.7.1 The Assumptions of the Model

The Jacchia-Nicolet model is based on certain simplifying assumptions and on empirically determined formulae. This is primarily due to the complexity and varied nature of the processes occurring in different regions of the atmosphere and the general lack of anything resembling a complete understanding of the fundamental mechanisms involved. The actual derivation of the model is based upon assumptions first proposed by Nicolet (see Reference 8); Jacchia selected the Nicolet approach to generate a model suitable for satellite dynamics.

The model of the atmosphere proposed by Nicolet considers that the fundamental parameter is the temperature. Other physical parameters such as the pressure and density were derived from the temperature. Thus the first concern is the temperature variation in the atmosphere.

This temperature variation is controlled by the following conditions:

1. Above the thermopause, the temperature of the atmosphere does not vary with altitude. The thermopause varies with solar activity (and the time of day), ranging between about 220 km to 400 km. The

\*Reference 9, "U.S. Standard Atmosphere Supplements, 1966" contains a fairly comprehensive description and summary.

temperature above the thermopause is called the exospheric temperature and is directly responsive to solar effects.

DENSITY

2. At an altitude of 120 km, the temperature, density, and atmospheric conditions are independent of time. This is an obvious simplification. However, the variations of these parameters above 120 km are considerably larger than those occurring at 120 km, and, considering the other assumptions, this assumption represents a reasonably good approximation.
3. The atmosphere is assumed to be in static equilibrium. With the large day-to-night temperature variations, having a period of the same order of magnitude as the conduction time in the lower thermosphere, and with the occasional occurrence of severe magnetic storms which give rise to fairly rapid and large temperature variations the validity of this assumption is open to question. The best argument for this assumption is its relative simplicity. It should be anticipated, however, that in times of rapid change of the solar or geophysical parameters the predictions of this model will be in error due to the invalidity of this assumption.

The atmosphere is considered to be in diffusive equilibrium above 120 km; that is, the density distributions of each atmospheric constituent with height are

governed independently by gravity and temperature. The governing equations are the hydrostatic law, relating the pressure variation with height to the acceleration of gravity, and the perfect gas law, which relates the pressure, density and temperature.

DENSITY

With this approach, Nicolet showed that above 250 km the observed density profiles were reproduced satisfactorily if the (exospheric) temperature was assumed to be a different constant. He also indicated that the problem of representing the density between 120 km and the thermopause was largely a problem of deducing the vertical distribution of temperature.

The contribution of Jacchia to the so-called Jacchia-Nicolet model is largely the development of empirical formulas to compute both the exospheric temperature and vertical temperature distribution as a function of exospheric temperature. These formulae are based on satellite observations coupled with physical reasoning. In addition, Jacchia has updated the boundary conditions of Nicolet. Thus in effect Jacchia has provided all but the basic assumptions behind the model.

The fundamental parameter of the model is therefore the exospheric temperature. This temperature, together with the boundary conditions, implies a particular vertical temperature profile. These three items - exospheric temperature, boundary conditions, and temperature profile - define the density at any altitude over 120 km through the diffusive equilibrium equation.

Figure 1, which was taken from Reference 3, shows a comparison of density and exospheric temperatures derived from observations of Explorer 1 satellite with solar and geomagnetic parameters. Note the correspondence between the exospheric temperature and the density.

DENSITY

#### 2.8.7.2 The Exospheric Temperature Computations

To calculate the fundamental parameter, the exospheric temperature, Jacchia considered four factors which could cause variations:

1. Solar activity variation
2. Semi-annual variation
3. Diurnal variation
4. Geomagnetic activity variation

Each of these variations was determined to be related to one or more observable parameters (see Figure 1). The given empirical formulae are based on these parameters.

##### Solar Activity

There are many indices of solar activity but the one whose variations most closely parallel those of atmospheric density is the 10.7 cm. (2800 Mc.) solar flux line. The intensity of this line has been measured continuously since 1947, by the National Research Council in Ottawa on a daily basis. The values of the 10.7 cm. flux line are published

Reproduced from  
best available copy.

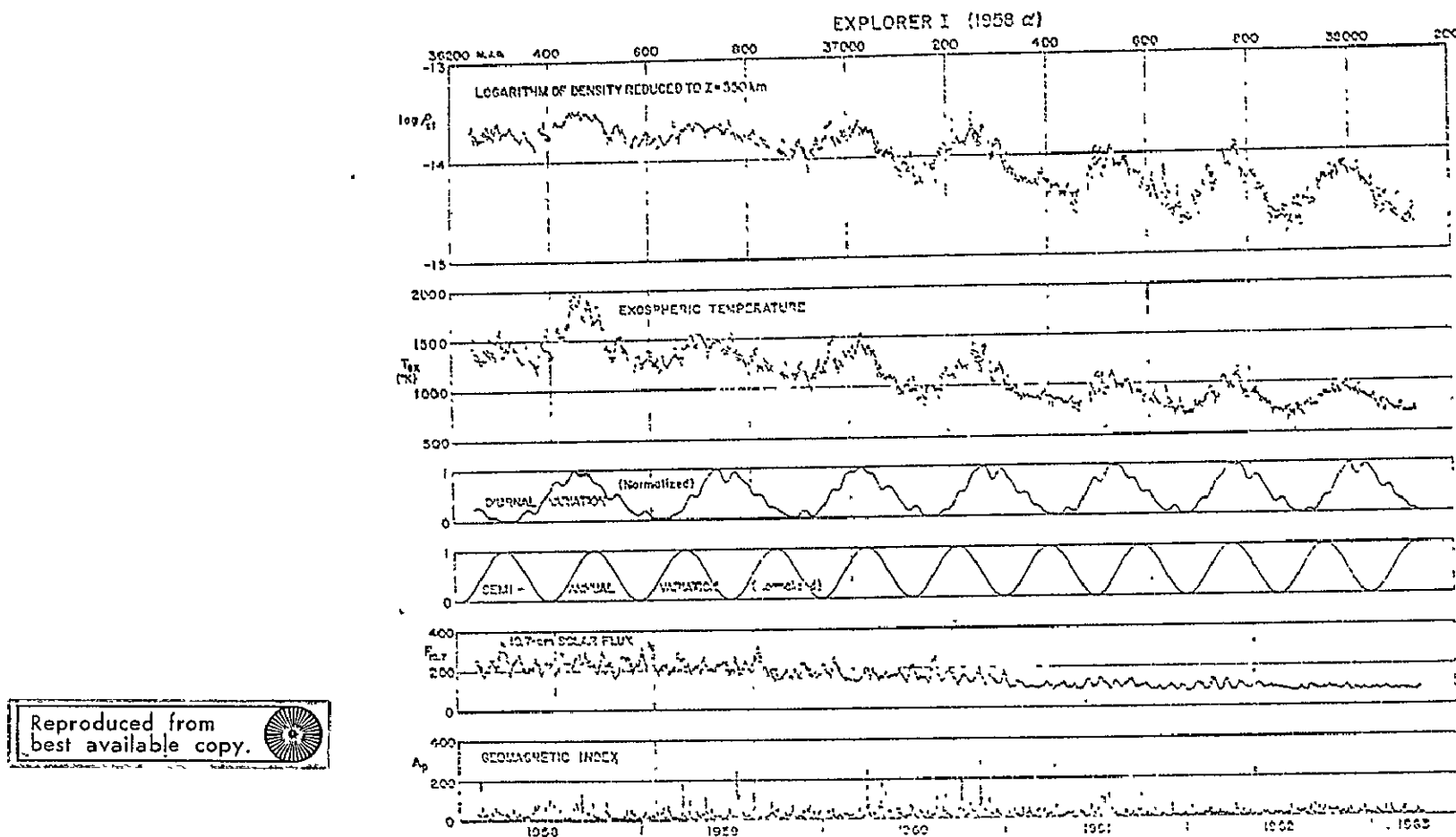


Figure 1. Densities and temperatures derived from the drag of the Explorer I satellite (1958 a), compared with solar and geomagnetic parameters. Notice the decrease in density and temperature which paralleled the decrease in the 10.7-cm solar flux during the five years covered by the diagram. The regular oscillations with a period of about 250 days are caused by the motion of the satellite perigee in and out of the diurnal bulge. Visible are also the 27-day oscillations in phase with those of the 10.7-cm flux and a few perturbations caused by major magnetic storm. Schematic curves of the diurnal and of the semiannual variations are added to aid the eye in recognizing them in the plots of satellite data. The wiggles in the diurnal diurnal-variation curve are caused by the rapid variations in latitude of the satellite orbit.  $X_1$  is the abscissa in the Modified Julian Day ( $JD$  minus 2400000.5). (Reproduced from Ref. 1)

monthly in the "Solar-Geophysical Data Reports" of the Environmental Science Services Administration in Boulder, Colorado (U.S. Department of Commerce).

DENSTY

Most of the time solar activity is much more intense in one solar hemisphere than the other so that the flux line appears to vary with the rotation period of the sun, 27 days. This periodicity frequently persists for a year or longer. In addition, there is a variation in the average flux strength with a period of about 11 years which is related to the solar cycle.

From satellite drag data a linear relation between the average 10.7 cm. flux and the average global nighttime minimum exospheric temperature has been obtained (Reference 2) and is expressed as

$$\bar{T}_0 = 357^\circ + 3.60^\circ \bar{F}_{10.7} \quad (1)$$

where

$\bar{F}_{10.7}$  is the average 10.7 cm. flux strength over 2 or 3 solar rotations measured in units of  $10^{-22}$  watts/ $\text{m}^2/\text{cycle/sec. bandwidth}$ .

$\bar{T}_0$  is the average global nighttime minimum temperature averaged over the same period.

This formula gives the relationship for absolutely quiet geomagnetic conditions; i.e., when  $a_p$  is zero.

The variation within one solar rotation is expressed (Reference 2) by

DENSITY

$$T_0' = \bar{T}_0 + 1.8^\circ (F_{10.7} - \bar{F}_{10.7}) \quad (2)$$

where

$F_{10.7}$  is the mean of the 10.7 cm solar flux for a given day in the same units as  $F_{10.7}$  and

$T_0'$  is the global nighttime minimum for the same day.

This formula accounts (approximately) for the day to day temperature variation superimposed on the average global nighttime minimum temperature determined by the previous formula.

There is some indication that the coefficient  $1.8^\circ$  actually varies from sunspot maximum to sunspot minimum. The indicated range of variation is from about  $2.4^\circ$  down to  $1.5^\circ$ .

#### Semi-Annual Variation

The semi-annual variation is the least understood of the several types of variation in the upper atmosphere. Yearly, the atmospheric density above 200 km reaches a deep minimum in July followed by a high maximum in October-November, a secondary minimum in January, and a secondary maximum in April. Jacchia

(Reference 1) found that the observed density variations could be explained by temperature variations in the thermopause, and are roughly proportional to the 10.7 cm flux line. It has been noted that the height of the ionospheric  $E_2$  layer shows a semi-annual variation almost exactly in phase with the observed density variations. Another suggestion by F.S. Johnson (Reference 7) concerning the cause of the semi-annual variation, involves convective transfer at ionospheric levels from the summer pole to the northern pole. This, as yet, does not seem to account correctly for all the details of this variation. The semi-annual variation is not as stable a feature as the diurnal variation. Jacchia (Reference 2) accounted for this feature in 1965 but has, with the recent information of drag data from six satellites, updated his empirical formula (Reference 6) as follows:

$$T_0 = T_0^* + 2.41 + F_{10.7} [0.349 + 0.206 \sin(2\pi\tau + 226.5^\circ) + \sin(4\pi\tau + 247.6^\circ)] \quad (3)$$

where

$$\tau = d/Y + 0.1145 \left( \left( \frac{1 + \sin[2\pi(d/Y) + 342.3^\circ]}{2} \right)^{2.16} - 0.5 \right) \quad (4)$$

d = day of the year counted from January 1.

DENSTY

Y = the tropical year in days.

$T_0$  = global nighttime minimum temperature for that day corrected for semi-annual variation.

Jacchia, Slowey, and Campbell (Reference 6) have more clearly defined this variation. As expected, the relationship between the temperature and the 10.7 cm flux line cannot be considered accurate. It was concluded that the observed density variations are the result of temperature variations at essentially the same level as in the case of the solar effect. However, a variable altitude shows that the semi-annual variation affects the whole atmosphere in the same manner, irrespective of latitude.

The most regular of the variations is the diurnal variation. One can picture the density distribution as an atmospheric bulge with its peak  $30^{\circ}$  east of the sub-solar point, degrading nearly symmetrically on all sides, but a little steeper on the morning side. The density peaks at 2 P.M. local solar time and the minimum occurs at 4 A.M. The ratio of the maximum temperature at the center of the bulge to the minimum in the opposite hemisphere remains constant throughout the solar cycle; the ratio is 1.28 in Jacchia's model atmosphere. The cause of the heating is in dispute. Some investigators believe it is due entirely to extreme ultra-violet (EUV) radiations; others, to ion drift; and still others, to a combination of the two.

The temperature,  $T$ , at a given hour and geographic location, can be computed in terms of the correct global nighttime minimum temperature for that day,  $T_0$ , using the following formula which approximates a mathematical description of the atmospheric bulge (Reference 2):

$$T = T_0 (1 + R \sin^m \theta) \left( 1 + \frac{R(\cos^m \eta - \sin^m \theta)}{1 + R \sin^m \theta} \cos^m \frac{\tau}{2} \right) \quad (5)$$

where

DENSTY

$$R = 0.26$$

$$n = m = 2.5$$

$$\tau = H + B + p \sin (H + \gamma) \quad (-\pi < \tau < \pi)$$

$$B = -45^\circ$$

$$p = 12^\circ$$

$$\gamma = 45^\circ$$

$$\eta = \text{ABS}[(\phi - \delta_\odot)/2]$$

$$\theta = \text{ABS}[(\phi + \delta_\odot)/2]$$

$\phi'$  = geographic latitude

$\delta_\odot$  = declination of the sun

$H$  = hour angle of the sun

( $H = 0$  occurs when the point considered,  
the sun, and the earth's axis are coplanar.  
 $H$  is measured westward  $0^\circ$  to  $360^\circ$ )

Based on satellite information, Jacchia (Reference 5) assumes a maximum day temperature 28% higher than the corresponding nighttime minimum. The variation is represented by  $R$  in the above equation. However, further investigation by Jacchia, Slowey, and Campbell (Reference 6), revealed that the diurnal-variation factor ( $R$ ) is somewhat variable. A value of 32% is considered valid for dates

prior to February 1963, and from August 1963<sup>1</sup>, onward, 26% variation is considered valid. Between these dates, R is made to decrease linearly.

DENSTY

Although in these equations the exponents m and n, which determine the mode of the longitudinal and latitudinal temperature variations respectively, are kept distinct, it was found in practice that m = n. These values are not really known accurately and could be as small as 2.0.

The constant B determines the lag of the temperature maximum with respect to the uppermost point of the sun; p introduces an asymmetry in the temperature curve whose location is determined by γ.

### Geomagnetic Activity

To the temperature, T, which is calculated above, a correction must be added which accounts for atmospheric heating related to changes in the Earth's magnetic field. The heating probably occurs in the E layer of the ionosphere, but the mechanism involved is not well understood. The temperature correction, ΔT, is given by Jacchia, Slobey, and Campbell (Reference 6):

$$\Delta T = 1.0^\circ a_p + 100^\circ [1 - \exp(-0.08a_p)] \quad (6)$$

where

$a_p$  is the three-hourly planetary geomagnetic index.

The quantity  $a_p$  is a measure of the variation in the earth's magnetic field in a given three hour period.

DENSTY

During magnetic storms the temperature changes generally lag behind the variations in  $a_p$  by about five hours, due to conduction. There is some evidence of larger temperature changes for given values of  $a_p$  as one proceeds to higher geomagnetic latitudes. However, the amount of data indicating this is negligible at this time.

The DENSTY subroutine allows for the magnetic heating effects with one modification. To minimize the input data for NONAME, the 3-hourly index ( $a_p$ ) is replaced by a 24-hourly or daily index ( $A_p$ ). Generally, magnetic storms last for 2 or 3 days so that the temperature calculation using  $A_p$  will reflect a daily change, but not the 3-hourly fluctuations which occur with  $a_p$ .

The quantity  $A_p$  and the solar flux data is available from E.S.S.A., Boulder, Colorado. The publication is, "Solar Geophysical Data, Part I."

Accurate daily values for both the solar and geomagnetic flux are required for the computation of the exospheric temperature. In NONAME, these values are input via a BLOCK DATA routine, INPT. This information may be updated (cf subroutine ADFLUX) using the appropriate NONAME Input Cards. The user should be aware of the fact that these tables are expanded as new information becomes available.

INPT  
ADFLUX

At the beginning of each run, a file is generated for each satellite arc which contains the required flux data for the time span indicated. Subroutine JANTHG is the routine which sets up the flux tables, including averaging the daily values of solar flux over two solar rotation periods. The reason for this is to free the large amount of computer storage required for daily flux values over five and a half years. As a matter of reference, the associated COMMON BLOCK is PRIORI.

JANTHG

#### 2.8.7.3 The Density Computation

The density computation in NONAME subroutine DENSTY is based on the density distribution versus altitude and exospheric temperature presented in Table 1, which is reproduced from Jacchia's 1965 paper (Reference 2). This data was obtained by numerical integration of the diffusion equation using an empirical temperature profile for each indicated exospheric temperature.

DENSTY

This vast quantity of information was fitted (by WOLF) to various degree polynomials of the form:

$$\text{LOG}_{10} \rho_D = \sum_i \sum_j a_{ij} T^{(j-1)} h^{(i-1)} \quad (7)$$

where

$\rho_D$  is the density,

T is the exospheric temperature,

DENSITY

h is the spheroid height of the satellite  
(altitude), and

a is a set of appropriate coefficients

Unfortunately, a single polynomial of the type presented is not completely descriptive. An examination of Table 1 reveals that density is nearly independent of temperature for low altitudes, but becomes increasingly dependent for heights above 160 km. Accordingly, appropriate polynomials were chosen to account for the varying dependency of the variables. This necessitated the separation of Table 1 into three parts.

The lower region (120 km - 160 km) is expressed as a second degree polynomial which is solely a function of altitude. This is due to the fact that density is not appreciably dependent on temperature in this region. The remaining regions of 160 km to 420 km and 420 km to 1000 km are described by polynomials of fourth degree in both temperature and altitude.

The coefficients for the selected polynomials are presented in Table 2. These coefficients have been modified to compute the natural log rather than the decimal log of the density.

TABLE 2  
DENSITY POLYNOMIAL COEFFICIENTS  
(FOR NATURAL LOG OF DENSITY)

	$h^0$	$h^1$	$h^2$	$h^3$
420-1000 KM				
$T^0$	61.5177	48.60687	6.87280	0.305394
$T^1$	-173.970	93.4870	-14.1203	0.651270
$T^2$	111.908	-60.34177	9.349784	-0.440330
$T^3$	-23.3864	12.64406	-1.989456	0.0950336
160-420 KM				
$T^0$	0.514627	-26.4622	6.28711	-0.604854
$T^1$	-36.8141	37.5137	-9.994692	1.00192
$T^2$	22.6334	-23.9095	6.780537	-0.695452
$T^3$	-4.47654	4.83017	-1.41853	0.148026
120-160 KM				
	1.1335948	-31.858566	8.7827269	

The densities produced by these fitted polynomials differ from the densities in Table 1 by an RMS of 3.7 percent. However, the fit does vary in different regions of the table. In the region of worst fit, where the temperature is relatively low (700-1000° K) and the altitude varies from 620-840 km, the RMS is somewhat greater being about 8.5 percent. The largest percent difference between densities is 13.2 percent and falls within the region described.

DENSTY

The fits above could be improved by either going to higher degree polynomials or by additional segmentation of the table. However, these fits are considered to be as accurate as the model being used.

For satellite altitudes above 1000 km, the density is computed according to the extrapolation formula given by Jacchia (Reference 1):

$$\rho_D = \rho_\infty + (\rho_{1000} - \rho_\infty) e^{[b(h-1000)]} \quad (8)$$

where

$b = \frac{d}{dh} (\ln \rho_D)$  as evaluated at 1000 km.

$\rho_\infty$  - is a limiting value for the density.  
This is zero in subroutine DENSTY.

$h$  - is the spheroid height.

$\rho_{1000}$  - is the density evaluated at 1000 km.

$\rho_D$  - is the desired density at altitude  $h$ .

## 2.8.7.4 Density Partial Derivatives

DENSITY  
VIVAL

In addition to the density, NONAME also requires the partial derivatives of the density with respect to the Cartesian position coordinates. These partials are used in computing the drag contribution to the variational equations.

As demonstrated above, the density is given by

$$\rho_D = \exp (C_0 + C_1 h + C_2 h^2 + C_3 h^3) \quad (1)$$

where

$h$  is the spheroid height, and the  $C_i$  are coefficients which are polynomials in temperature.

We then have

$$\frac{\partial \rho_D}{\partial \bar{r}} = \rho_D (C_1 + 2 C_2 h + 3 C_3 h^2) \frac{\partial h}{\partial \bar{r}} \quad (2)$$

where

$\bar{r}$  is the true of date position vector of the satellite ( $x, y, z$ ). The partial derivatives  $\frac{\partial h}{\partial \bar{r}}$  are presented along with the computation of spheroid height in Section 2.5.1.

The partial derivatives  $\frac{\partial \rho_D}{\partial \bar{r}}$  are computed in subroutine VEVAL. The quantities  $h$ ,  $\rho_D$ , and the  $C_i$  are computed in DENSTY and passed through COMMON BLOCK DRGBLK.

SECTION 2.9  
INTEGRATION AND INTERPOLATION

NONAME uses Cowell's method for direct numerical integration of both the equations of motion and the variational equations to obtain the position and velocity and the attendant variational partials at each observation time. The integrator output is not required at actual observation times; it is output on an even integration step. NONAME uses an interpolation technique to obtain values at the actual observation time. The specific numerical methods used in NONAME for this integration and interpolation are presented below. These procedures are controlled by subroutine ORBIT.

2.9.1 Integration

Let us first consider the integration of the equations of motion. These equations are three second order differential equations in position, and may be formulated as six first order equations in position and velocity if a first order integration scheme were used for their solution. For reasons of increased accuracy and stability, the position vector  $\vec{r}$  is obtained by a second order integration of the accelerations  $\ddot{\vec{r}}$ , whereas the velocity vector  $\vec{r}$  is obtained as the solution of a first order system. These are both ten point multi-step methods requiring two derivative evaluations on each step.

ORBIT

COWELL

To integrate the position components, a Stormer predictor

COWEL

$$\bar{r}_{n+1} = 2\bar{r}_n - \bar{r}_{n-1} + (\Delta h)^2 \sum_{p=0}^q \gamma_{qp}^* \ddot{r}_{n-p} \quad (1)$$

is applied, followed by a Cowell corrector:

$$\bar{r}_{n+1} = 2\bar{r}_n - \bar{r}_{n-1} + (\Delta h)^2 \sum_{p=0}^q \gamma_{qp} \ddot{r}_{n-p+1} \quad (2)$$

The velocity components are integrated using an Adams-Basforth predictor;

$$\dot{r}_{n+1} = \dot{r}_n + \Delta h \sum_{p=0}^q \beta_{qp}^* \ddot{r}_{n-p} \quad (3)$$

followed by an Adams-Moulton corrector;

$$\dot{r}_{n+1} = \dot{r}_n + \Delta h \sum_{p=0}^q \beta_{qp} \ddot{r}_{n-p+1} \quad (4)$$

In these integration formulae,  $\Delta h$  is the integration step size,  $q$  has the value 9, and  $\gamma_{qp}^*$ ,  $\gamma_{qp}$ ,  $\beta_{qp}^*$  and  $\beta_{qp}$  are coefficients whose values are presented in Table 1.

TABLE 1  
INTEGRATION SCHEME COEFFICIENTS

$i$	$D\beta_{qi}^*$	$D\beta_{qi}$	$D\gamma_{qi}^*$	$D\gamma_{qi}$
0	- 262 426 878	7 217 406	57 739 248	2 153 844
1	2 631 486 186	- 73 512 810	- 579 546 324	- 21 861 404
2	-11 882 722 320	38 670 864	2 620 127 664	100 226 448
3	31 829 896 224	- 931 648 032	7 028 936 208	-273 727 440
4	-56 041 292 412	1 702 270 332	12 398 969 520	494 279 552
5	67 833 843 588	- 217 739 396	15 044 569 848	-618 300 144
6	-57 287 383 776	2 016 292 320	-12 743 542 224	540 551 504
7	33 507 517 680	-1 420 184 304	7 469 061 264	-242 102 448
8	-13 229 393 814	1 190 664 342	- 2 840 368 608	875 698 740
9	3 814 933 122	262 426 878	1 453 091 220	57 739 248

where  $D = 9144457600$  and is the common denominator

Let us next consider the integration of the variational equations. These equations may be written as

COWELL

$$\ddot{Y} = [A \ B] \begin{bmatrix} Y \\ \dot{Y} \end{bmatrix} + f \quad (5)$$

where

$$\begin{bmatrix} Y \\ \dot{Y} \end{bmatrix} = X_m$$

and, partitioning according to position and velocity partials,

$$[A \ B] = \begin{bmatrix} U_{2C} + D_r \end{bmatrix} \quad (6)$$

Note that equation (5) is the same as equation (7) of Section 2.8.2, with  $Y$  corresponding to the matrix  $F$ . The variational particle  $X_m$  and the partial derivative matrices  $U_{2C}$ ,  $D_r$ , and  $f$  are completely defined in that section.

Because  $A$ ,  $B$ , and  $f$  are functions only of the orbital parameters, the integration can be and is performed using only corrector formulae. (Note that  $A$ ,  $B$ , and  $f$  must be evaluated with the final corrected values of  $\bar{r}_{n+1}$  and  $\dot{\bar{r}}_{n+1}$ .)

In the above corrector formulae, we substitute the equation for  $Y$  and solve explicitly for  $Y$  and  $\dot{Y}$ :

$$\begin{bmatrix} Y_{n+1} \\ \vdots \\ \dot{Y}_{n+1} \end{bmatrix} = S^{-1} \begin{bmatrix} C \\ \vdots \\ \dot{C} \end{bmatrix} \quad (7)$$

where

$$S = \begin{bmatrix} I - \gamma_{q0} A & -\gamma_{q0} B \\ -\beta_{q0} A & I - \beta_{q0} B \end{bmatrix}$$

$$C = \begin{bmatrix} 2Y_n - Y_{n-1} + \sum_{p=1}^q \gamma_{qp} \ddot{Y}_{n-p+1} + \gamma_{q0} f \\ \dot{Y}_{n-1} + \sum_{p=1}^q \gamma_{qp} \ddot{Y}_{n-p+1} + \beta_{q0} f \end{bmatrix}$$

$$\dot{C} = \begin{bmatrix} \ddot{Y}_{n-1} + \sum_{p=1}^q \gamma_{qp} \ddot{Y}_{n-p+1} + \beta_{q0} f \end{bmatrix}$$

Under certain conditions, a reduced form of this solution is used. It can be seen from the variational and observation equations that if drag is not a factor and there are no range rate, doppler, or altimeter rate measurements, the velocity variational partials are not used. There is then no need to integrate the velocity variational equations. This represents a significant time saving. In the integration algorithm, the B matrix is zero and S is reduced to a three by three.

Backwards integration involves only a few simple modifications to these normal or forward integration procedures. These modifications are to negate the step size, invert the time completion test, and invert the entire table of back values.

BAKINT

The above integration procedures are implemented in NONAME in the subroutine COWELL. The inversions for backwards integration are performed by BAKINT. The matrix inversion is performed by subroutine DNVERT.

BAKINT

COWELL

DNVERT

The default step size for these integration procedures is selected on the basis of perigee height and the eccentricity of the orbit. The default step size selection is explained in detail in the Operations Manual, Volume III of the NONAME System Documentation. This may be reset to some other fixed value on input. (See the STEP control card description in the above manual.)

#### Variable Step Mode

There is an optional variable step mode which is the default mode for high eccentricity orbits. The selection of this mode of operation, its default initial step size, halving error bound, and doubling error bound are also explained in Volume III with the STEP control card.

In the variable step mode, the local error is compared against upper and lower error bounds to determine whether the step size should be halved or doubled. This local error is computed as the difference between the predicted and corrected values of position. Both the halving and doubling procedures require the tables of

COWELL

REARG

HUEMIR

back values to be modified so as to be compatible with the new step size. The halving requires a Hermite interpolation for mid-points. This interpolation is of course on the back position, velocity and acceleration values. The doubling is achieved by discarding every other time point in the table of back values. REARG HHEMIT

It should be noted that twenty sets of back values are saved when NONAME is operating in variable step mode. Doubling of the step size is disabled for the following ten steps after a step size change; i.e., until the table of back values is again filled.

These halving and doubling procedures are contained in subroutine REARG. In the case of halving, subroutine HHEMIT is invoked to interpolate for the mid-points.

### 2.9.2 The Integrator Starting Scheme

The predictor-corrector combination employed to proceed with the main integration is not self-starting. That is, each step of the integration requires the knowledge of past values of the solution that are not available at the start of the integration. The method presented here is that implemented in the NONAME subroutine INTGST. INTGST

A method first proposed by W. Romberg provides the ten values required to start the main predictor-corrector scheme. The Euler-Cauchy single step method is combined with Richardson's  $h^2$ -extrapolation to generate a sequence of approximate solutions,  $X(h)$ , for a fixed time interval  $h$ . Successive approximations

to  $X(h)$  are formed by subdividing the interval into subintervals of lengths  $\Delta t_1 > \Delta t_2 > \Delta t_3 \dots$  and by applying the Euler-Cauchy method to yield the sequence of approximations  $X(\Delta t_1)$ ,  $X(\Delta t_2)$ ,  $X(\Delta t_3) \dots$ . An Aitken-Neville interpolation scheme is then used to find successive extrapolations to  $X(\Delta t=0)$ . A complete analysis of this very stable and accurate technique has been published by Rutishauser, Stiefel, and Bauer (Reference 2).

The subintervals  $\Delta t_i$ ,  $i=1, \dots, 7$  are defined as  $\frac{h}{s_i}$ , by step-ratios  $s_i$ ,  $i=1, \dots, 7$ , which must form a monotonic increasing series. In the NONAME starting scheme this step-ratio series is a fixed program parameter  $\{1, 2, 3, 5, 8, 12, 17\}$ , chosen to maintain the scheme's accuracy by considering a broad range of step-ratios, without consuming the computation time needed for very large step-ratios.

At each subinterval, an Euler-Cauchy scheme is used to predict a value of the position-velocity vector  $X$  as the solution of a first order system of equations, using the Euler formula.

$$X [(j+1)\Delta t_i] = X [j\Delta t_i] + \Delta t_i \dot{X} [j\Delta t_i], \quad (1)$$

$$j = 0, \dots, s_i - 1, \quad i = 1, \dots, 7$$

This predicted vector is next refined using the formula

$$X[(j+2)\Delta t_i] = X[j\Delta t_i] + \Delta t_i \dot{X}[(j+1)\Delta t_i], \quad (2) \quad \text{INTGST}$$

$$j = 0, \dots, s_i - 2, \quad i = 1, \dots, 7$$

and finally corrected using the equation

$$X[(j+1)\Delta t_i] = X[j\Delta t_i] + \frac{\Delta t_i}{2} \{X[j\Delta t_i] + \dot{X}[(j+1)\Delta t_i]\},$$

$$j = 0, \dots, s_{i-1}, \quad i = 1, \dots, 7 \quad (3)$$

The approximations  $X(s_i \Delta t_i)$ ,  $i=1, \dots, 7$  to the position velocity vector  $X(h)$  over a full step  $h$ , given by each sequence of subinterval integrations are then used in an Aitken-Neville interpolation scheme:

$$X(h) = X(\Delta t_i) + r_{ji} [X(j\Delta t_i) - X(j\Delta t_{i-1})] \quad (4)$$

$$j = 1, \dots, s_i, \quad i = 1, \dots, 7$$

The Aitken-Neville factors  $r_{ji}$  are computed from the monotonic increasing series  $t_1, t_2, \dots, t_7$  from the formula

$$r_{jk} = \left[ \left( \frac{t_{k+1}}{t_j} \right)^2 - 1 \right]^{-1} \quad k = 1, \dots, 6$$

$$j = 1, \dots, k \quad (5)$$

The final approximation  $X(h)$  to the integrated vector is then used to repeat the above process for the next time-step  $h$ , until nine values of the position-velocity vector have been generated. Together with the epoch position-velocity vector, these values are used to start the much faster predictor-corrector sequence employed to integrate the remainder of the orbit.

INTGSI

### 2.9.3 Interpolation

NONAME uses Hermite interpolation for two functions. The first is the interpolation of the orbit elements and variational partials to the observation times; the second is the interpolation for mid-points when the integrator is halving the step size. These functions are separate largely because they have entirely different accuracy requirements. In particular, when the step size is being halved, the accuracy of the interpolation for the new points is critical because any errors introduced will build up in the subsequent integration.

HERMIT

HIERMIT

The Hermite interpolation formula uses osculating polynomials of contact order  $n$ ; i.e., they have the properties

$$X(t_j) = P(t_j) \quad (1)$$

$$X^{(i)}(t_j) = P^{(i)}(t_j) \quad i = 0, 1, \dots, n \quad (2)$$

where the  $X^{(i)}(t_j)$  are the  $i^{\text{th}}$  derivatives of  $X(t)$  evaluated at  $t = t_j$ . Also, the derivatives of  $P(t)$  higher than  $n$  are zero.

These Hermite polynomials have the form (see Reference 3):

$$P(t_j) = \sum_{i=0}^n \sum_{j=1}^k h_{ij} x^{(i)}(t_j) \quad (3)$$

HERMIT  
HHERMIT

where

$n$  is the number of derivatives being utilized,

$k$  is the number of values available for each  $x^{(i)}$ , and

$h_{ij}$  is a polynomial having properties similar to those of the Lagrange polynomials.

Let us consider the case where  $n$  is one. This produces the usual Hermite interpolation formula in the literature. For this case, only the function and its first derivative are used. The two sets of coefficients are given by

$$h_{0j} = \left[ 1 - 2 L_j^{(1)}(t_j) (t - t_j) \right] \left[ L_j(t_j) \right]^2 \quad (4)$$

$$h_{1j} = \left( t - t_j \right) \left[ L_j(t_j) \right]^2 \quad (5)$$

HERMIT

where the  $L_j(t)$  are the familiar Lagrange polynomials of degree  $k$ . This is the case for interpolating the orbital elements and is implemented in NONAME subroutine HERMIT. Note that the same two sets of coefficients are used for all of the variables being interpolated. The variational partials are interpolated using the Lagrange polynomials. This is also implemented in HERMIT.

We also take advantage of the fact that the data is evenly spaced according to the current integrator step size. The  $h_{ij}$  are used as

$$h_{0j} = \left[ 1 - 2(s-j) \sum_{\substack{i=0 \\ i \neq j}}^n \frac{1}{j-i} \right] \left[ L_j(t_j) \right]^2 \quad (6)$$

$$h_{1j} = h(s-j) \left[ L_j(t_j) \right]^2 \quad (7)$$

where  $h$  is the step size,

$$s = \frac{t-t_0}{h},$$

and the Lagrange polynomials take the form\*

$$L_j(t_j) = \frac{(-1)^{n-j} \pi^{(s-i)}}{j! (n-j)!}$$

\*  $\pi^{(s-i)}$  is a standard notation for the derivative of  $\pi(s-i)$  evaluated at  $i=j$ ; i.e.,  $\sum_{i=j}^{o,n} \pi^{(s-i)}$ .

Let us now consider the case where  $n$  is two, where the function and two derivatives are required. In this case there are three sets of coefficients:.

$$h_{0j} = \left[ 1 + 6(t-t_j)^2 \left\{ \left[ L^{(1)}(t_j) \right]^2 - \frac{1}{4} L^{(2)}(t_j) \right\} \right] \left[ \frac{3(t-t_j)}{L^{(1)}(t_j)} \right] \left[ \frac{L(t_j)}{L^{(1)}(t_j)} \right]^2 \quad (8)$$

$$h_{1j} = \left[ (t-t_j) - 3(t-t_j)^2 L^{(1)}(t_j) \right] \left[ \frac{L(t_j)}{L^{(1)}(t_j)} \right]^2 \quad (9)$$

$$h_{2j} = \frac{1}{2} (t-t_j)^2 \left[ L(t_j) \right]^2 \quad (10)$$

This is the case for the mid-point interpolation for position when the integrator is halving the step size. It is implemented in subroutine HHEMIT, along with the  $n$  equals one case for the velocity and variational partials.

In interpolating for the mid-points advantage is taken of both the fact that the data is evenly spaced and that the mid-points are being determined. The quantity  $s$  becomes  $\ell + \frac{1}{2}$ ; the  $h_{ij}$  are therefore given by

$$h_{0j} = \left[ 1 + \frac{3}{2} \left( \ell - j + \frac{1}{2} \right)^2 \left\{ \sum_{\substack{i=0 \\ i \neq j}}^n \frac{1}{j-i} \right\}^2 + \sum_{\substack{i=0 \\ i \neq j}}^n \frac{1}{(j-i)^2} \right] \quad (11)$$

$$= 3 \left( \ell - j + \frac{1}{2} \right) \sum_{\substack{i=0 \\ i \neq j}}^n \frac{1}{j-i} \left[ L_j(t_j) \right]^2$$

$$h_{1j} = \left[ h \left\{ \left( \ell - j + \frac{1}{2} \right) - 3 \left( \ell - j + \frac{1}{2} \right)^2 \sum_{\substack{i=0 \\ i \neq j}}^n \frac{1}{j-i} \right\} \right] \left[ L_j(t_j) \right]^2 \quad (12)$$

$$\frac{1}{j-1} \left\{ \right\} \left[ L_j(t_j) \right]^2$$

$$h_{2j} = \frac{h^2}{2} \left( \ell - j + \frac{1}{2} \right)^2 \left[ L_j(t_j) \right]^2 \quad (13)$$

for  $n$  equals two. For the case of  $n$  equal to one, the  $h_{ij}$  become

$$h_{0j} = \left[ 1 - 2 \left( \ell - j + \frac{1}{2} \right) \sum_{\substack{i=0 \\ i \neq j}}^n \frac{1}{j-i} \right] \left[ L_j(t_j) \right]^2 \quad (14)$$

$$h_{1j} = h \left( k - j + \frac{1}{2} \right) \left[ L_j(t_j) \right] \quad \text{HERMIT} \quad (15)$$

it should be noted that both interpolation  
schemes are tenth order. HERMIT  
HERMIT

## SECTION 2.10 THE STATISTICAL ESTIMATION SCHEME

The basic problem in orbit determination is to calculate, from a given set of observations of the spacecraft, a set of parameters specifying the trajectory of a spacecraft. Because there are generally more observations than parameters, the parameters are overdetermined. Therefore, a statistical estimation scheme is necessary to estimate the "best" set of parameters.

The estimation scheme selected for NONAME is a partitioned Bayesian least squares method. The complete development of this procedure is presented in this section.

It should be noted that the functional relationships between the observations and parameters are in general non-linear; thus an iterative procedure is necessary to solve the resultant non-linear normal equations. The Newton-Raphson iteration formula is used to solve these equations.

### 2.10.1 Bayesian Least Squares Estimation\*

Consider a vector of  $N$  independent observations  $\underline{z}$  whose values can be expressed as known functions of  $M$  parameters denoted by the vector  $\underline{x}$ . The following non-linear regression equation holds:

$$\underline{z} = \underline{f}(\underline{x}) + \underline{\sigma}, \quad (1)$$

where  $\underline{\sigma}$  is the  $N$  vector denoting the noise on the observations. Given  $\underline{z}$ , the functional form of  $\underline{f}$ ; and the statistical properties of  $\underline{\sigma}$ , we must obtain the estimate of  $\underline{x}$  that is "best" in some sense.\*\*

Bayes theorem in probability holds for probability density functions and can be written as follows:

$$p(\underline{x}|\underline{z}) = \frac{p(\underline{x})}{p(\underline{z})} p(\underline{z}|\underline{x}). \quad (2)$$

where

$p(\underline{x}|\underline{z})$  is the joint conditional probability density function for the parameter vector  $\underline{x}$ , given that the data vector  $\underline{z}$  has occurred

\*Vector notation in this section is that used by statisticians; i.e., an underscore denotes a vector. The symbol " $\hat{\cdot}$ " denotes the "best" estimate of the superscripted quantity.

\*\*For a complete discussion of the properties of estimators see Maurice G. Kendall and Alan Stuart, Reference 1

$p(\underline{x})$  is the joint probability density function for the vector  $\underline{x}$ ;

$p(\underline{z})$  is the joint probability density function for the vector  $\underline{z}$ ;

and

$p(\underline{z}|\underline{x})$  is the joint conditional density function for the vector  $\underline{z}$  given that  $\underline{x}$  has occurred;

$p(\underline{x})$  is often referred to as the a priori density function of  $\underline{x}$ , and  $p(\underline{x}|\underline{z})$  is referred to as the a posteriori conditional density function. In any Bayesian estimation scheme, we must determine this a posteriori density function and from this function determine a "best" estimate of  $\underline{x}$ , which can be denoted  $\hat{\underline{x}}$ .

To obtain the a posteriori conditional density function, we must make an assumption concerning the statistical properties of the noise on the observations: the noise vector  $\underline{\sigma}$  has a joint normal distribution with mean vector  $\underline{0}$  and a variance-covariance matrix  $\sum_z$ .  $\sum_z$  is an NxN matrix and is assumed diagonal, that is, the observations are considered to be independent and uncorrelated. The "best" estimate of  $\underline{x}$ ,  $\hat{\underline{x}}$ , is defined as that vector maximizing the a posteriori density function; this is equivalent to choosing the mean value of this distribution. An estimator of this type has been referred to as the maximum likelihood estimate in the Bayesian sense. (Reference 2)

A further assumption is that the a priori density function  $p(\underline{x})$  is a joint normal distribution and is written as follows:

$$p(\underline{x}) = \left[ \frac{\text{Det}(\Sigma_A^{-1})}{2\pi} \right]^{\frac{M}{2}} \exp \left\{ -\frac{1}{2} \left( \underline{x} - \underline{x}_A \right)^T \sum_A^{-1} \left( \underline{x} - \underline{x}_A \right) \right\} \quad (3)$$

where

$\underline{x}_A$  is the a priori estimate of the parameter vector,

$\sum_A$  is the a priori variance-covariance matrix associated with the a priori parameter vector.

$\sum_A$  is an  $M \times M$  matrix, which may or may not be diagonal.

The conditional density function  $p(\underline{z}|\underline{x})$  can be written as follows:

$$p(\underline{z}|\underline{x}) = \left[ \frac{\text{Det}(\Sigma_z^{-1})}{2\pi} \right]^{\frac{N}{2}} \exp \left\{ -\frac{1}{2} \left[ \underline{z} - \underline{f}(\underline{x}) \right]^T \sum_z^{-1} \left[ \underline{z} - \underline{f}(\underline{x}) \right] \right\} \quad (4)$$

It can be shown that maximizing the a posteriori density function  $p(\underline{x}|\underline{z})$  is equivalent to maximizing the product  $p(\underline{x})p(\underline{z}|\underline{x})$  because the density function  $p(\underline{z})$  is a constant valued function. Further, this reduces to minimizing the following quadratic form:

$$\left( \underline{x} - \underline{x}_A \right)^T \sum_A^{-1} \left( \underline{x} - \underline{x}_A \right) + \left( \underline{z} - \underline{f}(\underline{x}) \right)^T \sum_z^{-1} \left( \underline{z} - \underline{f}(\underline{x}) \right). \quad (5)$$

This results in the following set of M non-linear equations:

$$B^T \sum_z^{-1} \left( \underline{z} - \underline{f}(\hat{\underline{x}}) \right) + \sum_A^{-1} \left( \underline{x} - \underline{x}_A \right) = 0 \quad (6)$$

where B is an NxM matrix with elements

$$B_{NM} = \frac{\partial f_N(\underline{x})}{\partial x_M} \Big|_{\underline{x}=\hat{\underline{x}}}$$

This equation defines the Bayesian least squares estimation procedure. We have not stated how the a priori parameter vector and variance-covariance matrix were obtained. In practice these a priori values are almost always estimates that have been obtained from some previous data. In these cases the Bayesian estimates are identical to the classical maximum likelihood estimates that would be obtained if all the data were used; in this context the a priori parameters can be considered as additional observations.

The variance-covariance matrix of  $\hat{\underline{x}}$ ,  $V$ , is given by the following formula:

$$V = \left[ B^T \sum_z^{-1} B + \sum_A^{-1} \right]^{-1} \quad (7)$$

### Solution of the Estimation Formula

Equation 6 defines a set of  $M$  non-linear equations in  $M$  unknowns  $\hat{\underline{x}}$ ; these equations are solved using the Newton-Raphson iteration formula. Equation 6 can be written as follows:

$$\underline{F}(\hat{\underline{x}}) = 0$$

The iteration formula is

$$\hat{\underline{x}}^{(n+1)} = \hat{\underline{x}}^{(n)} - \left( \frac{\partial \underline{F}(\hat{\underline{x}})}{\partial \hat{\underline{x}}} \right)^{-1} \underline{F} \left( \hat{\underline{x}}^{(n)} \right) \quad (8)$$

where

$\hat{\underline{x}}^{(n)}$  is the  $n^{\text{th}}$  approximation to the true solution  $\hat{\underline{x}}$ .

Now

$$F(\hat{\underline{x}}) = B^T \sum_z^{-1} \left( \underline{z} - \underline{f}(\hat{\underline{x}}) \right) + \sum_A^{-1} \left( \hat{\underline{x}} - \underline{x}_A \right) = 0 \quad (9)$$

Then differentiating and neglecting second derivatives,

$$\left( \frac{\partial F(\hat{\underline{x}})}{\partial \hat{\underline{x}}} \right) = \left[ \left( B^T \sum_z^{-1} B \right) \right] + \sum_A^{-1} \quad (10)$$

Substituting equation 10 in equation 8 gives

$$\begin{aligned} \hat{\underline{x}}^{(n+1)} - \hat{\underline{x}}^{(n)} &= \left( B^T \sum_z^{-1} B + \sum_A^{-1} \right)^{-1} \left\{ B^T \sum_z^{-1} \left( \underline{z} - \underline{f}(\hat{\underline{x}}^{(n)}) \right) \right. \\ &\quad \left. + \sum_A^{-1} \left( \hat{\underline{x}}^{(n)} - \underline{x}_A \right) \right\} \end{aligned} \quad (11)$$

Now let  $\hat{\underline{x}}^{(n+1)} - \hat{\underline{x}}^{(n)}$ , the correction to the  $n^{\text{th}}$  approximation, be denoted by  $\underline{d}\underline{x}^{(n+1)}$ , and let  $\underline{z} - \underline{f}(\hat{\underline{x}}^{(n)})$ , the vector of residuals from the  $n^{\text{th}}$  approximation, be  $\underline{d}\underline{z}^{(n)}$ . Equation 11 becomes

$$\underline{d}\underline{x}^{(n+1)} = \left( B^T \sum_z^{-1} B + \sum_A^{-1} \right)^{-1} \left\{ B^T \sum_z^{-1} \underline{d}\underline{z}^{(n)} + \sum_A^{-1} \left( \hat{\underline{x}}^{(n)} - \underline{x}_A \right) \right\} \quad (12)$$

2.10.2 The Partitioned Solution

ESTIM

In a multi-satellite, multi-arc estimation program such as NONAME, it is necessary to formulate the estimation scheme in a manner such that the information for all satellite arcs are not in core simultaneously. The procedure used in NONAME is a partitioned Bayesian Estimation Scheme which requires only common parameter information and the information for a single arc to be in core at any given time. The development of the NONAME solution is given here.

The Bayesian estimation formula has been developed in the previous section as

$$\underline{\underline{x}}^{(n+1)} = \left( B^T W B + V_A^{-1} \right)^{-1} \left[ B^T W \underline{\underline{d}}_m + V_A^{-1} \left( \underline{\underline{x}}^{(n)} - \underline{\underline{x}}_A \right) \right] \quad (1)$$

where

$\underline{\underline{x}}_A$  is the a priori estimate of  $\underline{\underline{x}}$ .

$V_A$  is the a priori covariance matrix associated with  $\underline{\underline{x}}_A$ .

$W$  is the weighting matrix associated with the observations.

$\underline{\underline{x}}^{(n)}$  is the  $n^{\text{th}}$  approximation to  $\underline{\underline{x}}$ .

$\underline{\underline{d}}_m$  is the vector of residuals ( $0 - C$ ) from the  $n^{\text{th}}$  approximation.

$\underline{dx}^{(n+1)}$  is the vector of corrections to the parameters; i.e.,

1811

$$\underline{x}^{n+1} = \underline{x}^n + \underline{dx}^{(n+1)}$$

$B$  is the matrix of partial derivatives of the observations with respect to the parameters where the  $i, j^{\text{th}}$  element is given by

$$\frac{\partial m_i}{\partial x_j}$$

The iteration formula given by this equation solves the non-linear normal equations formed by minimizing the sum of squares of the weighted residuals.

We desire a solution wherein  $\underline{x}$  is partitioned according to  $\underline{a}$ ; the vector of parameters associated only with individual arcs; and  $\underline{k}$ , the vector of parameters common to all arcs. For geodetic parameter estimation  $\underline{a}$  consists of the sets of orbital elements, satellite parameters, and measurement biases associated with each arc, whereas  $\underline{k}$  consists of the geopotential coefficients and station coordinates.

As a result of this partitioning, we may write  $B$ , the matrix of partial derivatives of the observations, as

$$B = \begin{bmatrix} B_a & B_k \end{bmatrix} \quad (2)$$

where

FSTM

$$[B_a]_{i,j} = \frac{\partial m_i}{\partial a_j}$$

and

$$[B_k]_{i,j} = \frac{\partial m_i}{\partial k_j}$$

We may also write  $V_A$ , the covariance matrix of the parameters as

$$V_A = \begin{bmatrix} V_a & 0 \\ 0 & V_k \end{bmatrix} \quad (3)$$

where we have assumed the independence of the a priori information on the arc parameters and common parameters (in practice valid to an extremely high degree).

we may now rewrite our iteration formula:

ESTIM

$$\begin{bmatrix} \frac{da}{da} \\ \frac{da}{dk} \end{bmatrix} = \begin{bmatrix} B_a^T WB_a + V_a & B_a^T WB_k \\ B_k^T WB_k & B_k^T WB_k + V_k \end{bmatrix}^{-1} \begin{bmatrix} X \\ \end{bmatrix} \quad (4)$$

$$\begin{bmatrix} B_a^T Wdm^{(n)} + V_a (a^{(n)} - a_A) \\ B_k^T Wdm^{(n)} + V_k (k^{(n)} - k_A) \end{bmatrix}$$

$$\begin{bmatrix} A & A_k \\ A_k^T & K \end{bmatrix}^{-1} \begin{bmatrix} c_a \\ c_k \end{bmatrix}$$

The required matrix inversion is obtained by partitioning. We write

$$\begin{bmatrix} N_1 & N_2 \\ N_2^T & N_4 \end{bmatrix} \begin{bmatrix} A & A_k \\ A_k^T & K \end{bmatrix} = I \quad (5)$$

and, solving the resulting equations, determine

$$N_1 = A^{-1} + \begin{bmatrix} A^{-1} & A_k \\ A_k^T & A^{-1} \end{bmatrix} N_4 \begin{bmatrix} A^T & A^{-1} \end{bmatrix} \quad (6)$$

$$N_2 = -A^{-1} A_k N_4 \quad (7) \quad \text{ESTIM}$$

and

$$N_4 = \left[ K - A_k^T A^{-1} A_k \right]^{-1} \quad (8)$$

There is no problem associated with inverting  $A$  because the existence of the a priori information alone guarantees this property. On the other hand, the inverse of  $K - A_k^T A^{-1} A_k$  is not guaranteed to exist. High correlations between the parameters could make the matrix near singular. In practice, however, the use of a reasonable amount of a priori information eliminates any inversion difficulties.

The iteration formula may now be written as

$$\begin{bmatrix} \frac{da}{dk} \end{bmatrix} = \begin{bmatrix} N_1 & N_2 \\ N_2^T & N_4 \end{bmatrix} \begin{bmatrix} C_a \\ C_k \end{bmatrix} \quad (9)$$

or

$$\frac{da}{dk} = \left[ A^{-1} + (A^{-1} A_k) N_4 (A_k^T A^{-1}) \right] C_a - A^{-1} A_k N_4 C_k \quad (10)$$

$$\frac{dk}{dk} = -N_4 A_k^T A^{-1} C_a + N_4 C_k \quad (11)$$

Noting the similarities between  $\underline{da}$  and  $\underline{dk}$ , we write

ESTIM

$$\underline{da} = \Lambda^{-1} C_a - \Lambda^{-1} \Lambda_k \underline{dk} \quad (12)$$

and rewrite  $\underline{dk}$  as

$$\underline{dk} = N_4 (C_k - \Lambda_k^T \Lambda^{-1} C_a). \quad (13)$$

Note that most of the elements of  $\Lambda$  are zero because the measurements in any given arc are independent of the arc parameters of any other arc. Also, the covariances between the a priori information associated with each arc is assumed to be zero. Thus both  $\Lambda$  and  $V_a$  are composed of zeroes except for matrices,  $\Lambda_r$  and  $V_r$ , respectively, along the diagonal, where

$r$  is a subscript denoting the  $r^{\text{th}}$  arc,

e.g.,  $\underline{a}_r$

$$\left[ \Lambda_r \right]_{i,j} = \sum_{\ell} \frac{\partial m_{\ell}}{\partial a_{r_i}} \frac{1}{\sigma_{\ell}^2} \frac{\partial m_{\ell}}{\partial a_{r_j}} + \left[ V_r^{-1} \right]_{i,j} \quad (14)$$

where  $\ell$  ranges over the measurements in the  $r^{\text{th}}$  arc and  $i, j$  range over the parameters in the  $r^{\text{th}}$  arc,  $\underline{a}_r$ .

$V_r$  is the partition of  $V_a$  associated with the  $r^{\text{th}}$  arc.

ESTIM

The reader should note that  $\Lambda^{-1}$ , like  $\Lambda$ , is composed of zeroes except for matrices  $\Lambda_r^{-1}$  along the diagonal.

We shall also require the partitions of  $\Lambda_k$  and  $C_a$  according to each arc. These partitions are given by

$$\left[ \Lambda_{rk} \right]_{i,j} = \sum_{\ell} \frac{\partial m_{\ell}}{\partial a_{r_i}} \frac{1}{\sigma_{\ell}^2} \frac{\partial m_{\ell}}{\partial k_j} \quad (15)$$

and

$$\left[ C_r \right]_{i,j} = \sum_{\ell} \frac{\partial m_{\ell}}{\partial a_{r_i}} \frac{1}{\sigma_{\ell}^2} \frac{\partial m_{\ell}}{\partial k_j} \quad (16)$$

where the subscript  $r$  again denotes the  $r^{\text{th}}$  arc and  $\ell$  ranges over the measurement partials and residuals in the  $r^{\text{th}}$  arc.

Let us now investigate the matrix partitions in the solutions for  $\underline{da}$  and  $\underline{dk}$ . We consider  $\Lambda^{-1}$  to be a diagonal matrix with diagonal elements  $\Lambda_r^{-1}$  and  $C_a$  to be a column vector with elements  $C_r$ . Hence

$$\left[ \begin{matrix} \Lambda^{-1} & C_a \end{matrix} \right]_r = \Lambda_r^{-1} C_r \quad (17) \quad \text{ESTLY}$$

is the  $r^{\text{th}}$  element of the product matrix.  $\Lambda_k$  is considered to be a column vector with elements  $\Lambda_{rk}$ , thus

$$\left[ \begin{matrix} \Lambda_k^T & \Lambda^{-1} & C_a \end{matrix} \right] = \Lambda_{rk}^T \Lambda_r^{-1} C_r \quad (18)$$

The elements in the product  $\Lambda^{-1} \Lambda_k$  are given by

$$\left[ \begin{matrix} \Lambda^{-1} & \Lambda_k \end{matrix} \right]_r = \Lambda_r^{-1} \Lambda_{rk}. \quad (19)$$

We also require the product  $\Lambda_k^T \Lambda^{-1} \Lambda_k$ . Its elements are given by

$$\left[ \begin{matrix} \Lambda_k^T & \Lambda^{-1} & \Lambda_k \end{matrix} \right]_{r,r} = \Lambda_{rk}^T \Lambda_r^{-1} \Lambda_{rk} \quad (20)$$

The solutions for  $\underline{da}$  and  $\underline{dk}$  may now be rewritten taking into account the partitioning by arc:

$$\underline{da}_r = \Lambda_r^{-1} C_r - \Lambda_r^{-1} \Lambda_{rk} \underline{dk} \quad (21)$$

$$\underline{dk} = N_4 \left( C_k - \sum_r \Lambda_{rk}^T \Lambda_r^{-1} C_r \right) \quad (22)$$

where

ESTIM

$$N_4 = \left[ K - \sum_r \Lambda_{rk}^T \Lambda_r^{-1} \Lambda_{rk} \right]^{-1} \quad (23)$$

These solutions form the partitioned Bayesian estimation scheme used in NONAME.

Additionally, the covariance matrix for the arc parameters must be updated to account for the simultaneous adjustment of the common parameters:

$$\left[ N_1 \right]_r = \Lambda_r^{-1} + \left( \Lambda_r^{-1} \Lambda_{rk} \right) N_4 \left( \Lambda_{rk}^T \Lambda_r^{-1} \right) \quad (24)$$

### Summary

The procedure for computer implementation is illustrated in Figure 1. This procedure is:

1. Integrate through each arc forming the matrices  $\Lambda_r$ ,  $\Lambda_{rk}$ , and  $C_r$ ; and simultaneously accumulate into the common parameter matrices  $K$  and  $C_k$ .
2. At the end of each arc, form

$$\underline{da}_r = \Lambda_r^{-1} C_r \quad (25)$$

and modify the common parameter matrices as follows:

$$K = K - A_{rk}^T A_r^{-1} A_{rk} \quad (26)$$

ESTIM

and

$$C_k = C_k - A_{rk}^T \underline{da}_r \quad (27)$$

The matrices  $\underline{da}_r$ ,  $A_{rk}$ , and  $A_r^{-1}$  must also be put in external storage.

3. After processing all of the arcs; i.e., at the end of a global or "outer" iteration, determine  $\underline{dk}$ . Note that  $K$  has become  $N_4^{-1}$  and  $C_k$  has been modified so that

$$\underline{dk} = K^{-1} C_k \quad (28)$$

The updated values for the common parameters are of course given by

$$\underline{k}^{(n+1)} = \underline{k}^{(n)} + \underline{dk} \quad (29)$$

The arc parameters are then updated to account for the simultaneous solution of the common parameters. Information for each arc is input in turn; that is, the previously

stored  $\underline{da}_r^t$ ,  $\Lambda_{rk}$ , and  $\Lambda_r^{-1}$ . The correction vector to the updated arc parameters is given by

ESTIM

$$\underline{da}_r = \underline{da}_r^t - (\Lambda_r^{-1} \Lambda_{rk}) \underline{dk} \quad (30)$$

and hence

$$\underline{a}_r^{(n+1)} = \underline{a}_r^{(n)} + \underline{da}_r \quad (31)$$

The covariance matrix for the arc parameters,  $\Lambda_r^{-1}$ , is updated by

$$\Lambda_r^{-1} = \Lambda_r^{-1} + (\Lambda_r^{-1} \Lambda_{rk}) K^{-1} (\Lambda_{rk} \Lambda_r^{-1}) \quad (32)$$

This completes the global iteration.

It should be noted that if only the arc parameters are being determined, as is the case for "inner" iterations, the solution vector is  $\underline{da}_r^t$  and hence the updated arc parameters are computed by

$$\underline{a}_r^{(n+1)} = \underline{a}_r^{(n)} + \underline{da}_r^t \quad (33)$$

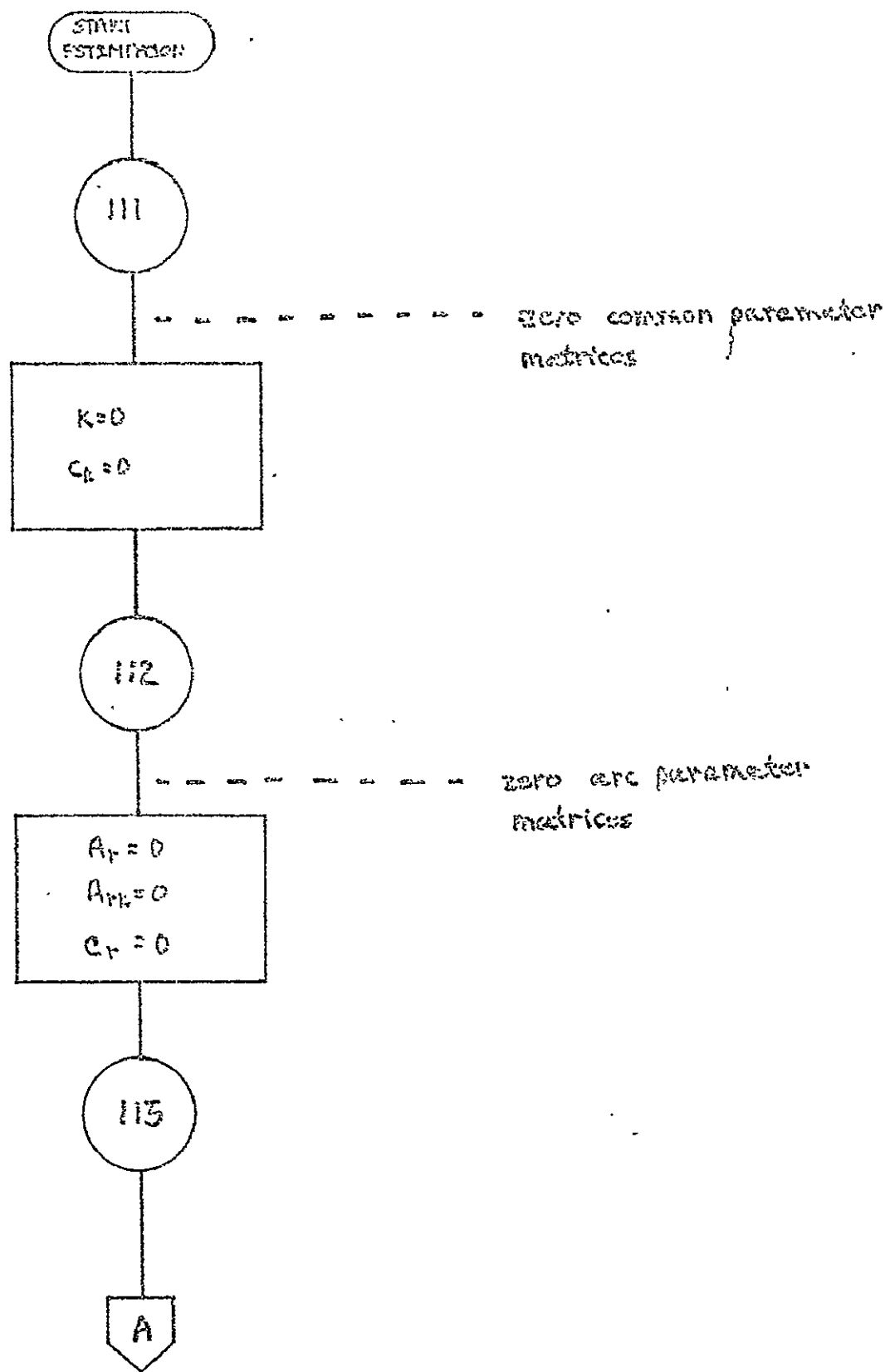


Figure 1: Partitioned Estimation Procedure

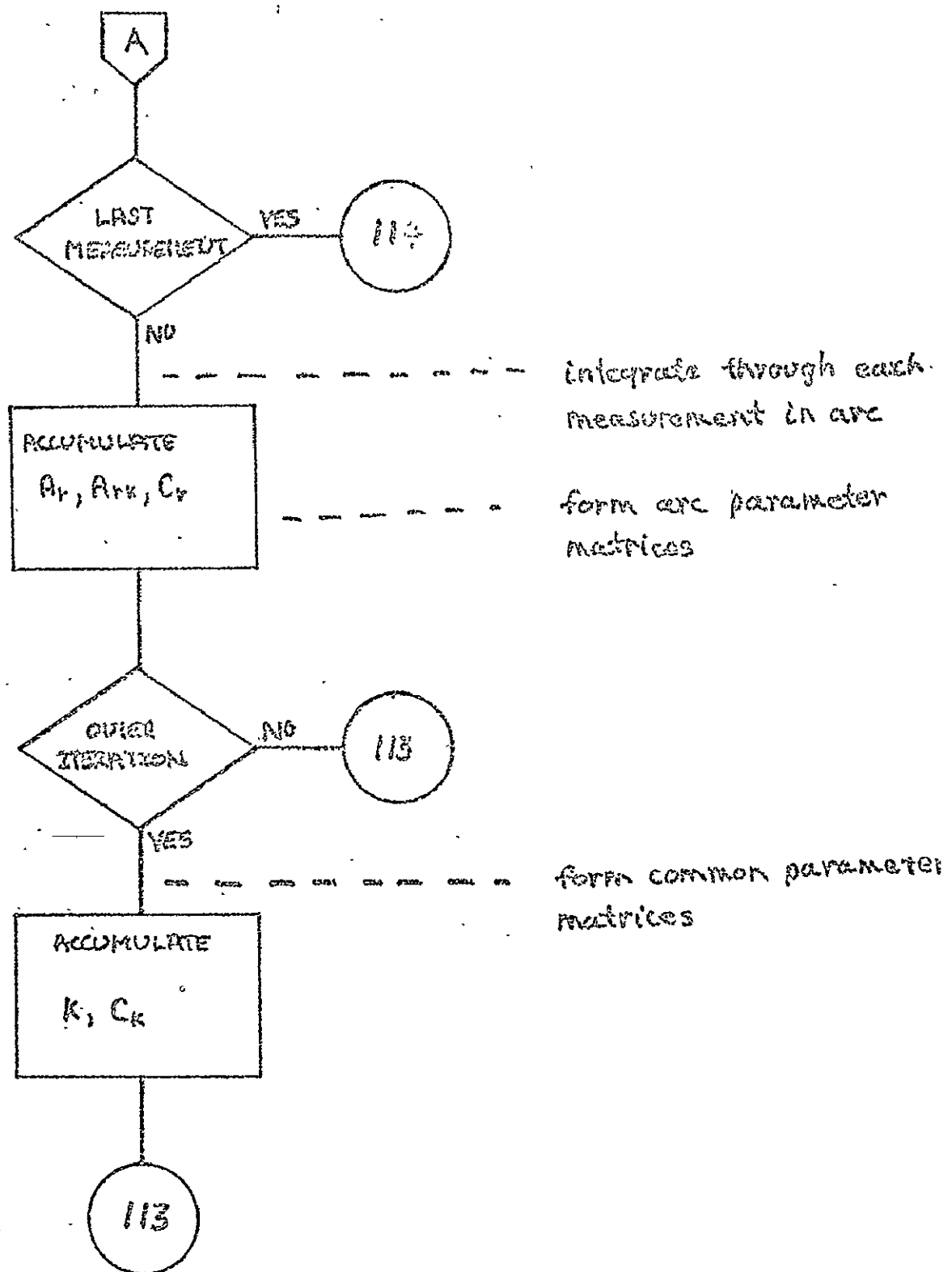


Figure 1: Partitioned Estimation Procedure (Cont.)

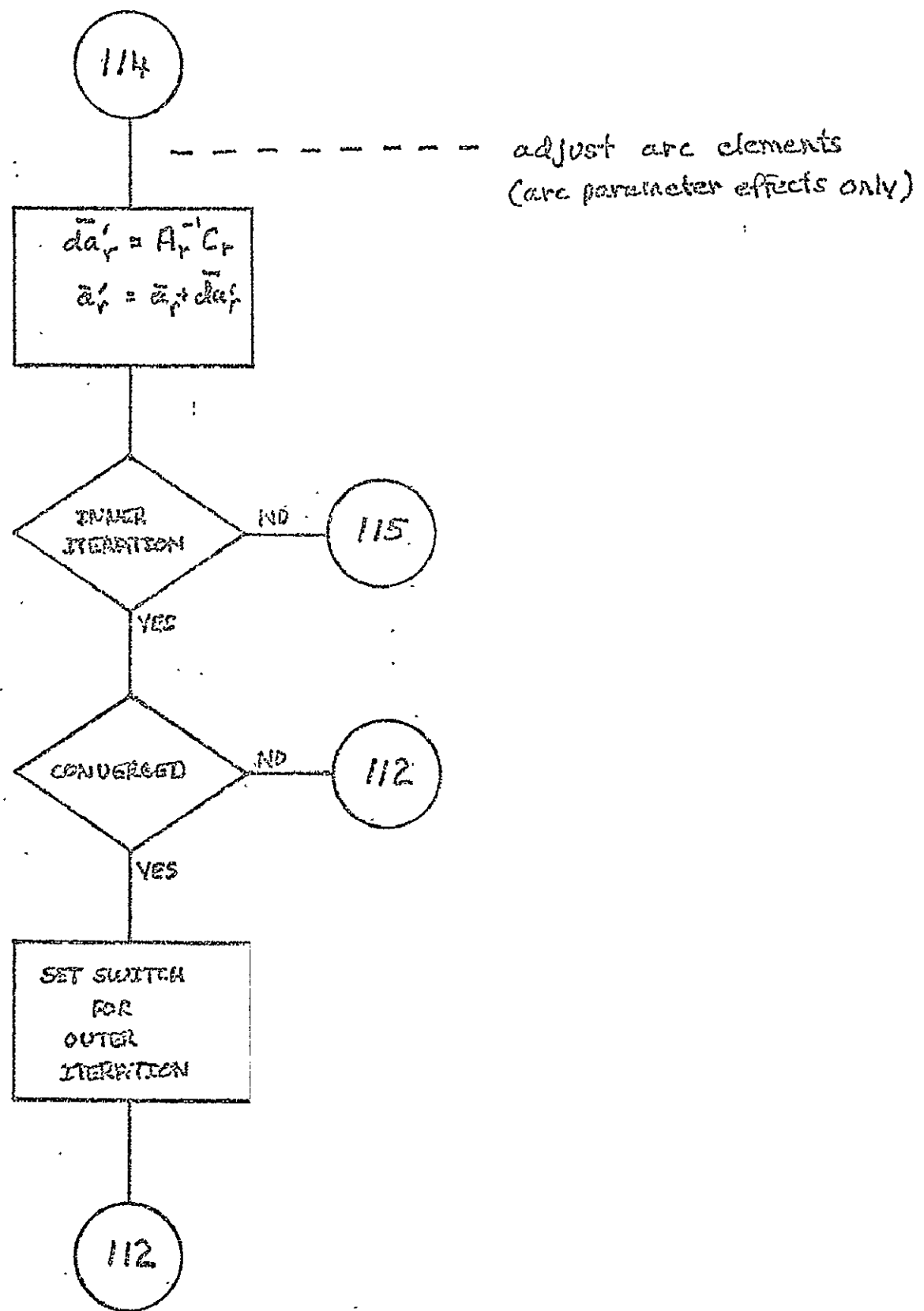


Figure 1: Partitioned Estimation Procedure (Cont.)

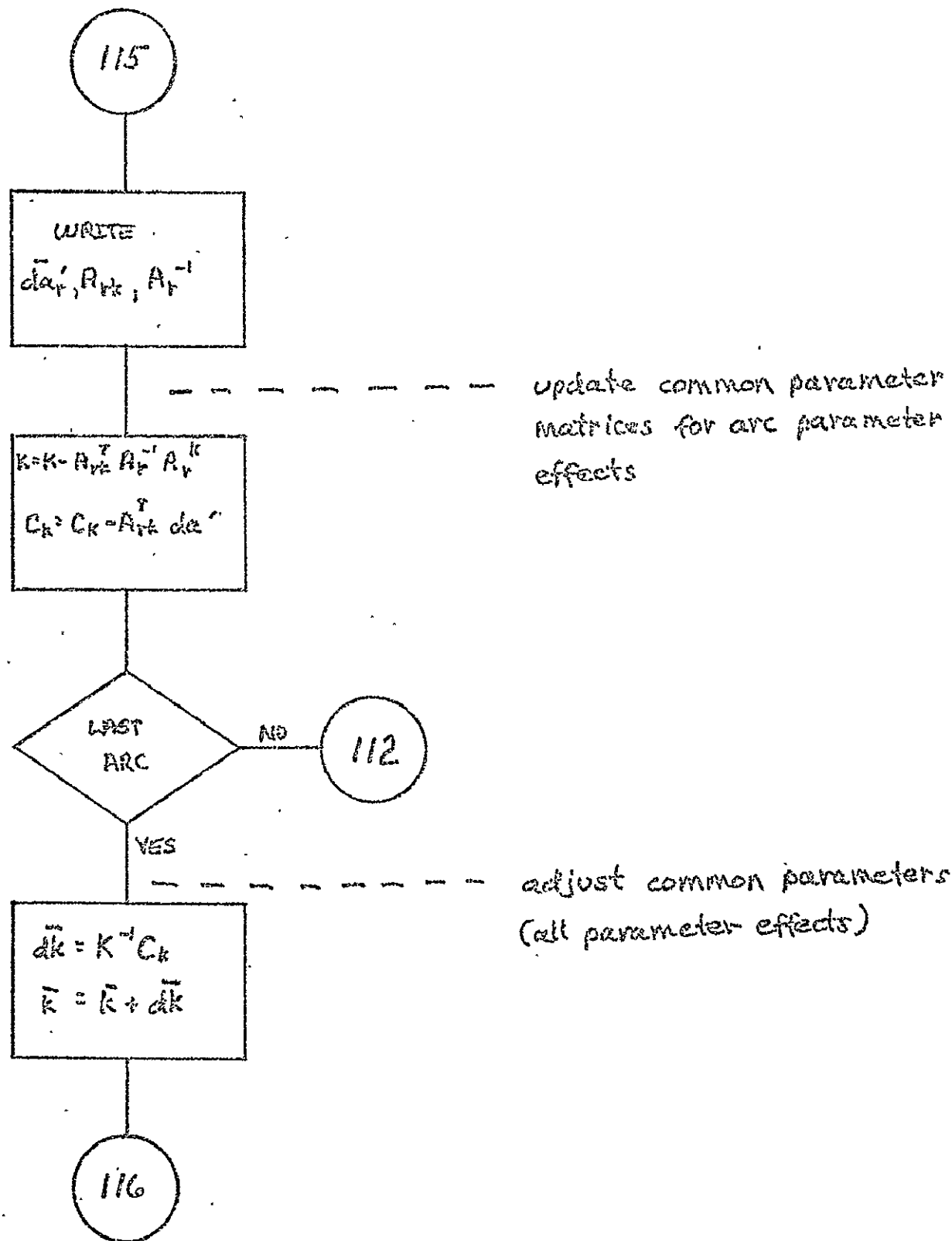


Figure 1: Partitioned Estimation Procedure (Cont.)

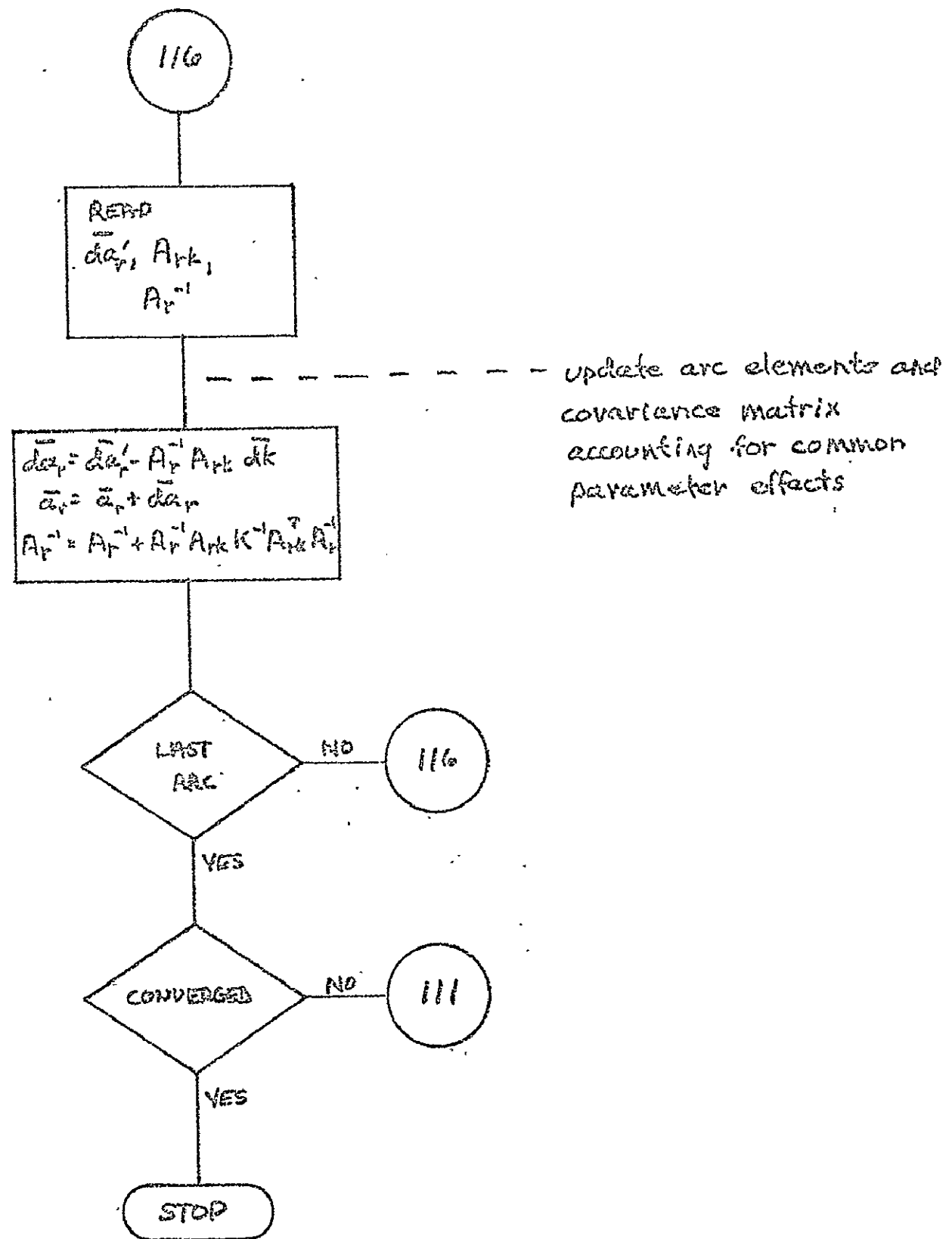


Figure 1: Partitioned Estimation Procedure (Cont.)

The common parameter matrix  $K$  is carried as a symmetric matrix. It is core-resident throughout the estimation procedure. Its dimension is set by the number of common parameters being determined and remains constant throughout the procedure.

The arc parameter matrices  $A_r$  are also carried as symmetric matrices. Their dimensions vary from arc to arc according to the number of arc parameters being determined. Only one arc parameter matrix  $A_r$  and the corresponding covariance matrix  $A_{rk}$  are resident in core at any given time. These arc parameter matrices are stored on disk during step 2 of the above summary and recovered during step 3.

The a priori covariance matrix  $V_k$  is not carried as a full matrix. The correlation coefficients between each coordinate of a given station position are carried. The position coordinates of different stations and the geopotential coefficients are considered to be uncorrelated.

The a priori covariance matrices  $V_r$  are also not carried as full matrices. The drag coefficient, radiation pressure coefficient, and each bias are considered to be uncorrelated. The covariance matrix for the epoch elements is carried.

In terms of a subroutine breakdown within NONAME, this entire section is implemented in subroutine ESTIM with the exception of the matrix inversions. These inversions are done by subroutine SYMINV.

### 2.10.3 Data Editing

The data editing procedures for NONAME have two forms:

- o hand editing using input cards to delete specific points or sets of points, and
- o automatic editing depending on the weighted residual as component to a given rejection level.

The hand editing is a simple matching of the appropriate NONAME control card information with the set of observations. This calling procedure is done in NONAME subroutines GEOSRD or DODSRD.

The automatic editing of bad observations from a set of data during a data reduction run is performed in the NONAME main program. Observations are rejected when

$$\left| \frac{O - C}{\sigma} \right| > k \quad (1)$$

where

NONAMP

$o$  is the observation

$c$  is the computed observation

$\sigma$  is the a priori standard deviation  
associated with the observation (input)

$k$  is the rejection level.

The rejection level can apply either for all observations of a given type or for all observations of a given type from a particular station. This rejection level is computed from

$$k = E_M \cdot E_R \quad (2)$$

where

$E_M$  is an input multiplier, and

$E_R$  is the weighted RMS of the previous "outer"  
or global iteration. The initial value of  
 $E_R$  is set on input.

It should be noted that both  $E_M$  and  $E_R$  have default values.

## SECTION 2.11 GENERAL INPUT/OUTPUT DISCUSSION

NONAME is a powerful yet flexible tool for investigating the problems of satellite geodesy and orbit analysis. This same power and flexibility causes extreme variation in both input and output requirements. Consequently, NONAME contains a great deal of programming associated with input and output.

### 2.11.1 Input

There are two major functions associated with the input structure:

These are the input of

- o Observation data, and
- o NONAME Input Cards.

The observation data utilized by NONAME includes data from all the major satellite tracking networks. The observational types used to date, together with their originating networks and instrument types, are:

- o Right Ascension and Declination

SAO	Baker-Nunn cameras
STADAN	MOTS-cameras

USAF	PC-1000 cameras
USC&GS	BC-4 cameras
SPEOPT	All of above except Baker-Nunn cameras

• Range

STADAN	GRARR S-Band
	GSFC Laser
SAO	Laser
AMS	SECOR
C-Band	FPQ-6 Radar
	FPS-16 Radar
MSFN	S-Band Radar

• Range Rate

STADAN	GRARR S-Band
MSFN	S-Band Radar

• Frequency Shift

TRANET - Doppler

• Direction Cosines

STADAN	Minitrack interferometer
--------	--------------------------

• X and Y Angles

STADAN	GRARR
MSFN	S-Band Radars

• Azimuth and Elevation Angles

STADAN	GSFC Laser
C-BAND	FPQ-6, Radar
	FPS-16 Radar

The observations are required to be in either the format specified by the National Space Science Data Center (NSSDC) or the GSFC DODS System.

The NSSDC format includes indicators to identify observation type, instrumentation source, reduction method, coordinate system, and information concerning tropospheric and ionospheric refraction corrections. Data in this format is input via subroutine GEOSRD.

GEOSRD

The DODS format includes indicators to identify observation type, satellite identification, ambiguity corrections, transponder channel when applicable, timing correction, and time reference system information. It also contains flags to indicate the need for transit time correction or other types of pre-processing corrections. Data in this format is input via subroutines DODSRD and DATBSE.

DODSRD

DATBSE

The NONAME Control Cards are the complete specifications for the problem to be solved including special output requests. Their input, controlled through subroutines ADFLUX and INOUPt, consists of data and perhaps variances for

ADFLUX

INOUPt

- Cartesian orbital elements
- Satellite drag coefficient

- Satellite emissivity
- Zero set measurement biases to be adjusted
- Station positions
- Geopotential coefficients

and data for

- Satellite cross-sectional area
- Satellite mass
- Integration times for the orbit
- Epoch time of elements
- Criteria for iteration convergence and data editing
- Solar and geomagnetic flux

Subroutine ADFLUX modifies the program internal data tables of solar and magnetic flux according to the input requests. It also generates the scratch file of flux information to be used with each arc.

Subroutine INOUPt interprets the NONAME Control Cards and sets the appropriate run parameters. It also generates the NONAME run description and the descriptions for all arcs.

ADFLUX  
INOUPt

Subroutine INOUPt references other routines to set up certain run parameters or to list selected run parameters in a particular format. Notable among the former are STA1NP, BLKSTA, SQUANT, and PLHOUT. These are all concerned with station position processing.

INOUPt  
STA1NP  
BLKSTA  
SQUANT  
PLHOUT

It should be noted that the starting orbital elements for some arcs may be recovered from the DODS Data Base by subroutine DODELM.

DODELM

#### 2.11.2 Output

Most of the output from NONAME, not counting the descriptions of the input or run parameters, is produced by the main program. The exception to this is the ORB1 tape output, which has a special subroutine, named ORB1, to produce the required output.

ORB1

The printed output consists of a measurement and residual printout, residual summaries, and solution summaries as detailed below.

For each arc:

##### Measurement and Residual Printout

- Measurement date
- Measurement station
- Measurement type
- Measurement value

- Measurement residual
- Ratio to sigma
- Satellite elevation

#### Residual Summary by Station and Type

- Station
- Measurement type
- Number of measurements
- Mean of residuals
- Randomness measure
- Residual RMS about zero
- Number of weighted residuals
- Mean ratio to sigma for weighted residuals
- Randomness measure for weighted residuals
- RMS about zero for weighted residuals

## Residual Summary by Type

- Measurement type
- Number of weighted residuals
- Weighted RMS about zero
- Weighted RMS about zero for all types together

## Element Summary

- a priori Cartesian elements
- Previous Cartesian elements
- Adjusted Cartesian elements
- Adjustment to Cartesian elements (delta)
- Standard deviations of fit (sigmas)
- Position RMS
- Velocity RMS
- a priori Kepler elements
- Previous Kepler elements

- Adjusted Kepler elements
- Adjustment to Kepler elements (delta)
- Double precision adjusted Cartesian elements  
(current best elements for arc)

#### Adjusted Force Model Parameter Summary for Arc

- Drag Coefficient and/or Solar Radiation Pressure Coefficient
- a priori coefficient value
- Adjusted coefficient value
- a priori standard deviations for coefficient
- Standard deviation of fit for coefficient

#### Adjusted Parameter Summary

- Instrument biases - timing bias and/or constant bias
- a priori bias value
- Adjusted bias value
- a priori standard deviation for bias
- Standard deviation of fit for bias

- Time period of coverage

The following items are printed on the last inner iteration of every outer iteration.

- Apogee and perigee heights
- Node rate and perigee rate
- Period of the orbit
- Drag rate and period decrement if drag is being applied
- Updated covariance matrix for Cartesian arc elements
- Adjusted arc parameter correlation coefficients

After all arcs:

Total Residual Summary

- Total number of weighted measurements for each measurement type
- Total weighted RMS for each measurement type
- Total number of weighted measurements
- Total weighted RMS

## Station Summary

- Earth-fixed rectangular coordinates and geodetic ( $\phi, \lambda, h$ ) coordinates
- a priori coordinate values
- a priori standard deviations for coordinate values
- Adjusted coordinate values
- Standard deviation of fit for coordinate values
- Correlations between determined coordinate values

## Geopotential Summary

- $C_{nm}$  and  $S_{nm}$  coefficients for each  $n,m$  set determined
- a priori values
- Adjusted values
- Ratios of a priori value to a priori sigma for each coefficient
- Standard deviations of fit for coefficients

Arc Summary for Outer Iteration - For each arc

- Updated Cartesian elements for arc
- Correlation coefficients between individual arc parameters
- Standard deviation of fit for arc parameters
- Correlation coefficients between individual arc parameters and parameters common to all arcs

Common Parameter Correlation Coefficients

- Geopotential coefficients
- Cartesian station positions

NONAME also produces an XYZ and Ground Track listing upon request. This is the normal printout for Orbit Generation Mode.

The tape output from NONAME consists of

- the ORB1 tape,
- the XYZ and Ground Track tape,
- a DODS formatted data tape, and
- a binary residual tape.

The XYZ and Ground Track tape and the binary residual tapes are used as input to NONAME support programs.

### 2.11.3 Computations for Residual Summary

The residual summary information is computed in subroutine STAINF for printing by the main program. The formulas used in this subroutine for computing each statistic are presented below.

STAINF

The mean is the familiar average:

$$\mu_C = \frac{1}{n} \sum_{i=1}^n R_i. \quad (1)$$

where

the  $R_i$  are the residuals and  $n$  is the number of residuals.

The RMS is the square root of the sample variance:

STATINF

$$\text{RMS} = \sqrt{s^2} \quad (2)$$

where

$$s^2 = \frac{1}{n} \sum_{i=1}^n (x_i - \mu_c)^2$$

The expected value of the sample variance differs from the population variance  $\sigma^2$ :

$$E(s^2) = \sigma^2 - \text{var } (\mu_c) \quad (3)$$

or rather

$$E(s^2) = \sigma^2(1 - \frac{1}{n}) \quad (4)$$

Hence we may make a better estimate of  $\sigma^2$  by computing

$$\sigma^2 = \frac{n}{n-1} s^2 \quad (5)$$

This is known as Bessel's correction. This computed value for the standard deviation,  $\sigma$ , is also called the RMS about zero.

STAINF

The randomness measure used in NONAME is from a mean square successive difference test. We have

$$RND = \frac{d^2}{s^2} \quad (6)$$

when

$RND$  is the random normal deviate, our statistic;

$s^2$  is the unbiased sample variance; and

$$d^2 = \frac{1}{2(n-1)} \sum_{i=1}^{n-1} (R_{i+1} - R_i)^2$$

Note that  $d^2$  is the mean square successive difference. For each  $i$  the difference  $R_{i+1} - R_i$  has mean zero and variance  $2\sigma^2$  under the null hypothesis that  $(R_1, \dots, R_n)$  is a random sample from a population with variance  $\sigma^2$ . The expected value of  $d^2$  is then  $\sigma^2$ . If a trend is present  $d^2$  is not altered nearly so much as the variance estimate  $s^2$ , which increases greatly. Thus the critical region  $RND$  constant is employed in testing against the alternative of a trend. (Reference 1)

In order to use this test, of course, it is necessary to know the distribution of the RND. It can be shown that in the case of a normal population the expected value is given by

STAINF

$$E(RND) = 1, \quad (7)$$

the variance is given by

$$\text{var}(RND) = \frac{1}{n+1} \left(1 - \frac{1}{n-1}\right), \quad (8)$$

and that the test statistic, RND, is approximately normal for large samples ( $n > 20$ ).

#### 2.11.4 Kepler Elements

The Kepler elements describe the position of the satellite as referred to an ellipse inclined to the orbit plane. This is shown in Figures 1 and 2. The definitions of these elements are:

$a$  - semi-major axis of the orbit

$e$  - eccentricity of the orbit

$i$  - inclination of the orbit plane

$\Omega$  - longitude of the ascending node

$\omega$  - argument of perigee

$M$  - mean anomaly

$E$  - eccentric anomaly

$f$  - true anomaly

Apogee height and perigee height are sometimes used in place of  $a$  and  $e$  to describe the shape of the orbit. As can be seen in Figure 1, the radius at perigee is  $a(1-e)$  and that at apogee is  $a(1+e)$ . The heights are determined by subtracting the radius of the reference ellipsoid at the given latitude from the spheroid height of the satellite. The computations of these last are detailed in section 2.5.1.

APPENDIX

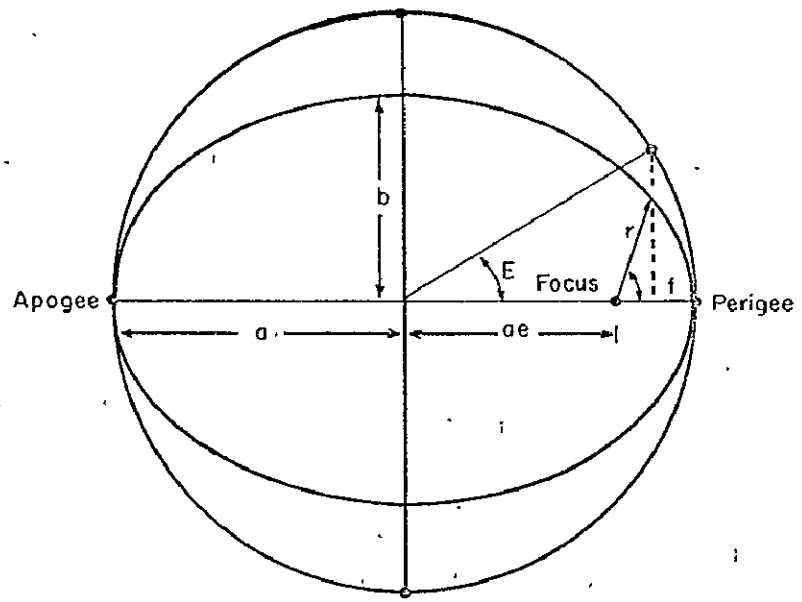


Figure 1: Orbital Ellipse

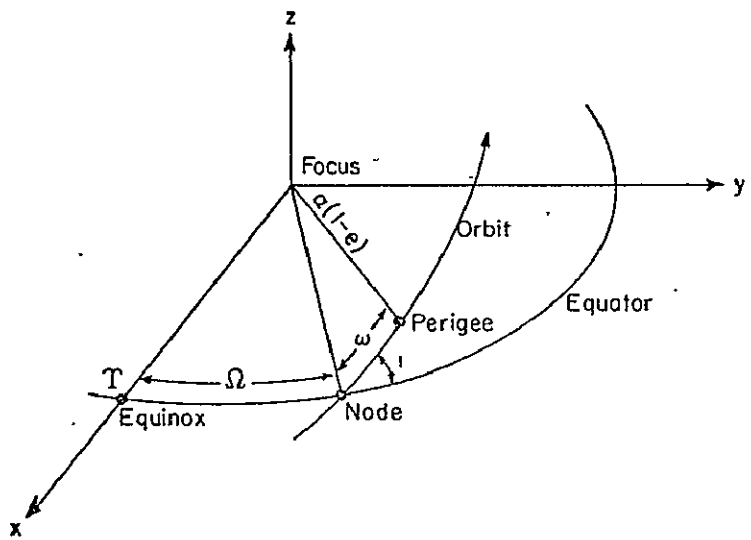


Figure 2: Orbital Orientation

## Conversion to Kepler Elements

ELE

The computation of Kepler elements from the Cartesian positions and velocities  $x, y, z, \dot{x}, \dot{y}, \dot{z}$  is as follows:

Compute the angular momentum vector per unit mass:

$$\bar{h} = \bar{r} \times \dot{\bar{r}} \quad (1)$$

where  $\bar{r}$  is the position vector and  $\dot{\bar{r}}$  is the velocity vector. Note that  $v^2 = \dot{\bar{r}} \cdot \dot{\bar{r}}$ . The inclination is given by

$$i = \cos^{-1} \left[ \frac{h_z}{h} \right] \quad (2)$$

From the vis-viva or energy integral we have

$$v^2 = GM \left( \frac{2}{r} - \frac{1}{a} \right), \quad (3)$$

where  $G$  is the universal gravitational constant and  $M$  is the mass of the primary about which the satellite is.

orbiting. Thus we have

ELEM

$$a = \left[ \frac{2}{r} - \frac{v^2}{GM} \right]^{-1} \quad (4)$$

Recalling Kepler's Third Law,

$$h^2 = GM a (1 - e^2), \quad (5)$$

we determine

$$e = 1 - \left( \frac{h^2}{aGM} \right)^{1/2} \quad (6)$$

The longitude of the ascending node is also determined from the angular momentum vector:

$$\Omega = \tan^{-1} \left( \frac{h_x}{-h_y} \right) \quad (7)$$

The true anomaly,  $f$ , is computed next. Note that in integrating

$$\ddot{\mathbf{r}} \times \dot{\mathbf{h}} = GM \ddot{\mathbf{r}} / r \quad (8)$$

one arrives at

$$\dot{\bar{r}} \times \bar{h} = GM (\bar{r} + \bar{e})$$

(9) ELEM

where  $\bar{e}$  is a constant of integration of magnitude equal to the eccentricity and pointing toward perihelion. Thus,

$$\bar{r} \times \bar{e} = re \sin f \left( \frac{-h}{h} \right), \quad (10)$$

or, performing a little algebra,

$$\sin f = \frac{a (1-e^2)}{reh} \frac{\bar{r} \cdot \dot{\bar{r}}}{}. \quad (11)$$

The cosine of the true anomaly comes from

$$r = \frac{a (1-e^2)}{1-e \cos f}, \quad (12)$$

that is

$$\cos f = \frac{a (1-e^2)}{er} - \frac{1}{e}. \quad (13)$$

The true anomaly is then

$$f = \tan^{-1} \left( \frac{\sin f}{\cos f} \right) \quad (14)$$

The eccentric anomaly is computed from the true anomaly: ELEM

$$\cos E = \frac{f+e}{1+e \cos f}, \quad (15)$$

$$\sin E = \frac{\sqrt{1-e^2} \sin f}{1+e \cos f}, \quad (16)$$

and

$$E = \tan^{-1} \left( \frac{\sin E}{\cos E} \right), \quad (17)$$

The mean anomaly is then computed from Kepler's equation:

$$M = E - e \sin E. \quad (18)$$

The central angle  $u$  is the angle between the satellite vector and a vector pointing toward the ascending node:

$$\cos u = \frac{x \cos \Omega + y \sin \Omega}{r} \quad (19)$$

$$\sin u = \frac{(y \cos \Omega - x \sin \Omega) \cos i + z \sin i}{r} \quad (20)$$

$$u = \tan^{-1} \left( \frac{\sin u}{\cos u} \right) \quad (21)$$

The argument of perigee is then

ELEM

$$\omega = u - f \quad (22)$$

In NONAME, this conversion from  $x, y, z, \dot{x}, \dot{y}, \dot{z}$  to  $a, e, i, \Omega, \omega, M$  is performed by subroutine ELEM.

#### Conversion From Kepler Elements

The input elements are considered to be  $a, e, i, \Omega, \omega$ , and  $M$  and the Cartesian elements are required. POSVE

An iterative procedure, Newton's method, is used to recover the eccentric anomaly,  $E$ , from Kepler's equation ( $M = E - e \sin E$ ).

The vectors  $\bar{A}$  and  $\bar{B}$  are computed.  $\bar{A}$  is a vector in the orbit plane directed toward peri center with a magnitude equal to the semi-major axis of the orbit:

$$\bar{A} = a \begin{bmatrix} \cos \omega \cos \Omega - \sin \omega \sin \Omega \cos i \\ \cos \omega \sin \Omega + \sin \omega \cos \Omega \cos i \\ \sin \omega \sin i \end{bmatrix} \quad (23)$$

$\bar{B}$  is a vector in the orbit plane directed  $90^\circ$  counter clockwise from  $\bar{A}$  with a magnitude equal to the semi-minor axis of the orbit.

$$\bar{B} = a \sqrt{1-e^2} \begin{bmatrix} -\sin \omega \cos \Omega & -\cos \omega \sin \Omega \cos i \\ -\sin \omega \sin \Omega & +\cos \omega \cos \Omega \cos i \\ \cos \omega \sin i \end{bmatrix} \quad \text{POSVEL} \quad (24)$$

The position vector  $\bar{r}$  is then

$$\bar{r} = (\cos E - e) \bar{A} + (\sin E) \bar{B} \quad (25)$$

The velocity vector is given by

$$\dot{\bar{r}} = E \left[ (-\sin E) \bar{A} + (\cos E) \bar{B} \right] \quad (26)$$

where  $E$  is given by

$$E = \frac{\sqrt{\frac{GM}{a^3}}}{1-e \cos E} \quad (27)$$

This conversion procedure for converting  $a, e, i, \Omega, \omega, M$  to  $x, y, z, x, y, z$  is performed in the NONAME system by subroutine POSVEL.

#### 2.11.4.1 Node Rate and Perigee Rate

The node rate  $\dot{\Omega}$  and perigee rate  $\dot{\omega}$  are computed from Lagrange's Planetary Equations. As these are for printout only, NONAME uses just the Earth oblateness term in the geopotential. From Reference 4, page 39, we have

$$\dot{\Omega} = \left[ \frac{3}{2} C_{20} \sqrt{\frac{GM}{a_e^3}} \right] \left( \frac{a}{a_e} \right)^{-3.5} \frac{\cos i}{(1-e^2)^2} \quad (1)$$

$$\dot{\omega} = \left[ \frac{3}{4} C_{20} \sqrt{\frac{GM}{a_e^3}} \right] \left( \frac{a}{a_e} \right)^{-3.5} \frac{(1-5 \cos^2 i)}{(1-e^2)^2} \quad (2)$$

in radians per second, or rather

$$\dot{\Omega} = -9.97 \left( \frac{a}{a_e} \right)^{-3.5} \frac{\cos i}{(1-e^2)} \quad (3)$$

$$\dot{\omega} = -4.98 \left( \frac{a}{a_e} \right)^{-3.5} \frac{(1-5 \cos^2 i)}{(1-e^2)^2} \quad (4)$$

in degrees per day. The quantities used in the above equations are defined as:

$a_e$  is the semi-major axis of the Earth

$GM$  is the product of the universal gravitational constant  $G$  and the mass of the Earth  $M$

$C_{20}$  is the Earth oblateness term in the geo-potential (see Section 2.8.3).

$a$  semi-major axis of the orbit

$e$  eccentricity of the orbit

$i$  inclination of the orbit

#### 2.11.4.2 Period Decrement and Drag Rate

The period decrement and the drag rate are determined from the partial derivatives of the position and velocity with respect to the drag coefficient at the final integrator time step in the given arc. These (multiplied by the drag coefficient) represent the sensitivity of the position or velocity to drag effects. Let us define

$$\overline{\Delta D} = \frac{\partial}{\partial C_D} (\bar{r}) \cdot C_D \quad (1)$$

where

$\bar{r}$  is the satellite (inertial) position vector

$C_D$  is the drag coefficient

We also define

$$\dot{\overline{\Delta D}} = \frac{\partial}{\partial C_D} (\dot{\bar{r}}) \cdot C_D \quad (2)$$

The (two-body) period of the orbit is

$$P = 2\pi \sqrt{\frac{a^3}{GM}} \quad (3)$$

where

$a$  is the semi-major axis of the orbit

$GM$  is the product of  $G$ , the universal gravitational constant, and  $M$ , the mass of the Earth.

Thus

$$\Delta P = 3\pi \sqrt{\frac{a}{GM}} \Delta a. \quad (4)$$

The vis viva or energy integral has

$$v^2 = GM \left( \frac{2}{r} - \frac{1}{a} \right), \quad (5)$$

hence

$$a = \frac{1}{\left[ \frac{2}{r} - \frac{\dot{r}}{v} \right]} \quad (6)$$

Recognizing that  $\Delta(\bar{r})$  is  $\bar{AD}$  and  $\Delta(\dot{r})$  is  $\bar{AD}$ ,

$$\Delta a = \frac{2}{\left[ \frac{2}{r} - \frac{\dot{r}}{v} \right]^2} \left[ \frac{\bar{r} + \bar{AD}}{r^3} + \frac{\dot{r} + \dot{AD}}{GM} \right] \quad (7)$$

The effect of the drag on the period is then given by

$$\Delta P = \frac{6\pi}{a^2} \sqrt{\frac{a}{GM}} \left[ \frac{\dot{r} \cdot \overline{\Delta D} + \dot{\dot{r}} \cdot \overline{\Delta D}}{r^3} + \frac{\dot{r} \cdot \overline{\Delta D}}{GM} \right] \quad (8)$$

The daily rate or period decrement is computed as  $\Delta P / \Delta t$  where  $\Delta t$  is the elapsed time (in days) between the last integrator time point and epoch.

The drag rate is computed from the along track (actually normal) portion of  $\overline{\Delta D}$ , that is  $\Delta D_N$ . We need to construct the unit vector along track,  $\hat{L}$ . The velocity vector  $\dot{r}$  may be resolved into a radial component and a component normal to the radius vector. The magnitude of the normal component is found by the Pythagorean Theorem:

$$A = \sqrt{\dot{r} \cdot \dot{r} - \left( \frac{1}{r} \dot{r} \cdot \dot{r} \right)^2} \quad (9)$$

The unit normal vector  $\hat{L}$  is then

$$\hat{L} = \left( \dot{r} - \frac{1}{r} \dot{r} \cdot \dot{r} \right) / A \quad (10)$$

The normal portion of  $\overline{\Delta D}$  is then

$$\Delta D_N = \hat{L} \cdot \overline{\Delta D} \quad (11)$$

This  $\overline{\Delta D}_N$  represents the along-track position effect due to drag over the integrated time span. The drag rate is computed as  $\Delta D_N / \Delta t^2$  where  $\Delta t$  is again the elapsed time in days.

SECTION 3.0  
NONAME ANALYSES AND GRAPHICS SUPPORT PROGRAMS

There exist three ancillary programs which are used with the NONAME program in the analysis of NONAME determined trajectories and residuals. These programs are entirely independent of the NONAME program.

DELTA is used to print and/or plot along track, cross track and radial differences between two trajectories. GEORGE performs a regression analysis of the residuals for each pass of data about a trajectory to determine trends in possible timing and measurement biases. GROUNDTRACK simply plots the groundtrack of the satellite over a particular tracking station or stations to provide geometric insights into data trends.

### 3.1 DELTA

#### INTRODUCTION

The graphic support program DELTA prints and/or plots trajectory differences. The two trajectories enter the program from two magnetic tapes in either an R-V tape format or ORBL1 tape format. If the tapes are in the ORBL1 format, the subroutine READER is called to obtain each trajectory point; DELTA itself can read the R-V tapes. The subroutine READER is the driver for the sequence of calls to the Plot Package, which provides the plots of the trajectory differences.

## PROGRAM MATHEMATICS

The trajectory tapes input to DELTA consist of the satellite positions ( $X, Y, Z$ ) and velocities ( $\dot{X}, \dot{Y}, \dot{Z}$ ) in the Cartesian system at given time intervals.

If  $X_1, Y_1, Z_1$  are the Cartesian coordinates of satellite position from tape 1 and  $X_2, Y_2, Z_2$  are the coordinates from tape 2 then the position difference vector is

$$\Delta \bar{P} = (\Delta X = X_2 - X_1, \Delta Y = Y_2 - Y_1, \text{ and } \Delta Z = Z_2 - Z_1).$$

The velocity difference vector  $\Delta \bar{V} = (\Delta \dot{X}, \Delta \dot{Y}, \Delta \dot{Z})$  is computed similarly.

These vectors are then resolved into a radial vector,  $\underline{H}$ , a cross track vector  $\underline{C}$ , and an approximation to an along track vector,  $\underline{L}$  (for nearly circular orbits).

First the distance from the geocenter to the satellite,  $R$ , is computed where

$$R = \sqrt{X^2 + Y^2 + Z^2}$$

and the square of the magnitude of the velocity vector ( $\bar{V}$ ),

$$V^2 = \dot{X}^2 + \dot{Y}^2 + \dot{Z}^2.$$

Thus the unit vector,  $\hat{U}$ , in the radial direction is

$$\hat{U} = \left( \frac{X}{R}, \frac{Y}{R}, \frac{Z}{R} \right)$$

DELT

Then to calculate the magnitude of the vector in our along track direction (normal to  $\hat{U}$  in the orbit plane),  $A$ , we must compute  $\hat{U} \cdot \bar{V}$  because

$$A = \sqrt{v^2 - (\hat{U} \cdot \bar{V})^2}$$

Now we compute the unit vectors in our along track direction  $\bar{A} = (a_1, a_2, a_3)$  where

$$a_1 = \left( \dot{X}_2 - (\hat{U} \cdot \bar{V}) \left( \frac{X}{R} \right) \right) / A$$

$$a_2 = \left( \dot{Y}_2 - (\hat{U} \cdot \bar{V}) \left( \frac{Y}{R} \right) \right) / A$$

$$a_3 = \left( \dot{Z}_2 - (\hat{U} \cdot \bar{V}) \left( \frac{Z}{R} \right) \right) / A$$

and the cross track direction  $\bar{C} = (c_1, c_2, c_3)$  where

$$\bar{C} = \bar{A} \times \hat{U}$$

or

$$C_1 = \left( a_2 \right) \left( \frac{Z}{R} \right) - \left( \frac{Y}{R} \right) \left( a_3 \right)$$

DELTA

$$C_2 = \left( a_3 \right) \left( \frac{X}{R} \right) - \left( \frac{Z}{R} \right) \left( a_1 \right)$$

$$C_3 = \left( a_1 \right) \left( \frac{Y}{R} \right) - \left( \frac{X}{R} \right) \left( a_2 \right)$$

Finally we compute the position differences in radial,  $H_p$ , cross track  $C_p$ , and approximation to along track,  $L_p$ ;

$$H_p = \hat{U} \cdot \Delta \bar{p}$$

$$C_p = \bar{C} \cdot \Delta \bar{p}$$

$$L_p = \bar{A} \cdot \Delta \bar{p}$$

and the velocity differences in the radial,  $H_v$ , cross track,  $C_v$ , and approximation to along track,  $L_v$ :

$$H_v = \hat{U} \cdot \Delta \bar{V}$$

$$C_v = \bar{C} \cdot \Delta \bar{V}$$

$$L_v = \bar{A} \cdot \Delta \bar{V}$$

## INTRODUCTION

The support program GEORGE analyzes NONAME measurement residuals. The residuals enter GEORGE from a tape generated by NONAME and are analyzed on a pass by pass basis for either the station and/or measurement type specified by card input to GEORGE.

The main routine GEORGE selects the residuals to be analyzed and breaks them up into individual passes. GEORGE also controls which types of plots are to be made, if any.

REGANL performs the regression analysis and can edit data points on the basis of their standard deviations from the mean.

The subroutines HISTO and PLOTER provide visual aids in analyzing the residuals. HISTO plots a histogram of either the residuals or the ratios to sigma for each pass and a grand summation histogram for all the passes analyzed. PLOTER plots either residuals versus time or measurement rate versus residuals for each pass of data. Both subroutines are drive routines for the Plot Package.

The subroutine DIFF computes the difference in days between any two dates, and the subroutine RYMDI resolves a date in one word into three words; the year, the month, and the day. Both of these subroutines are members of the NONAME program.

The subroutine REGANL determines measurement biases (or zero-set errors) and timing errors in each pass of data and then performs a regression and analysis of the residuals.

The zero-set error, A, and timing error, B, are determined by using a least squares method of solving the following equation: REGANL

$$Y = A + BX \quad (1)$$

where

Y is the residual and

X is the measurement rate.

Taking the partials of (1) with respect to B and then with respect to A and setting them to zero, we get

$$\sum_{i=1}^N x_i y_i - B \sum_{i=1}^N x_i^2 - A \sum_{i=1}^N x_i = 0 \quad (2)$$

$$\sum_{i=1}^N Y_i - B \sum_{i=1}^N X_i - NA = 0 \quad (3)$$

where  $N$  is the number of points in the pass.

REGANL

The two equations are solved simultaneously for  $A$  and  $B$ .

First REGANL computes the sums of the rates,

$$\sum_{i=1}^N X_i,$$

and residuals,

$$\sum_{i=1}^N Y_i,$$

the products of  $X_i$  and  $Y_i$ ,

$$\sum_{i=1}^N X_i Y_i,$$

the squares of the rates,

$$\sum_{i=1}^N X_i^2$$

and finally, the squares of the residuals,

REGAN

$$\sum_{i=1}^N Y_i^2.$$

Then the corrected sum of the products,  $CSXY$ , and the corrected sums of the squares,  $CSX^2$  and  $CSY^2$ , are computed as follows:

$$CSXY = \sum_{i=1}^N X_i Y_i - \sum_{i=1}^N X_i \sum_{i=1}^N Y_i / N$$

$$CSX^2 = \sum_{i=1}^N X_i^2 - \left( \sum_{i=1}^N X_i \right)^2 / N$$

$$CSY^2 = \sum_{i=1}^N Y_i^2 - \left( \sum_{i=1}^N Y_i \right)^2 / N$$

Now, solving for  $B$  we get

$$B = CSXY/CSX^2,$$

and solving for  $A$  using  $B$  we get

$$A = \left( \sum_{i=1}^N Y_i - B \sum_{i=1}^N X_i \right) / N.$$

The regression analysis is performed next. (See Anderson, R.L., and Bancroft, J.A., Statistical Theory in Research, 1952, McGraw-Hill Book Co., Inc., New York, pp. 156-157.)

The regression sum of squares, RSS, is

REGAC

$$RSS = CSXY^2 / CSX^2$$

and the regression mean, RM, is

$$RM = (CSY^2 - RSS) / (N - 1),$$

which is nothing more than the square of the standard deviation of the residuals about the trajectory.

The standard deviations of the zero-set error, SDZ, and timing error, SDT, are

$$SDZ = \sqrt{RM \sum_{i=1}^N x_i^2 / NCSX^2}$$

and

$$SDT = \sqrt{RM / (N-1)}$$

The noise about the fitted line, D, is

$$D = \sqrt{RM}$$

The residual mean square, RMSQ, is computed as

$$RMSQ = \frac{CSY^2 - RSS}{N - 1}$$

To test the randomness of the result, we compute the residuals corrected for zero-set and timing error biases, CR<sub>i</sub>, as

$$CR_i = RESID_i - A_i - B_i X_i$$

where RESID<sub>i</sub> is the residual.

Then we compute difference sum of squares between subsequent residuals, DSQ, as

$$DSQ = \sum_{i=1}^N (CR_{i+1} - CR_i)^2$$

The random normal deviate, RND, is then

$$RND = \frac{\left(\frac{DSQ}{2RM}\right) - 1}{\sqrt{(N-2)/(N^2-1)}}$$

The noise is random if

$$|RND| < 2.58$$

and non-random if

$$|RND| > 2.58.$$

### 3.3 GROUNDTRACK

#### INTRODUCTION

GROUNDTRACK provides geometric insights into NONAME results by plotting the satellite groundtrack for each pass over a particular station.

The main routine GROUNDTRACK controls the type of plot (groundtrack only or groundtrack with land plots), fixes the size of the grid, reads the data required for the groundtrack requested, and makes the required calls to the Plot Package.

The subroutine CENTER centers the station position on the plotting grid. The subroutine LAND finds the required data in the WRLMAP block data to plot the land masses on the grid. WRLMAP is part of the Plot Package.

The subroutine DATIME converts minutes into days, hours, and minutes. The subroutines ADDYMD, DIFF, and RYMDI are members of the NONAME program and are used to handle the dates and times in the program.

### 3.4 WOLF SC4020 PLOT PACKAGE

#### INTRODUCTION

The WOLF Plot Package is a complete system for producing SC4020 and/or printer plots. The package has been designed to be highly flexible and easy to use. Any plot from a quick simple plot (which requires only one call to the package) to highly sophisticated plots (including motion picture plots) can be easily generated with only a basic knowledge of FORTRAN being necessary.

The SC4020 (Stromberg Carlson 4020) is a cathode ray plotter whose outstanding feature is its plotting speed. As such, any user who is producing series of plots should use this plotter. Film (35 mm and 16 mm) and hardcopy are available and the WOLF Plot Package also allows for printer plots which can be used as a quick look for the SC4020 output.

A typewriter mode is available which conveniently allows plotting of character information on the SC4020. This is especially useful as a printer substitute for large amounts of output.

## PROGRAM DESCRIPTION

The WOLF Plot Package is a system of FORTRAN callable subroutines which are used to create plots. It is structured into four major levels as follows:

1. Basic Level - The basic level routines perform the primary functions of the plot package. Except for a few auxiliary routines, the basic level routines are necessary for all other routines. However, few of the basic routines are user called.

The primary basic routine assembles the instructions for the SC4020 tape. There is a printer simulation (of the SC4020) in this routine. This allows for SC4020 plots, printer plot or both simultaneously. The other major basic level routine is used for initialization and termination of the Plot Package.

2. Intermediate Level - The intermediate level contains the major user called routine. Some of the functions of this level are

- a. Grid Overlays (both Cartesian and Polar)  
with labels
- b. Scaling functions
- c. Plotting of vectors or characters in any of  
the following coordinate systems:

Linear

Semi-Log

Log-Log

Polar

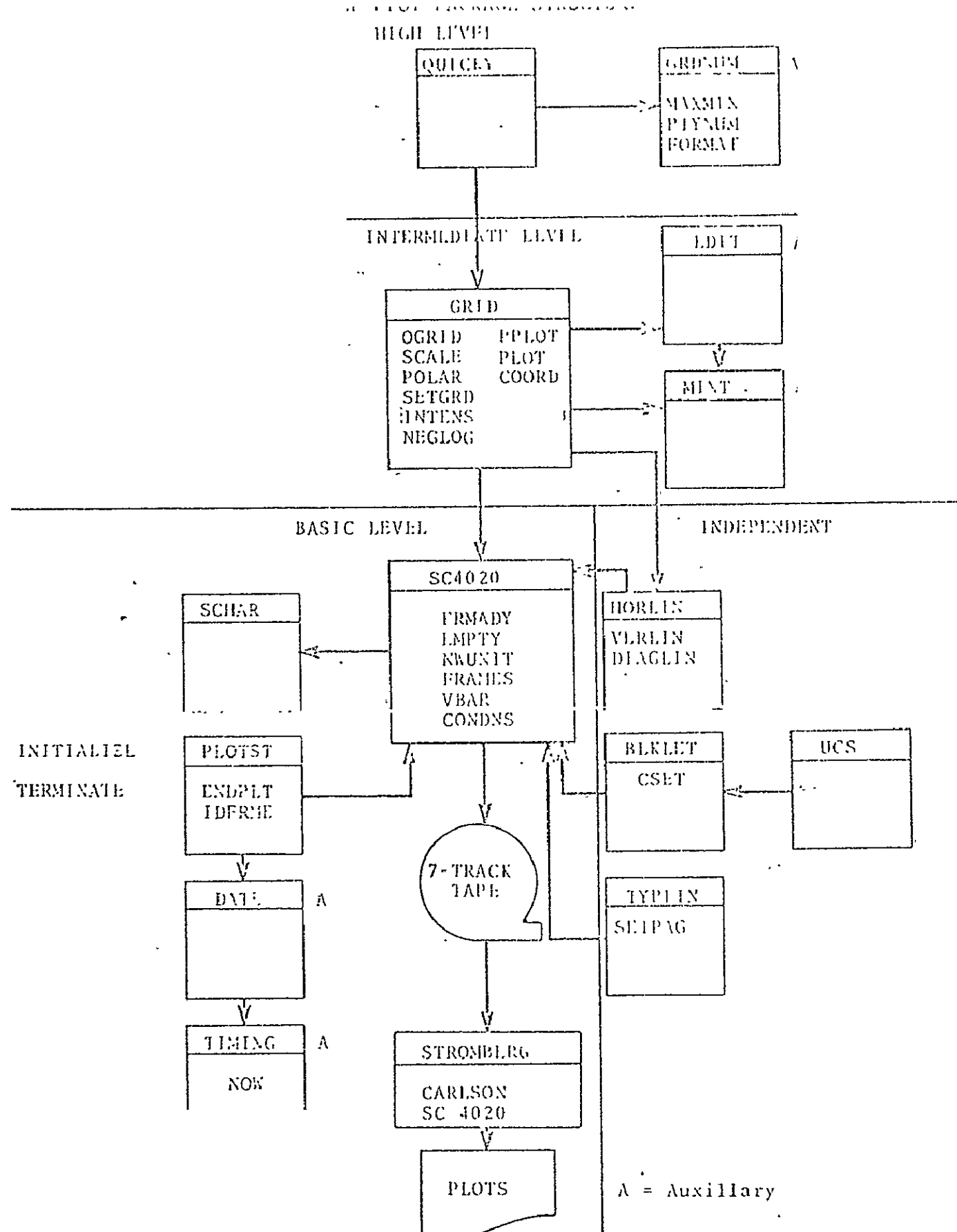
3. High Level - This level is for quick plots with a minimum of programming effort. At this level, all of the other levels are called upon. Only one FORTRAN statement is necessary to produce a plot of any array of data complete with a labeled grid overlay.

4. Independent Level - These routines perform functions that are independent of all other levels except the basic level. The following are among the functions of this level:

- a. Labels: A string of characters can be plotted horizontally, vertically or diagonally (at any inclination and direction).
- b. Graphic Letters: Letters can be output in any size and in any font design (i.e., standard block letters, mathematical symbols or even old English script).
- c. Typewriter Mode: The typewriter function in the SC4020 plotter can be used by calling the various typewriter routines. These allow for information to be typed (strings of characters output in page format) on either the SC4020 or printer.

In addition to these four levels, there are also a number of auxillary routines. These perform such functions as conversion of decimal (binary) numbers to EBCDIC equivalents and dump of the SC4020 plot tape.

The functional structure of the Plot Package is illustrated in Figure 1.



SECTION 4.0  
NONAME DATA HANDLING SUPPORT PROGRAMS

The three data handling programs are used to merge or modify existing data tapes for use with the NONAME system.

DODS SORT-MERGE sorts and merges data from two data tapes in the DODS data tape format described in detail in Volume III-NONAME SYSTEM OPERATIONS DESCRIPTION. GEOS SORT-MERGE performs the same task for tapes in the GEOS format described in section C.4 of the above reference. The ORB1 conversion program converts a NONAME generated ORB1 tape of the format described in Section C.6 of the same reference on a 9-track tape to the same format on a 7-track tape.

No input cards are required for any of these programs as there are no options.

#### 4.1 GEOS SORT-MERGE

The GEOS SORT-MERGE program sorts data from two GEOS format data tapes into chronological, station, and then measurement type order, eliminating duplicate data records.

SORT-MERGE first reads and sorts a block of 250 data records onto a scratch file. It then reads and sorts another block of 250 records and merges it with the first block. The same procedure is followed until all the data has been sorted and merged. The output from the final merge operation is an ordered magnetic data tape in the GEOS data format.

#### 4.2 DODS SORT-MERGE

The DODS SORT-MERGE program sorts data from two DODS format data tapes by satellite identification numbers into chronological, station and then measurement type order, eliminating duplicate data records.

SORT-MERGE first reads and sorts a block of 250 data records onto a scratch file. It then reads and sorts another block of 250 records and merges it with the first block. The same procedure is followed until all the data has been sorted and merged. The output from the final merge operation is an ordered magnetic data tape in the DODS data format in blocks by satellite.

#### 4.3 ORB1 CONVERSION

The ORB1 CONVERSION program is used to convert a 9-track 360 double-precision ORB1 tape to a 7-track 7094 single-precision tape.

The main routine reads in 360 double-precision words and writes on a 7-track tape the 7094 single-precision word.

The subroutine WORD94 does the conversion from the 360 64-bit floating point format to the 7094 36 bit floating point format.

SECTION 5.0  
REFERENCES

GENERAL:

1. Explanatory Supplement to the Astronomical Ephemeris and the American Ephemeris and Nautical Almanac, Published by Her Majesty's Stationery Office, London, 1961.
2. William M. Kaula. "Theory of Satellite Geodesy," Blaisdell Publishing Company, Waltham, Massachusetts, 1966.

SECTION 2.3:

1. A Joint Supplement to the American Ephemeris and the British Nautical Almanac," Improved Lunar Ephemeris 1952-1959," pages IX and X.
2. Astronomical Papers Prepared for the Use of the American Ephemeris and Nautical Almanac, Volume 15, Part 1, page 153, "Theory of the Rotation of the Earth Around its Center of Mass," published by the United States Government Printing Office, Washington, D.C., 1953.
3. Explanatory Supplement to the Astronomical Ephemeris and the American Ephemeris and Nautical Almanac, published by Her Majesty's Stationery Office, London, 1961.

REFERENCES (CONT.)

SECTION 2.3:

4. S. Newcomb. "A New Determination of the Precessional Constant with the Resulting Precessional Motions," Astronomical Papers prepared for the use of the American Ephemeris, 1897.
5. Edgar W. Woolard. "A Redevelopment of the Theory of Nutation," Astronomical Journal, February 1953, Vol. 58, No. 1, pages 1-3.

SECTION 2.4:

1. C.J. Devine. "JPL Development Ephemeris Number 19," JPL Technical Report 32-1181, Pasadena, California, November 15, 1967.

SECTION 2.5:

1. Bernard Guinot and Martine Feissal. "Annual Report for 1968," Bureau International De L'Heure, published for the International Council of Scientific Unions, Paris, 1969.

## REFERENCES (CONT.)

### SECTION 2.7:

1. "GEOS-A Clock Calibration for Days 321, 1965 to 50, 1966," Johns Hopkins University Applied Physics Laboratory Report, 1966.
2. C.A. Lundquist and G. Veis. "Geodetic Parameters for a 1966 Smithsonian Institution Standard Earth," Smithsonian Astrophysical Observatory Special Report No. 200, 1966.
3. S.J. Moss, R.L. Brooks and E. Hyman. "GEOS-A Preprocessing Report," Wolf Research and Development Corporation Contract NAS 5-9756-8A.

### SECTION 2.8:

1. L.G. Jacchia. "The Temperature Above the Thermo-pause," 1964, Special Report 150, Smithsonian Institution Astrophysical Observatory (SAO), Cambridge, Massachusetts.
2. L.G. Jacchia. "Static Diffusion Models of the Upper Atmosphere with Empirical Temperatures Profiles," 1965, Special Report 170, SAO.
3. L.G. Jacchia. "Density Variation in the Hetrosphere, 1965, Special Report 184, SAO (September 20).

REFERENCES (CONT.)

SECTION 2.8:

4. L.G. Jacchia. "Recent Results in the Atmospheric Region Above 200 km and Comparisons with CIRA 1965," 1967, Special Report 245 SAO, (July 7).
5. L.G. Jacchia. "IV. The Upper Atmosphere," Philosophical Transactions of the Royal Society, 1967, A, Vol. 262, pp. 157-171.
6. L.G. Jacchia, I.G. Campbell and J.W. Showey. "Semi-annual Density Variations in the Upper Atmosphere, 1958 to 1966," 1968, Special Report 265, SAO, (January 15).
7. F.S. Johnson. "Circulation at Ionospheric Levels," 1964, Southwest Center for Advanced Studies, Report on Contract CWb 10531, (January 30).
8. M. Nicolet. "Density of the Hetrosphere Related to Temperature," 1960, Special Report 75, SAO, Cambridge, Massachusetts.
9. U.S. Standard Atmosphere, 1966. Sponsored by National Aeronautics and Space Administration, U.S. Air Force and U.S. Weather Bureau, Washington, D.C. (December).

## REFERENCES (CONT)

### SECTION 2.9:

1. Peter K. Henrici. "Elements of Numerical Analysis," John Wiley & Sons, Inc., New York, 1964.
2. H. Rutishauser, F.L. Bauer and E. Stiefel. "New Aspects in Numerical Quadrature," Proceedings of the XV Symposium on Applied Mathematics, 1962.
3. C.E. Velez. "General Lagrangian Interpolation Formulas," NASA TND-4424, Goddard Space Flight Center, Greenbelt, Maryland.

### SECTION 2.10:

1. Maurice G. Kendall and Alan Stuart. "The Advanced Theory of Statistics," Vol. II, London, 1961.
2. Robert C.K. Lee. "Optimal Estimation, Identification and Control," Cambridge, Massachusetts, 1964.
3. "The GEOSTAR Plan for Geodetic Parameter Estimation," Wolf Research and Development Corporation, Contract No. NAS 5-9756-132, November 1968.

REFERENCES (CONT.)

SECTION 2.11:

1. B.W. Lindgren. "Statistical Theory," The Macmillan Company, New York, 1968.
2. "Support Activity of the Geodetic Satellite Data Service," National Space Science Data Center Report, Goddard Space Flight Center, November 1965.
3. J. Topping. "Errors of Observation and Their Treatment," Chapman and Hall, Ltd., London, 1965.
4. William M. Kaula. "Theory of Satellite Geodesy," Blaisdell Publishing Company, Waltham, Massachusetts, 1966.

APPENDIX A  
INDEX OF SUBROUTINE REFERENCES  
FOR NONAME PROGRAM

<u>SUBROUTINE</u>	<u>SECTION</u>
ADFLUX	2.8.7.2, 2.11.1
BAKINT	2.9.1
BLKSTA	2.11.1
COWELL	2.9.1
DATBSE	2.11.1
DENORM	2.8.3
DENSTY	2.8.2, 2.8.6, 2.8.7
DNVERT	2.9.1
DODELM	2.11.1
DODSRD	2.7.1, 2.7.2, 2.10.3, 2.11.1
DRAG	2.5.1, 2.8.2, 2.8.6
EGRAV	2.8.3
ELEM	2.11.4
EPHEM	2.3.5, 2.4
EQN	2.3.6, 2.3.6.2
EQUATR	2.3.6, 2.7.2
ESTIM	2.10
F	2.3.5, 2.8.1, 2.8.2, 2.8.5
GEOSRD	2.7.1, 2.7.2, 2.7.6, 2.10.3, 2.11.1
GRHRAN	2.3.4, 2.3.5, 2.6.1
HERMIT	2.9.3
HHEMIT	2.9.1, 2.9.3
INOUP	2.5.1, 2.11.1
INPT	2.8.7.2
INTGST	2.9.2
JANTHG	2.3.5, 2.8.7.2
NUTATE	2.3.6, 2.3.6.2

APPENDIX A (CONT.)

<u>SUBROUTINE</u>	<u>SECTION</u>
OBSDOT	2.3.4, 2.5.2, 2.6, 2.6.1, 2.6.3
ORBIT	2.8.2, 2.9-1
ORB1	2.11.2
PLHOUT	2.5.1, 2.11.1
POLE	2.5.4
POSVEL	2.11.4
PRECES	2.3.6, 2.3.6.1
PREDCT	2.3.4, 2.5.1, 2.5.2, 2.6, 2.6.1, 2.6.2, 2.82
PROCES	2.7.1, 2.7.3, 2.7.4, 2.7.5
REARG	2.9.1
REFCOR	2.3.6, 2.8.1
REFION	2.7.5
RESPAR	2.8.2, 2.83
SATCL2	2.7.1
SATCLC	2.7.1
SQUANT	2.5.1, 2.5.2, 2.11.1
STAINF	2.11.3
STAINP	2.11.1
SUNGRV	2.8.4
SYMINV	2.10.2
TDIF	2.5.3
TRUEP	2.5.4
VCONV	2.5.1
VEVAL	2.5.1, 2.8.2, 2.8.3, 2.8.4, 2.8.5, 2.8.6, 2.8.7.2
XEFIX	2.3.4, 2.6.3
XINERT	2.3.4
YEFIX	2.3.4, 2.6.3
YINERT	2.3.4